



# ***ELyT Workshop 2019***

*10th annual workshop*

*Naruko Kanko Hotel, Osaka, Japan*

*March 10th-12th, 2019*

## ***Abstract Book***



## *Program of ELyT Workshop 2019*

### ***Sunday, March 10th***

- 10:00 Leaving Katahira Campus for Naruko by chartered bus
- 12:00 Lunch

<b>Session 1</b>			
<b>Time</b>	<b>Title</b>	<b>Author(s)</b>	<b>Project</b>
13:20	Welcome address		
13:40	INVITED 1 : Welding and Joining Researches at Sato Laboratory	Y. S. SATO	
14:10	High-order accurate flow simulation for aeronautical problems	Y. ABE	
14:30	Self-sustained superlubricity of glycerol in a steel/ta-C contact	Y. LONG, M.-I. DE BARROS BOUCHET, J. M. MARTIN	SuperLub
14:50	Liquid metal dealloying: formation and coarsening	P.-A. GESLIN, T. WADA, H. KATO, T. SUGA	DeProMiNa
15:10	FeCr composites: liquid metal dealloying process and its applications	M. MOKHTARI, C. LE BOURLOT, P.-A. GESLIN, E. MAIRE, J. DUCHET-RUMEAU, H. KATO, T. WADA	DeProMiNa

<i>Time</i>	<i>Title</i>	<i>Author(s)</i>	<i>Project</i>
15:30	Optimizing surface finish to Prevent SCC initiation in energy industries	H. ABE, N. MARY, T. MIYAZAKI, Y. WATANABE, B. TER-OVANESSION, B. NORMAND, K. JAFFRE	OPSCC
15:50	Charge kinetic effect and electrostriction in polyurethane	G. DIGUET, K. YUSE, Y. TANAKA, H. MIYAKE, T. TAKAGI, J.-Y. CAVAILLE	TEmpuRA
16:10	Coffee break		

<b>Session 2</b>			
<i>Time</i>	<i>Title</i>	<i>Author(s)</i>	<i>Project</i>
16:30	NeuroRobotics	M. HAYASHIBE	
16:50	Investigation of the effect of surface roughness on human stiffness feeling	S. KANG, T. OKUYAMA, C. THIEULIN, H. ZAHOUANI, C. PAILLER-MATTEI, M. TANAKA	
17:10	Advanced scintillating fibres and Cerenkov fibres for new hadron and jet calorimeters for future colliders	K. LEBBOU, A. YOSHIKAWA, G. BOULON	INTELUM

<i>Time</i>	<i>Title</i>	<i>Author(s)</i>	<i>Project</i>
17:30	Transition of Solid-phase Dynamic Alloying Behavior of Powder Particles under Repetitive Tangential Force	S. TAKEDA, H. MIKI, J. FONTAINE, M. GUIBERT, H. TAKEISHI, T. TAKAGI	COSMIC
17:50	In-flight behavior of polymeric particle during Cold-spray process	C. A. BERNARD, H. TAKANA, G. DIGUET, K. RAVI, O. LAME, K. OGAWA, J.-Y. CAVAILLE	PolymColdSprayCoat
18:10	Potential of double network gel for low friction system	K. KANDA, L. JAY, H. ZAHOUANI, K. ADACHI	TriArtiJoints
18:30	Opportunity of student exchange via ElyTSchool and Strategy of Université de Lyon in Japan	V. FRIDRICI A. FAVE J.-Y. CAVAILLE	
18:50	End of session		

- 19:00 Dinner
- 20:30 Group sessions, Free Discussions

## **Monday, March 11th**

• 7:00 Breakfast

<b>Session 3</b>			
<b>Time</b>	<b>Title</b>	<b>Author(s)</b>	<b>Project</b>
8:40	New electron microscopy techniques for ceramic materials characterization	L. JOLY-POTTUZ, I. ISSA, A. KRAWCZYNSKA, T. PLOCINSKI, D. STAUFFER, S. LE FLOCH, D. MACHON, V. GARNIER, J. AMODEO, T. EPICIER, K. MASENELLI-VARLOT	
9:00	Quantitative measurement of interfacial heat and mass transfer using high-speed phase-shifting interferometer	Y. KANDA, J. OKAJIMA, A. KOMIYA	
9:20	Tribological characterization of natural bones and bone substitutes for simulating bone drilling in dry conditions	Y. MURAMOTO, V. FRIDRICI, P. KAPSA, G. BOUVARD, M. OHTA	BoneDrill
9:40	Polymer-Metal-Fiber Adhesion Delamination Control (POMADE) by EB-Irradiation	Y. NISHI, H. T. UCHIDA, M. KANDA, M. C. FAUDREE, K. YUSE, D. GUYOMAR, M. SALVIA, J.-Y. CAVAILLE	POMADE & COSMIC

<i>Time</i>	<i>Title</i>	<i>Author(s)</i>	<i>Project</i>
10:00	Magneto Rheological Elastomers and energy harvesting	G. DIGUET, G. SEBALD, M. NAKANO, M. LALLART, J.-Y. CAVAILLE	MARECO
10:20	Coffee break		

<b>Session 4</b>			
<i>Time</i>	<i>Title</i>	<i>Author(s)</i>	<i>Project</i>
10:40	Possibilities of the Gleeble machine at MATEIS laboratory	F. MERCIER	
11:00	Advancement of acoustic emission inspection using system invariant analysis technology	T. SOMA, T. TAKAGI, T. UCHIMOTO, S. CAI	
11:20	Future prospects in the MISTRAL (Miniature-Scale Energy Generation by Magnetic Shape Memory Alloys) project	H. MIKI, M. KOHL, M. LALLART, L. YAN	MISTRAL
11:40	Polymer-Metal-Fiber Adhesions DElamination control	L. OLLIVIER-LAMARQUE, N. MARY, T. UCHIMOTO, S. LIVI, S. YUAN, S. MARCELIN, B. TER-OVANEISSIAN, B. NORMAND	POMADE
12:00	Effect of wettability of carbon fiber on interfacial shear stress on PP/PA polymer blend	H. KOSUKEGAWA, F. DALMAS, T. TAKAGI, J.-Y. CAVAILLE	DESIRE
12:20	Lunch		

<b>Session 5</b>			
<b>Time</b>	<b>Title</b>	<b>Author(s)</b>	<b>Project</b>
14:00	INVITED 2 : Double Keynote Team Science and Interdisciplinary Research in Lyon Collaborative Decision Making in a Visualized, Data Driven Environment	K. LUND  J. MILLER	
14:50	Study on composite materials in NARITA laboratory	F. NARITA, H. KURITA	
15:10	Piping system, risk management based on wall thinning monitoring and prediction	T. TAKAGI, P. GUY	PYRAMID
15:30	Recent advances in PYRAMID project : EMAT experimental results for corrosion characterization	P. GUY, B. NORMAND, H. NAKAMOTO, T. TAKAGI, D. MALLICK	PYRAMID
15:50	Advanced simulation tools for nondestructive assessment of corrosion affecting steel pipes	P. CALMON, C. REBOUD, E. DEMALDENT	PYRAMID
16:10	Coffee break		

<b>Session 6</b>			
<b>Time</b>	<b>Title</b>	<b>Author(s)</b>	<b>Project</b>
16:30	Molecular Simulation Analysis for Adhesion Mechanisms Involved in Polyethylene Processed by Cold Spray	Y. ISHIZAWA, R. MIURA	
16:50	Transonic buffet phenomenon by optimized extraction of transient structure based on physical sensitivity	A. YAKENO	
17:10	A new device based on a unique 6-axis force sensor for environment-controlled tribological and mechanical experiments	J. FONTAINE, M. GUIBERT, J. GALIPAUD, T. LE MOGNE, T. DURAND	
17:30	Modelisation and simulation of nanoscale phenomena	T. TOKUMASU, P. CHANTRENNE	CarboEDiffSim & SilicaGelSim
17:50	Robust Shape optimization under mechanical stability criteria	K. SHIMOYAMA, P. MOHANASUNDARAM, S. BESSET, F. GILLOT	MuORode
18:10	The Eddy Current Magnetic Signature (EC-MS) non-destructive micro-magnetic technique - Simulation	T. MATSUMOTO, B. DUCHARNE, T. UCHIMOTO, B. GUPTA, T. TAKAGI, G. SEBALD	BENTO
18:30	End of session		

- 19:00 Dinner
- 20:30 Group sessions, Free Discussions

## ***Tuesday, March 12th***

• 7:00 Breakfast

<b>Session 7</b>			
<b><i>Time</i></b>	<b><i>Title</i></b>	<b><i>Author(s)</i></b>	<b><i>Project</i></b>
8:30	Computational fluid dynamics for perfusion MRI simulation	M. DECROOCQ, M. OHTA, C. FRINDEL, G. LAVOUE	
8:50	On the potential of materials with a high elastic limit and moderate plasticity for dental implants	A. LIENS, B. TER OVANESSIAN, H. KATO, D. FABREGUE, H. REVERON, N. COURTOIS, J. CHEVALIER	
9:10	Understanding Creep Phenomenon in High Chromium Steel Samples: Characterisation and Modelling	B. GUPTA, B. DUCHARNE, T. UCHIMOTO, G. SEBALD, T. TAKAGI	BENTO
9:30	Low and ultralow friction of microcrystalline diamonds films towards smart and tribo-resistant coatings	H. MIKI, M. BELIN	lofDIAMS
9:50	Coffee break		

<b>Session 8</b>			
<b>Time</b>	<b>Title</b>	<b>Author(s)</b>	<b>Project</b>
10:10	Innovative Surface Treatments by Peening	D. NÉLIAS T. CHAISE	
10:30	Elaboration and characterization of new Titanium alloys for biomedical applications	M. LAURENÇON, D. FABREGUE, A. CHIBA	
10:50	Development of fluoropolymer coating using Cold-spray	W. A. LOCK SULEN, K. RAVI, C. A. BERNARD, N. MARY, Y. ICHIKAWA, K. OGAWA	PolymColdSprayCoat
11:10	Influence of the C composition on properties of Co based alloys	S. AOTA, A. CHIBA, E. MAIRE, D. FABREGUE, K. YAMANAKA	DECCOBABA
11:30	Concluding remarks		

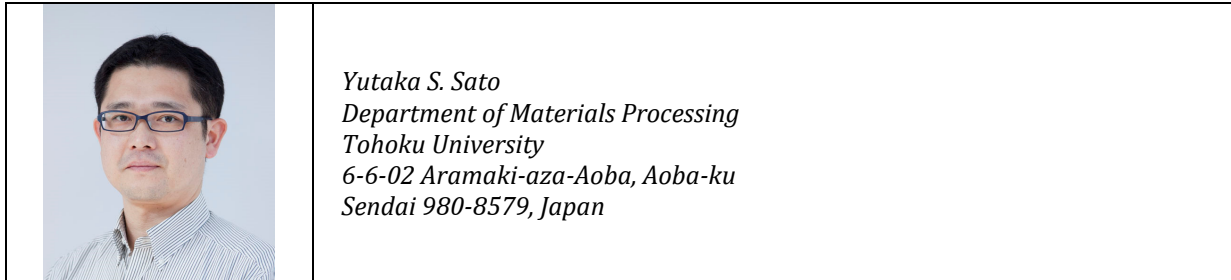
- 12:00 Lunch
- 13:30 Leaving hotel for sake brewery by chartered bus
- 17:00 Arriving at Sendai station



---

*Sunday, March 10<sup>th</sup> – Afternoon*  
*Session 1 – 13:20-16:10*

## **Welding and Joining Researches at Sato Laboratory**



### Abstract :

#### **1. Introduction**

In our laboratory, understanding of fundamental phenomena and mechanisms of welding, joining and bonding processes, and the control and design of the weld interface are conducted on the basis of metallurgy and materials science in order to produce the welded parts with better properties and higher reliability more efficiently during the actual manufacturing sequence. Especially, our laboratory focuses on production of the innovative welded parts through the precise control and design of the weld interface during welding and joining of dissimilar materials with mainly the low heat-input welding, joining and bonding processes, such as friction stir welding and ultrasonic welding. In this presentation, our research activities will be briefly shown.

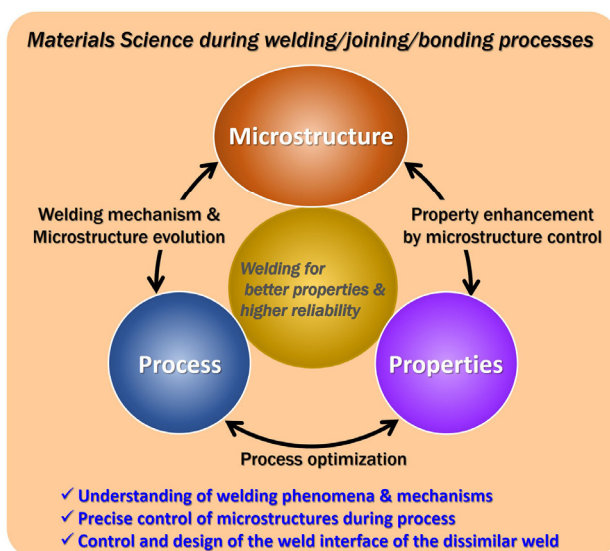


Fig. 1: Research concept of Sato Laboratory

#### **2. Research activities**

##### **2.1 Control of weld interface during dissimilar welding**

Welding of dissimilar materials is an important process to manufacture the future structures and devices, but it is hard to produce the high-performance welds because thick intermetallic compound layer, that deteriorates the weld properties, is generally formed at the weld interface through the excessive reaction during conventional welding processes. Since thickness reduction of the intermetallic compound layer improves the weld properties, many researchers on the dissimilar welding attempt to reduce the thickness of the intermetallic compound layer using low heat-input or solid-state welding processes, but drastic improvement of the weld properties is still difficult. On the other hand, the interfacial reaction during dissimilar welding should be chemically controlled, but the chemical effects on interfacial reaction and weld properties have hardly been clarified. In our group, development of new dissimilar welding process to create the new interface with the aimed properties has been attempted through design and control of interfacial reaction as well as usage of solid state welding processes [1,2].

## 2.2 Microstructural studies on friction stir welding

Friction stir welding (FSW) has been widely used in various industrial fields, such as construction of external fuel tank of rockets, rolling stock of railways, high speed vessels, bridges, etc. Many research attempts to expand the practical applications of FSW more, but understanding of the mechanisms and phenomena of FSW is still lacking. Our group is examining the FSW mechanisms and phenomena based on metallurgical aspects in various metallic materials, such as aluminum alloys, magnesium alloys, copper, steels and titanium alloys, to provide fundamental knowledge to enhance the weld quality and reliability [3,4]. Moreover, development of tool materials for steels and titanium alloys, feasibility of dissimilar welding [5], and modification of microstructure and properties using friction stir processing are also examined in our group.

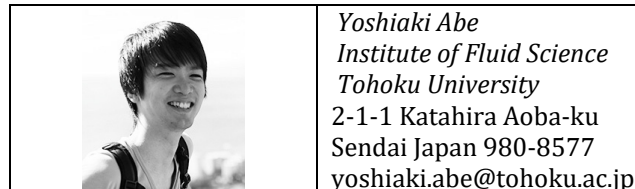
## 2.3 Interfacial phenomena in ultrasonic welding of thin metals

Ultrasonic welding (USW) is a solid state process which can produce a joint between thin metallic materials through ultrasonic vibrating energy and normal clamping force. The USW technique is characterized by a lower energy input, shorter welding time and thinner workpieces than the other welding techniques. Thus, USW technique has a great deal of potential as an environmentally-friendly and cost-effective tool in many industrial fields. However, there is currently little academic understanding on the ultrasonic welding mechanisms despite the engineering significance and past research efforts. Our works on USW technique aim to understand the welding mechanisms based on systematic examinations of the microstructural evolution and mechanical properties of the ultrasonic welds [6].

## References :

- [1] H.S. Furuya, Y.S. Sato, H. Kokawa, T. Huang, and R.S. Xiao, *Metall. Mater. Trans. A* **49A** (2018) 6215-6223
- [2] H.S. Furuya, Y.T. Sato, Y.S. Sato, H. Kokawa, and Y. Tatsumi, *Metall. Mater. Trans. A* **49A** (2018) 527-536
- [3] S. Mironov, Y.S. Sato, S. Yoneyama, H. Kokawa, H.T. Fujii, and S. Hirano, *Mater. Sci. Eng. A*, **717** (2018) 26-33
- [4] Y.S. Sato, T. Onuma, K. Ikeda, and H. Kokawa, *Sci. Technol. Weld. Join.* **21** (2016) 325-330
- [5] Y.S. Sato, A. Tsuji, T. Takida, A. Ikegaya, A. Shibata, H. Ishizuka, H. Moriguchi, S. Susukida, and H. Kokawa, in "Friction Stir Welding and Processing IX", ed. by Y. Hovanski, R. Mishra, Y.S. Sato, P. Upadhyay, D. Yan, Springer, (2017) 47-52
- [6] H.T. Fujii, H. Endo, Y.S. Sato, and H. Kokawa, *Mater. Characterization* **139** (2011) 233-240

## High-order accurate flow simulation for aeronautical problems



Abstract :

### 1. Introduction

Designing ‘greener’ aircraft that is more fuel-efficient is crucial to reduce environmental impact on air transportation system. To improve the performance and decrease fuel consumption, engine weight is a critical design parameter for the aircraft that uses gas turbine engines. Therefore, modern turbines are designed to use as few blades as possible, which however results in higher-loading blades to turn flows and extract an energy. Over these higher-loading blades, the flow is often fully separated in the aft portion of the blade, which exhibits unsteady flow phenomena in a high-Reynolds-number condition and involves small turbulent vortices. The high-fidelity scale resolving simulations such as a Direct Numerical Simulation (DNS) or Large-Eddy Simulation (LES) are hoped to accurately capture these complicated physics and contribute to improving the design of turbine blades. This study performs simulations of flows over an MTU-T161 low-pressure turbine blade with and without turbulent inflow condition, using high-order Flux-Reconstruction (FR) schemes [3] via the Python-based flow solver PyFR [2]. The simulations using laminar and turbulent inlet conditions are compared with the experiments in terms of skin friction, isentropic Mach number on the blade surface, and total pressure loss at the wake region.

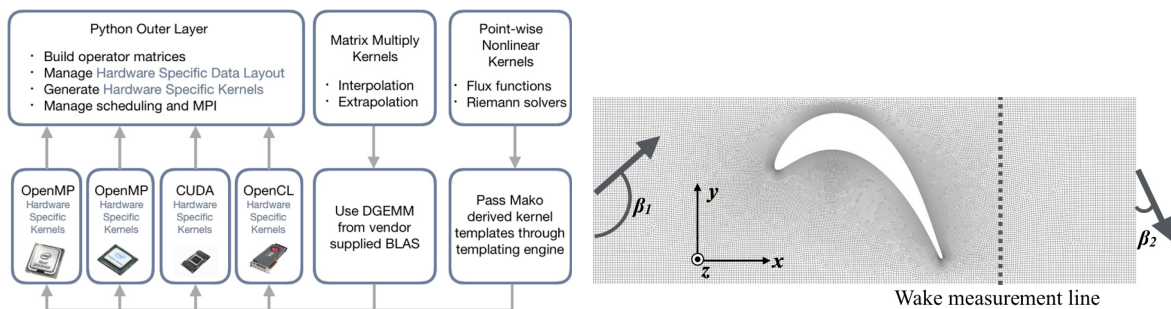


Figure 1 : PyFR (flow solver) implementation      Figure 2: Computational Domain and mesh

### 2. Simulations, discussion

Throughout this study, we adopt PyFR [2] to solve flows over the MTU-T161 low-pressure turbine blade. PyFR solves the compressible Navier–Stokes equations using the FR scheme first proposed by [3]. PyFR is a Python based implementation of the FR approach for heterogeneous clusters consisting

of both conventional CPUs and accelerators (Fig. 2). The computational domain and mesh are shown in Fig. 1. Inlet and outlet Mach number is 0.3857 and 0.5543, respectively. A blade-chord-based Reynolds number is 90,000. The other inlet and outlet variables are derived from isentropic relations. The mesh is periodic in the pitch-wise (vertical) direction and prismatic in the span-wise direction. Both sides of the blade are bounded by end walls which are diverging in the downstream direction. The mesh consists of 19,560,000 hexahedral elements defined by a second-order shape function, which was generated using Gmsh. The simulations are run with a p4 solution polynomial with full anti-aliasing option being activated for both surface and volume fluxes. Each simulation is performed using 1200 or 4000 NVIDIA K20X on Titan at Oak Ridge National Laboratory.

Figure 2 shows instantaneous flow fields of the laminar and turbulent inlet cases after approximately 27 flow passes. It is noteworthy that in the laminar inlet case of Fig. 2, the turbulent transition is not uniform across the span, which occurs at more upstream position in the mid-span plane. This implicates that a strong end-wall effects appears in the turbulent transition over the suction-side of the blade. By contrast, the turbulent inlet case shows relatively uniform transition line across the span. Comparing with the laminar inlet case, turbulent transition in the mid-span plane occurs at more downstream position, which suggests that the inlet turbulence can delay the turbulent transition, and therefore the separation can be effectively suppressed. From these results, it is observed that the lack of turbulence in the inflow profile results in the large separation on the suction side of the blade; meanwhile, the flow separation can be suppressed to some extent by introducing turbulent fluctuation in the inflow, which leads to an accurate prediction of the total wake pressure loss. Therefore, the use of turbulent inlet condition is critical in the present flow and airfoil conditions if we compare the simulation with the experiments which are performed with inflow disturbance.

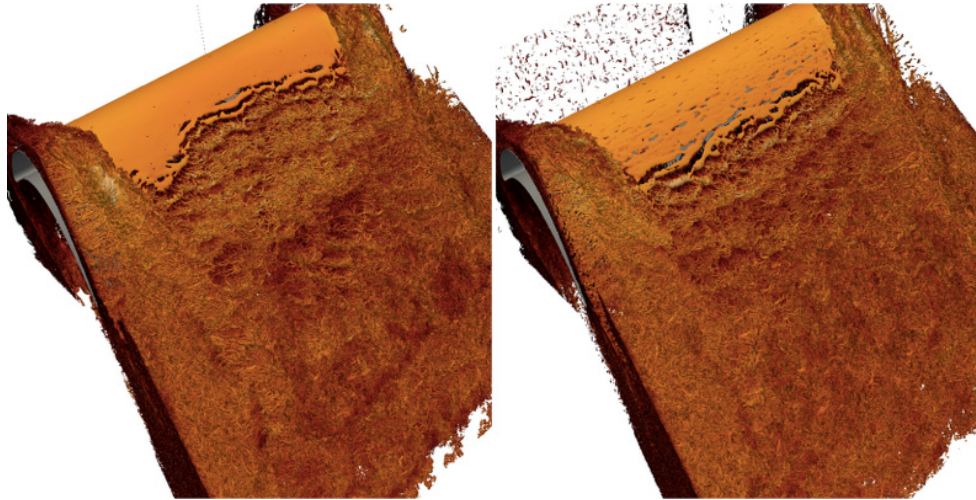


*Figure 1 : Instantaneous flow field laminar (left) and turbulent (right) inlet cases after approximately 27 flow passes. The iso-surfaces shows a  $Q$ -criterion colored by the velocity magnitude.*

## References :

- [1] P. E. Vincent, A. S. Iyer, F. D. Witherden, B. C. Vermeire, Y. Abe, Ralf-Dietmar Baier and A. Jameson, "High-order accurate scale- resolving simulations of low-pressure turbine lin- ear cascades using python at petascale" ICOSA- HOM2018, 9 Jul 2018.
- [2] F. D. Witherden, A. M. Farrington, and P. E. Vincent, "PyFR: An Open Source Frame- work for Solving Advection- Diffusion Type Problems on Streaming Architectures using the Flux Reconstruction Approach," Computer Physics Communications, 185 (11), pp.3028- 3040, (2014)
- [3] H. T. Huynh. "A Flux Reconstruction Ap- proach to High-Order Schemes Including Dis- continuous Galerkin Methods," AIAA-2007- 4079.

## Self-sustained superlubricity of glycerol in a steel/ta-C contact

	<p><i>Yun Long, Maria-Isabel De Barros Bouchet, Jean Michel Martin.</i></p>		<p>Laboratory of Tribology and systems Dynamics, Ecole Centrale de Lyon, 36 Avenue Guy de Collongue, 69134 Ecully</p>
---	---	--	---

### 1. Introduction

In the presence of glycerol, self-mated highly polished steels exhibit superlow friction under thin film EHL lubrication. However, the superlow friction isn't sustainable under high temperature in the boundary regime.<sup>[1]</sup> Hence, in this study, ta-C coated steel is used to replace steel flat. Lubricated by glycerol, the new combination steel/ta-C demonstrates an extremely steady low friction coefficient (0.004) in a long run and this under boundary conditions ( $\lambda < 1$ ). The wear status and superlubricity mechanism are also presented here.

### 2. Experimentation, discussion

#### 2.1. Tribometer and specimens

Ball-on flat sliding tests were performed with a linear reciprocating tribometer. The different tribotests of steel/steel (AISI 52100), steel/ta-C, and ta-C/ta-C friction pairs are conducted under maximum Hertzian contact pressure ( $P_{max}$ ) 577 MPa, 3 mm/s sliding speed for 1.7 h at 50°C. Additionally, for steel/ta-C, to understand the role of sliding speed and temperature, the cases of 1mm/s at 50°C and 3mm/s at 80°C are also studied. To check the stability of superlubricity regime, the test of steel/ta-C was prolonged to 7.4 h at 50°C.

#### 2.2. Material specimens

The ta-C coating was produced by PVD deposition process with graphite target through arc-ion plating and was casted on polished bearing steel (AISI 52100) with thickness around 0.5 micron. The different properties of the ta-C material are reported on the table below.

*Table 1 The relating properties of ta-C*

	Elastic modulus (Gpa)	Hardness (Gpa)	RMS (nm)	Ra (nm)
ta-C	500	55	6.5	2.7

#### 2.3. Lubricant

The lubricant pure glycerol ( $\geq 99.5\%$ ) was purchased at sigma Aldrich and used directly. The cinematic viscosity and piezoviscosity at 50 and 80 °C are listed in the table 2.

*Table 2 Temperature dependent properties of glycerol*

	Viscosity (Pa·s)	Piezoviscosity (Pa <sup>-1</sup> )
50°C	142	5.7
80°C	31.9	4.8

### 3. Results and Discussion

Under lubrication of glycerol, the friction properties of different tribo-pairs: steel/steel, steel/ta-C, ta-C/ta-C are compared at 3mm/s, 50°C. (Fig.1 (a)) The tribo-pair steel/ta-C stands out from the three combinations by reaching a friction coefficient (COF) as low as 0.004. As for the level of wear, no measurable wear has been observed on ta-C and a limited wear scar with diameter 120 μm is obtained on steel ball. Furthermore, studied by atomic force microscopy (AFM), the roughness of steel ball after sliding against ta-C was measured as 4.3 nm while the virgin steel ball roughness was 19.7 nm. (Fig.1 (b))

Steel and ta-C worn surfaces were analyzed by X-ray photoelectron spectroscopy (XPS). Both surfaces wear found to be terminated by FeOOH species. The OH terminations mainly derive from glycerol.<sup>[2]</sup> The FeOOH termination on ta-C comes from iron element transferred from steel during friction process. The easy shear property of OH termination is confirmed by molecular dynamic simulation. Moreover, the thickness of glycerol fluid is calculated as 4.7 nm suggesting that the mixed and boundary regimes are predominant in these experiments.

Hence, the superlubricity achieved by steel/ta-C is the coordination of three factors: smoothed worn surface, FeOOH termination on surfaces and a suitable nm-thick glycerol layer.

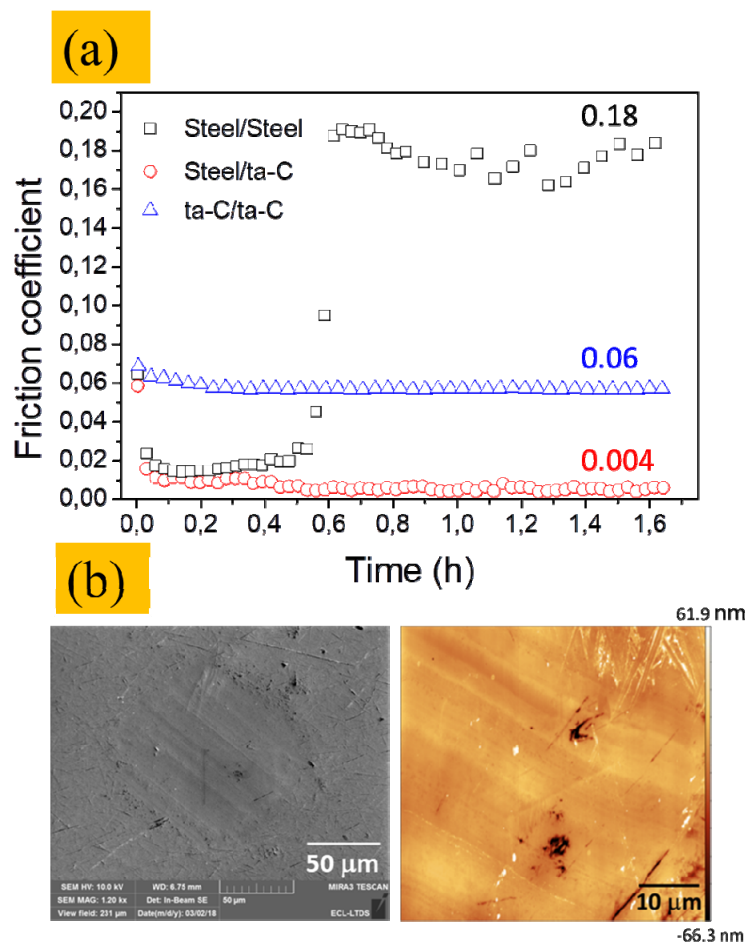


Figure 1 (a) Evolution of COF against time for three tribo-pairs. (b) SEM image and AFM image of steel wear scar after sliding against ta-C.

### References :

- [1] Joly-Pottuz, Lucile, Jean-Michel Martin, MI De Barros Bouchet, and Michel Belin. "Anomalous low friction under boundary lubrication of steel surfaces by polyols." Tribology letters 34, no. 1 (2009): 21-29.
- [2] Bachmann, Svenja, Marcus Schulze, Lisa Krell, Rolf Merz, Michael Wahl, and Robert W. Stark. "Ultra-Low Friction on Tetrahedral Amorphous Diamond-Like Carbon (ta-C) Lubricated with Ethylene Glycol." Lubricants 6, no. 3 (2018): 59.

## Liquid metal dealloying: formation and coarsening

	<i>Pierre-Antoine Geslin MATEIS laboratory INSA Lyon Bat. St Exupéry 23 Avenue Jean Capelle 69621 Villeurbanne</i>		<i>Takeshi Wada Institute for Materials Research, Bld. 2 2-1-1, Katahira, Aobaku, Sendai-city, Miyagi, Japan 980-8577</i>
	<i>Hidemi Kato Institute for Materials Research, Bld. 2 2-1-1, Katahira, Aobaku, Sendai-city, Miyagi, Japan 980-8577</i>		<i>Takumi Suga Institute for Materials Research, Bld. 2 2-1-1, Katahira, Aobaku, Sendai-city, Miyagi, Japan 980-8577</i>

### Abstract :

#### 1. Introduction

Liquid metal dealloying has emerged as a promising technique to elaborate finely porous structures of various nature (non-noble metals, refractory metals or semi-conductors) presenting a high surface area, valuable in numerous applications including catalysis, sensors or battery materials [1,2,3]. This process consists of immersing a binary precursor alloy in a liquid metal chosen such that only one element of the precursor alloy dissolves selectively into the metallic melt while the other element reorganizes into a porous structure. After its formation, the microstructure coarsens significantly by surface diffusion, leading to a decrease of the specific surface and a drop of properties. Therefore, the resulting microstructure and its properties depend both on the formation mechanism occurring at the dealloying front and the subsequent coarsening process. In this contribution, we present results on both processes (formation and coarsening) to better understand how to control the resulting microstructure of the materials.

#### 2. Formation process

In order to investigate the formation process in details, we choose to investigate the model system of Ni-Cu precursor immersed into liquid Ag. This system presents the advantage of having a simple phase diagram [4] (a unique solidus and liquidus lines connected by tie-lines) at the prescribed dealloying temperature (see Fig1.a). Assuming thermodynamic equilibrium at the dealloying interface and using a maximum velocity criteria enables to predict the dealloying rate and the composition profiles based on the phase-diagram. These predictions are then compared with experimental observations.

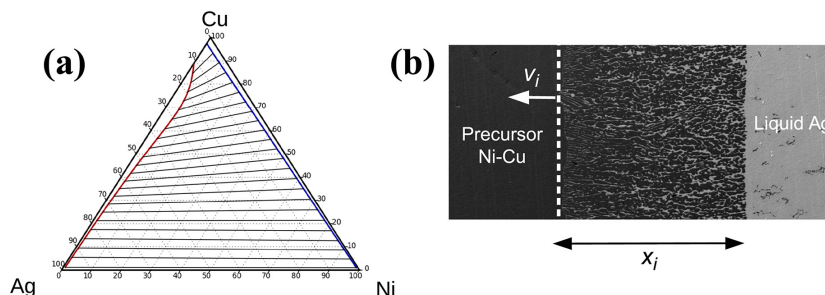


Figure 2: (a) Ternary phase diagram of Ni-Cu-Ag system at 1273 K [4] (b) Microstructure obtained after partial dealloying of a Ni50Cu50 precursor alloy in Ag for 50 sec at 1273K.

### 3. Coarsening process

Experimental observations (see Fig. 2.a) show that the coarsening mechanism is significant in these structures and occurs by surface diffusion. To better understand this process and discuss the evolution of a connected structure, we have used a phase-field model for surface diffusion [5]. Starting with artificial connected microstructures (see Fig. 2.b), our simulations show that the evolution of connected structures of different volume fractions follow expected trends with their characteristic length-scale increasing as  $\lambda \sim t^{1/4}$  [6]. The dependence of the coarsening rate on the volume fraction is discussed in light of the morphological characteristics of the microstructures. Also, the evolution of the topological characteristics of the structure (representing the number of connection per unit cell of the structure) remains constant after a short transient stage (see Fig.1c), showing that the microstructure evolves in a self-similar way.

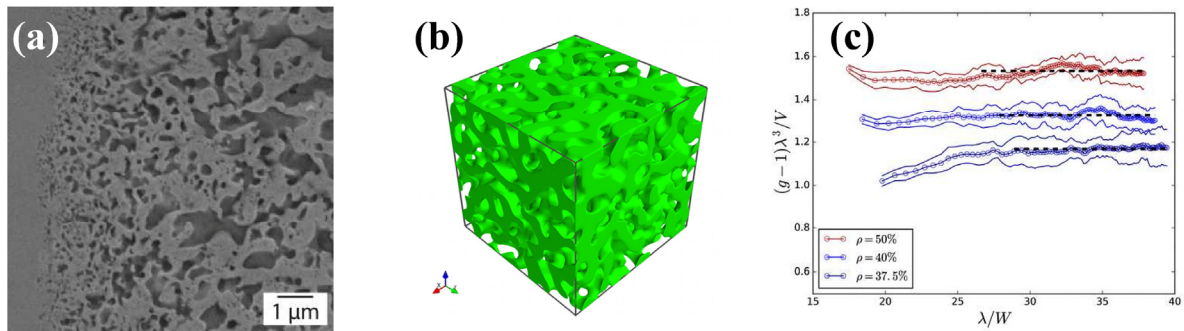


Figure 2: (a) SEM image of a partially dealloyed sample demonstrating the rapid coarsening of these structures. (b) Microstructure used as input of the phase-field model (c) Average connectivity as a function of characteristics length-scale showing the self-similar evolution of the structure.

### References :

- [1] T. Wada, K. Ybyta, A. Inoue and H. Kato, Materials Letters 65, pp. 1076-2078, 2011.
- [2] T. Wada, A.D. Setyawan, K. Yubuta, H. Kato, Scripta Materialia 65, pp. 532-535, 2011.
- [3] T. Wada, H. Kato, Scripta Materialia 68, pp. 723-726, 2013.
- [4] X.J. Liu, F. Gao, C.P. Wang, K. Ishida, Journal of Electronic Materials 37, 2008.
- [5] A. Rätz, A. Ribalta, A. Voigt Journal of Computational Physics 214, pp. 187-208, 2006.
- [6] C. Herring, Journal of Applied Physics 21, pp. 301, 1950.

## **FeCr composites: liquid metal dealloying process and its applications**

	<p><i>Morgane Mokhtari, Christophe Le Bourlot, Pierre-Antoine Geslin Eric maire (MATEIS) Jannick Duchet-Rumeau (IMP), INSA Lyon, Villeurbanne (Fr)</i></p>		<p><i>Hidemi Kato, Takeshi Wada Institute for Materials Research, Tohoku University, Sendai (JP)</i></p>
---	--	--	--

Morgane Mokhtari has recently defended her PhD, successfully conducted in collaboration between MATEIS (Lyon) and IMR (Sendai) laboratories. This presentation aims at exposing the results of her work on the dealloying process.

### Abstract :

Nanoporous metals have attracted considerable attention for their excellent functional properties [1]. The most promising technique used to prepare such nanoporous metals is dealloying in aqueous solution. Nanoporous noble metals including Au have been prepared from binary alloy precursors [2]. The less noble metals, unstable in aqueous solution, are oxidized immediately when they contact water at a given potential so this process is only possible for noble metals. Porous structures with less noble metals such as Ti or Fe are highly desired for various applications including energy-harvesting devices [3]. To overcome this limitation, a new dealloying method using a metallic melt instead of aqueous solution was developed [4]. Liquid metal dealloying consists in the selective dissolution phenomenon of a mono-phase alloy solid precursor: one component (referred as soluble component) being soluble in the metallic melt while the other (referred as targeted component) is not. When the solid precursor contacts the metallic melt, only atoms of the soluble component dissolve into the melt inducing a spontaneously organized bi-continuous structure (targeted+sacrificial phases), at a microstructure level. This sacrificial phase can finally be removed by chemical etching to obtain the final nanoporous materials. Because this is a water-free process, it enables the preparation of nanoporous structures of less noble metals such as Ti, Si, Fe, Nb, Co and Cr.

The objectives of this study are the fabrication and the microstructure and mechanical characterization of 3 different types of materials obtained from the dealloying process : (i) metal/metal composites (FeCr-Mg), (ii) porous metal (FeCr) (iii) metal/polymer composites (FeCr-epoxy resin). The microstructure study was based on 3D observation by X-ray tomography and 2D analysis with electron microscopy (SEM, SEM-EDX, SEM-EBSD). To have a better understanding of the dealloying, the process was followed in situ by X-ray tomography and X-ray diffraction. Finally the mechanical properties were evaluated by nano indentation and compression.

The main results of this study are the following [5,6,7]:

- Nanoporous foam morphology and characteristics (ligaments size, porosity, specific surface,...) can be controlled by precursors composition and dealloying time and temperature.
- Two recrystallization processes are observed at the dealloying front (diffusive or displacive transformation) as function of the precursor composition

- The mechanical properties of the Fe-Cr foam can be enhanced by polymer infiltration: full infiltration as been successfully performed.
- Commercial nickel alloy (*Incalloy* 800 and 825) can be used as precursors. The alloying elements slow-down the dealloying process, resulting in smaller ligament size and higher specific surface of the final materials. The corrosion resistance properties of the dealloyed *Incalloy* samples have been characterized.

#### References:

- [1] J. Snyder, T. Fujita, M. Chen, J. Erlebacher. *Nat. Mater.*, **9** (2010) 904-907 References:
- [2] A.J. Forty. *Nature*, **282** (1979) 597-598 References:
- [3] K. Sivula, R. Zboril, F.L. Formal, R. Robert, A. Weidenkaff, J. Tucek, J. Frydrych, M. Grätzel. *J. Am. Chem. Soc.*, **132** (2010) 7436-7444
- [4] T. Wada, K. Yubuta, A. Inoue, H. Kato. *Mater. Lett.*, **65**(2011) 1076-1078
- [5] M. Mokhtari et al., *Journal of Alloys and Compounds*, Elsevier, 2017, 707, pp.251 - 256.
- [6] M. Mokhtari et al., *Materials Characterization*, Elsevier, 2018, 144, pp.166-172.
- [7] M. Mokhtari et al., *Scripta Materialia*, Elsevier, 2019, 163, pp.5-8

## **Optimizing surface finish to Prevent SCC initiation in energy industries**

Project ElyT lab : OPSCC

	<p>H. Abe<sup>1</sup> N. Mary<sup>1,2</sup> T. Miyazaki<sup>1</sup> Y. Watanabe<sup>1,2</sup></p> <p><i>1: Tohoku University 2: ElyT MaX</i></p>		<p>B. Ter-Ovanessian<sup>1</sup>, B. Normand<sup>1</sup>, K. Jaffre<sup>1,2</sup></p> <p><i>1: MATEIS INSA Lyon 2: ElyT MaX</i></p>
---	--	--	---

### Abstract :

#### **1. Introduction**

The selection of structural materials for applications is usually done from their mechanical properties and adding a safety coefficient to take into account some environmental effect. If this methodology can be used in the most of applications, additional precautions are required in energy industries. Synergistic effects can be activated between the material metallurgy, the environment and mechanical stresses when the material are exposed under extremes conditions (pressure, temperature, strongly aggressive solution, etc.). In various kinds of environments, including boiling water reactor coolant, primary circuit of pressurized water reactor and chloride containing water, the material surface state is the key parameter to control the corrosion and Stress Corrosion Cracking (SCC) susceptibility of alloys. For example, it has been widely accepted that surface machining enhances SCC susceptibility of non-sensitized austenitic stainless steels in a boiling water reactor environment.

Surface finishing operations such as grinding, wire brushing, machining produce surface states that compromise the corrosion resistance of oxidative and passive materials [1]. These processes affect the electrochemical and mechanical stabilities of the material at the microstructure scale and also the passive film properties [2]. A part of our collaborative study (Project ElyT lab: R32 – Understanding and managing stress corrosion cracking) showed that even slight cold work introduced with fine emery finish has significant impact on oxidation properties[3] and cracking susceptibility of Ni base alloys in superheated steam.

Until now, researches focused on the relation between the microstructural modification induced by the surface preparation on the SCC behaviour of material or on the selection of the most suitable treatment [4,5]. However, industries need appropriate surface finish procedures to reasonably minimize SCC susceptibility of alloys. To achieve an effective answer on this demand, new knowledge are required on:

- Physical metallurgy of alloy surface (micro- and nano-structure of surface)
- Electrochemical properties, in particular, stability of passivity (re-passivation kinetic, growth mechanism)
- SCC initiation dynamic (embryo formation, re-passivation, coalescence of micro-cracks).

All those properties need to be linked each other to understand the effect of surface finish on SCC susceptibility of alloys.

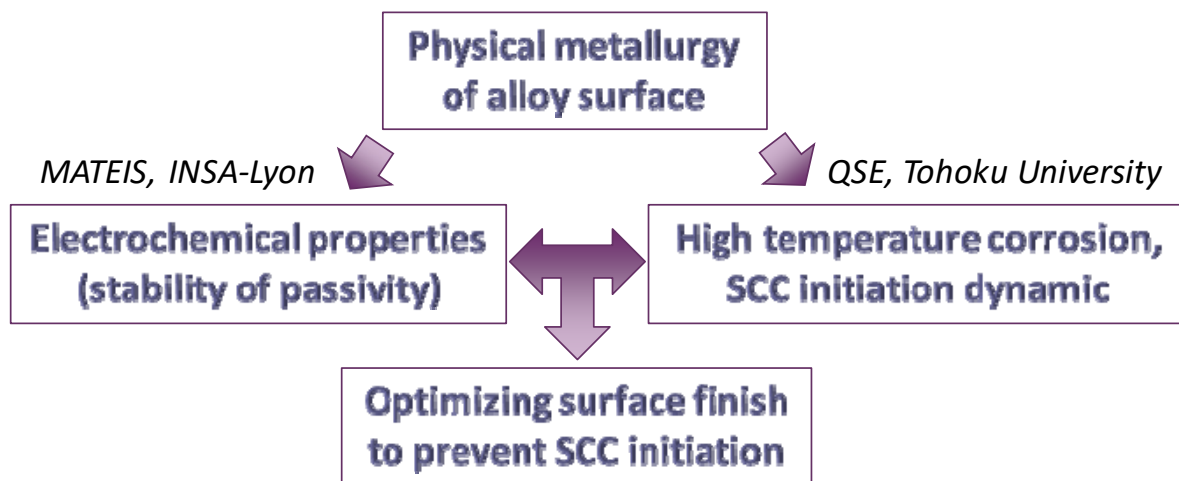


Figure 1 : Frame of the project

## 2. First results

To highlight the influence of surface finishing process used in maintenance, the corrosion and SCC behavior of grinded and mechanically polished samples (2400-SiC polishing or mirror polish) have been studied. It has been shown that the grinding sample exhibits a larger subsurface recrystallization zone than the mechanically polished sample. Such microstructural modification is suspected to affect the corrosion behavior in a simulated primary medium. Indeed, if the nature of the oxide layer is not fundamentally modified, its thickness and the depths affected by the intergranular oxidation are.

Thus, the goal of this study is to establish and quantify the effects of different surface mechanical treatments on the modification of the microstructure, the surface reactivity and the resistance to crack initiation by SCC.

The first step of this study was the understanding of the influence of different surface states of the steels (304L, 316L, 316NG) on the electrochemical properties of the passive film that forms on its surface. In order to characterize the passive film, electrochemical impedance spectroscopy measurements coupled with the Mott-Schottky approach were carried out following a methodology developed in the MATEIS laboratory based on the analysis of impedance diagrams. These analysis techniques make it possible to determine the type of semi-conductivity (type-n, type-p), the main charge carriers nature and their density as well as the thickness of the film. Relationship between the obtained parameters, the stability and the resistance of the passive film can be drawn regarding the microstructural modifications related to surface treatments. Measurements with the XPS technique were also carried out in order to correlate results from the electrochemical tests to the chemistry and nature of the passive films. The final purpose is to link the semiconducting properties, the chemistry of the passive layer to the resistance of materials to intergranular corrosion or pitting corrosion.

### References :

[1]M. Moine, N. Mary, B. Normand, L. Peguet, A. Gaugain, H.N. Evin, Tribo electrochemical behavior of ferrite and ferrite-martensite stainless steels in chloride and sulfate media, *Wear*. 292–293 (2012) 41–48. doi:10.1016/j.wear.2012.06.001.

[2]B. Ter-Ovanesian, N. Mary, B. Normand, Passivity Breakdown of Ni-Cr Alloys: From Anions Interactions to Stable Pits Growth, *J. Electrochem. Soc.* 163 (2016) C410–C419. doi:10.1149/2.0381608jes.

[3]F. Hamdani, H. Abe, B. Ter-Ovanesian, B. Normand, Y. Watanabe, Effect of Chromium Content on the Oxidation Behavior of Ni-Cr Model Alloys in Superheated Steam, *Metall. Mater. Trans. A.* 46 (2015) 2285–2293. doi:10.1007/s11661-015-2786-7.

[4]S. Ghosh, V. Kain, Microstructural changes in AISI 304L stainless steel due to surface machining: Effect on its susceptibility to chloride stress corrosion cracking, *J. Nucl. Mater.* 403 (2010) 62–67. doi:10.1016/j.jnucmat.2010.05.028.

[5]S.J. Lennon, F.P.A. Robinson, G.G. Garrett, The Influence of Applied Stress and Surface Finish on the Pitting Susceptibility of Low Alloy Turbine Disk Steels in Wet Steam, *CORROSION.* 40 (1984) 409–413. doi:10.5006/1.3593946.



## Charge kinetic effect and electrostriction in polyurethane

			G. Diguët <sup>1</sup> , K. Yuse <sup>3</sup> , Y. Tanaka <sup>4</sup> , H. Miyake <sup>4</sup> , T. Takagi <sup>1,2</sup> , J.-Y. Cavaillé <sup>1</sup>
<sup>1</sup> ELyTMax, UMI 3757, CNRS—Université de Lyon—Tohoku University International Joint Unit, Tohoku University, Sendai, Japan <sup>2</sup> Institute of Fluid Science, Tohoku University <sup>3</sup> LGEF, INSA Lyon, Université de Lyon, Villeurbanne, France <sup>4</sup> Measurement and Machine Control Lab, Tokyo City University			

### Abstract :

#### 1. Introduction

Polymers can be used as actuators based on their electromechanical coupling. By applying a metallic coating on top and bottom surfaces, electric field can be set inside soft polymers (elastomers), which induces their deformation. The first mechanisms to be considered is the electrostatic compressive stress due to the applied voltage on the electrodes, known as the Maxwell effect [1], but also the intrinsic deformation of the polymer induced by the electric field. The Maxwell effect yields to a strain  $S_M$  as a quadratic function of the electric field,  $E$ , such as:

$$S_M = M_M E^2, \quad M_M = \epsilon_0 \epsilon_r / Y \quad (1)$$

where  $\epsilon_0$  refers as to the vacuum permittivity,  $\epsilon_r$ , as to the average dielectric constant of the material,  $Y$ , as to its average Young modulus.  $M_M$  is so-called Maxwell electromechanical coefficient. In fact, both experimental strain  $S$  and electrical conductivity appear to be time dependent under constant applied field, as shown in Fig.1. Moreover, results in Fig.1(right) show that the electrical conductivity depends on the thermo-electrical history of the sample.

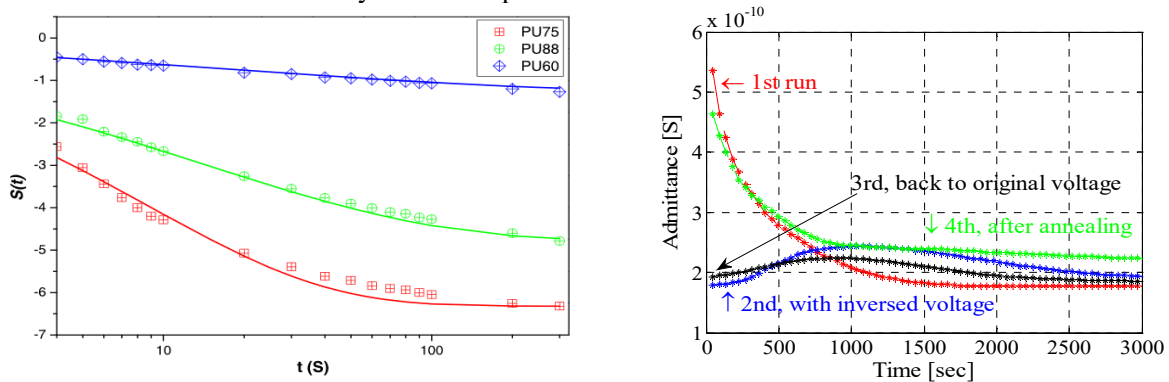


Figure.1: (left) PU electrostriction ( $E=2$  MV/m) versus time (from [2]); (right) PU 88 Admittance evolution versus time for different thermo-electrical histories ( $E=1.2$  MV/m)

## 2. Experimentation, discussion

The intrinsic mechanism, so-called "electrostriction," is often described by an empirical relationship, also linear with  $E^2$  [2]. This effect can be much stronger, i.e. by 1 to 2 orders of magnitude that the Maxwell effect in some polymers like polyurethane (PU):  $M \gg M_M$ , see Fig.1. It is always reported as a compressive effect. Up to now, no physical description of this effect has been proposed in the literature. A new lead has been revealed from cellular polypropylene (PP) film electromechanical properties change, after being submitted to a corona discharge: exposed films exhibit an enhanced electromechanical coefficient  $M$  compared to films without treatments. Moreover, such treatments at different temperatures yield to a larger coefficient with higher temperature. In this process, electrical charges were injected into the polymer during the discharge, and these space density depends on temperature. This proves that internal electrical charges have a direct effect on the electromechanical coefficient. Similar results were obtained by electron beam exposition [3].

In this way, we perform a space charge density measurement [4], under electric field, on PU samples to probe any internal charges under high electric field. The results (Fig.2) show that some charges are accumulating at the interfaces between polymer and electrodes, positives at the anode and negatives at the cathode. More importantly, there is, within the volume, a large accumulation of negative charges near the anode, and a relatively smaller accumulation of positive charges near the cathode.

By integrating the charge density  $\rho$ , inside polymer, the internal charge  $Q$  can be estimated, and by plotting the internal charge versus time ( $Q(t)$ ), it appears that this internal charge reaches a plateau in a time-scale of few hundreds of seconds. This time constant order is actually similar to the electrostriction time constant (as seen in Fig.1).

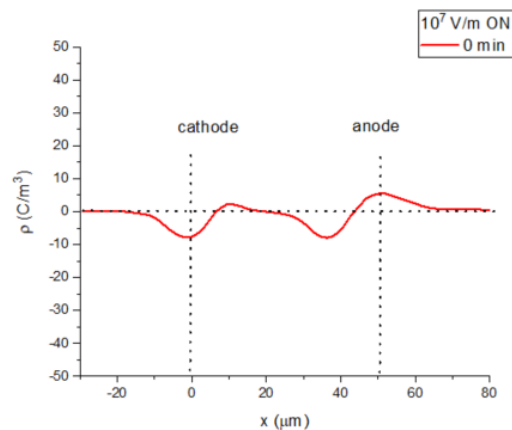


Figure.2: Space charge density of PU

More experiments are required to determine the nature and origin of these electrical charges, as well as their diffusion mechanisms. On the other hand, the relationship between the features of this space charges and the macroscopic electrostriction needs to be elucidate, and the effect of filler as well [5].

### References:

- [1] R. Pelrine and R. Kornbluh in "Dielectric Elastomers as Electromechanical Transducers", ed. by F. Carpi, D. de Rossi, R. Kornbluh, R. Pelrine, P. Sommer-Larsen Elseviers, New York, 2008.
- [2] Jomaa, M. H., Seveyrat, L., Perrin, V, Lebrun, L, Masenelli-Varlot, K; Diguët, G, Cavaille, J.Y., Difference between electrostriction kinetics, and mechanical response of segmented polyurethane-based EAP", by *Smart Mater. Struct.* 26 (2017) 035049
- [3] Masae Kanda, Kaori Yuse, Benoit Guiffard, Laurent Lebrun, Yoshitake Nishi, Daniel Guyomar, "Improvement of Electric Field Induced Compressive Electrostriction of Polyurethane Composites Film Homogeneously Dispersed with Carbon Nanoparticles" *Materials Transactions*, **56**, (2015) 2029-33
- [4] K. Fukunaga, IEEE Electrical Insulation Magazine **15** (1999) 6-18
- [5] K. Wongtimnoi, B. Guiffard, A. Bogner-Van de Moortele, L. Seveyrat, C. Gauthier, J.Y. Cavaille, *Comp Sci Tech* **71** (2011) 885-892



---

*Sunday, March 10<sup>th</sup> – Afternoon*  
*Session 2 – 16:30-18:50*

## Investigation of the effect of surface roughness on human stiffness feeling

	<p><i>Semin KANG, Takeshi OKUYAMA, Mami TANAKA</i></p> <p><i>TOHOKU University 6-6-04, Aramaki, Aoba, Sendai</i></p>		<p><i>Coralie THIEULIN, Hassan ZAHOUANI, Cyril PAILLER-MATTEI,</i></p> <p><i>École Centrale Lyon, University of Lyon, FRANCE</i></p>
---	--	--	--

### Abstract :

#### 1. Introduction

The tactile sensation is perceived by mechanical interaction between the finger and the object. Several factors, such as ways to touch objects[1] and arrangements of sensory receptors[2], are involved to the sensation. However, the mechanism of perception has not been sufficiently elucidated. Furthermore, various mechanical properties of the object influence tactile sensation complexly. For example, it has been reported that texture and touching comfort can be improved by embossing an uneven shape on the surface of the object without changing the material[3]. However, the influence of the embossed shape on the tactile sensation has not been sufficiently elucidated.

In the previous study, the influence of the surface roughness on stiffness feeling is investigated[4]. It was suggested that surface roughness obviously affected the feeling of stiffness in the case of an instruction that subjects evaluated them with feeling the surface roughness. However, the investigation of mechanical properties of samples with difference surface roughness is not enough.

In this study, we focus on the mechanical properties of the sample's surface and human sensory evaluation in order to clarify the effect of surface roughness on human stiffness feeling.

#### 2. Methods

As shown in Table 1, six kinds of samples are prepared by combining two kinds of Young's modulus and three kinds of surface roughness. The surface roughness of sample is created by transferring by the abrasive paper. The abrasive paper ID, #120, #320, #1000, are defined by Japanese Industrial Standards(JIS). Smaller number of the ID indicates rougher surface.

The subject estimates tactile stiffness of the samples using the ranking method that the subjects arrange the samples according to stiffness feeling. Moreover, the mechanical properties on the surface of the samples such as the elastic modulus, the friction coefficient, and the viscoelasticity are measured by using the spherical indentation testing system.

Table 1. Conditions of silicone samples

Sample ID	S1	S2	S3	S4	S5	S6
Young's modulus	329kPa			197kPa		
Surface roughness	#120	#320	#1000	#120	#320	#1000

### 3. Results and discussion

The sensory evaluation scores are shown Figure 1. From the result of the sensory test, it was observed that subjects feel that the rougher surface sample is softer (Pattern 1) and that the rougher surface sample is harder (Pattern 2). And, it was found that the effect of roughness on the stiffness is changed by the sample Young's modulus.

The elastic modulus of the different samples evaluated for different normal loads are shown Figure 2. From the result of the indentation test, it was found that the rougher surface sample is the lower the elastic modulus on surface. This result is consistent with the result of sensory evaluation. In friction test, the effect of the Young's modulus and roughness on friction coefficient is not appeared.

In the comparison between results of sensory test and mechanical tests, it was suggested that subjects in Pattern 1 perceived the difference in the Young's modulus on surface of sample. However, subjects in Pattern 2, it was found that the perception of roughness may affect the perception of hardness. In the future, it is necessary to perform the sensory evaluation for more subjects, and to investigate mechanical properties of finger.

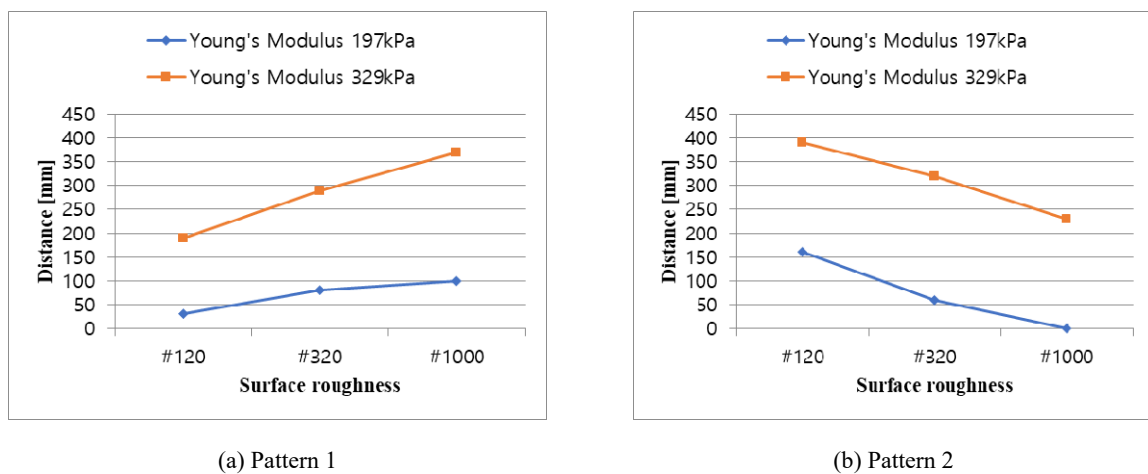


Figure 1. The results of the sensory evaluation

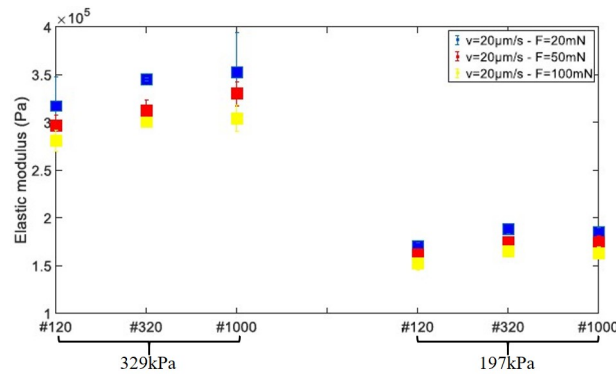


Figure 2. Elastic modulus for the different samples at different normal loads

### References :

- [1] S. J. Ledermann et al., "The hand as a perceptual system. In: K. J. Connolly editor. The psychobiology of the hand", London: Mac Keith Press, pp. 16-35, (1998)
- [2] R. S. Johansson et al., "Tactile sensibility in the human : Relative and absolute densities pf four types of mechanoreceptors in the glabrous skin area", The Journal of Physiology, Vol.286, pp.283-300, (1979)
- [3] S. Watanabe et al., "Recognition and language estimation of fine particles through tactile sensing with fingers(In Japanese)", Journal of the Japan society for precision engineering, Vol.71, No.11, pp.1421-1425, (2005)
- [4] Semin Kang et al., "The effect of surface roughness on human stiffness feeling", International Journal of Applied Electromagnetics and Mechanics, In-press,(2018)

## **Advanced scintillating fibres and Cerenkov fibres for new hadron and jet calorimeters for future colliders**

Project ELYT lab : INTELUM-Materials and structure design



**LEBBOU Kheirreddine**  
Luminescence team,  
Institut Lumière Matière  
(ILM)  
UMR 5306 CNRS- Université  
Claude Bernard Lyon 1.  
Campus Lyon Tech-La Doua  
69622 Villeurbanne, FRANCE  
BELSKEY Andrei  
**BOUITA Rekia**  
BOULON Georges  
DUJARDIN Christophe  
LEDOUX Gilles  
**VEBER Philippe**



**YOSHIKAWA Akira**  
Research Laboratory on  
Advanced Crystal  
Engineering, Institute for  
Materials Research (IMR),  
Tohoku University,  
2-1-1 Katahira, Aoba-ku,  
Sendai, 980-8577, JAPAN  
KAMADA Kei  
KUROSAWA Shunsuke  
YAMAJI Akihiro  
YOKOTA Yuui  
YOSHINO Masao



Presented by:  
**BOULON Georges**  
Luminescence team,  
Institut Lumière Matière  
(ILM)  
UMR 5306 CNRS- Université  
Claude Bernard Lyon 1.  
Campus Lyon Tech-La Doua  
69622 Villeurbanne, FRANCE

**Abstract :** Intelum is a European Marie Skłodowska-Curie Research and Innovation Staff Exchange (RISE 2020) and International and Intersectoral mobility to develop advanced scintillating and Cerenkov fibres for new hadron and jet calorimeters for future colliders in CERN (Geneva, Switzerland).

### **1-Introduction**

Currently, new concepts are being considered for hadron and jet calorimetry in high energy physics experiments, in order to improve the energy resolution of these detectors by a factor of at least two. This is a prerequisite for future studies at the high luminosity, large hadron collider as well as at future electron and proton colliders. Amongst the few concepts being proposed, scintillating and Čerenkov fibres are considered very promising candidates [1].

The INTELUM project coordinated by CERN consists in research and innovation staff exchange. It is an ambitious project funding international, industry-academia exchanges to develop micro-pulling-down crystal growth and other new types of fibre technology. This new fibre production technology has the potential to enable fast, low-cost, manufacture of

heavy crystal scintillating fibres. In order to prove the new fibre technology concept, two key technical issues will be addressed during the project:

- demonstrate feasibility of producing between 20-200km of fibres with consistent quality and well defined production costs;
- demonstrate sufficient radiation hardness of the fibres that the degradation of their optical properties is below 10% at 1 MGy level.

## **2-Cooperation Lyon-Tohoku on crystal growth and characterization of scintillating fibres**

Commun research activities of both the « Luminescence team » at the Institute of Light Matter (ILM) at UCBLyon1, France, and the « Laboratory on Advanced Crystal Engineering » at IMR & NICHe of Tohoku University in Sendai, Japan, are based on engineering process, developments and applications in the field of scintillators and crystal growth. The teams are now two leading groups in both, crystal growth fibres and shaped crystals using micro-pulling down ( $\mu$ -PD) and Czochralski techniques, structural and spectroscopic characterizations as well as mechanism analysis in scintillating crystals.

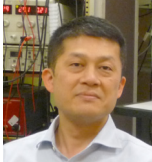
The two teams are cooperating together since many years and have the objective to create novel or improved materials based on  $Y_3Al_5O_{12}$  (YAG) and  $Lu_3Al_5O_{12}$  (LuAG) garnets [2-5] that match the challenging requirement specifications informed by CERN for the scintillating and Cerenkov fibres and identify the most suitable types of fibres in view of their use in high energy. The project will also lead to important impacts in other domains such as functional medical imaging and homeland security.

### References

- [1] S.DERENZO, M.BOSWELL, M. WEBER, K.BRENNAN, SCINTILLATION PROPERTIES, [HTTP://SCINTILLATOR.LBL.GOV/](http://scintillator.lbl.gov/)
- [2] C. DUJARDIN, C. MANCINI, D. AMANS, G. LEDOUX, D. ABLER, E. AUFFRAY, P. LECOQ, D. PERRODIN, A. PETROSYAN, K. L. OVANESYAN, LUAG:CE FIBERS FOR HIGH ENERGY CALORIMETRY, JAP 108, 013510 (2010)
- [3] KEI KAMADA ; TAKAYUKI YANAGIDA ; JAN PEJCHAL ; MARTIN NIKL ; TAKANORI ENDO ; KOUSUKE TSUTUMI ; YUTAKA FUJIMOTO, A.FUKABORI, A. YOSHIKAWA, CRYSTAL GROWTH OF CE-DOPED(LU,Y)3(GA,AL)5O12 SINGLE CRYSTAL BY THE MICRO-PULING-DOWN METHOD AND THEIR SCINTILLATION PROPERTIES, IEEE TRANSACTIONS ON NUCLEAR SCIENCE VOLUME: 59 ISSUE: 5, 2116-2219 (2012)
- [4] X.XU, K.LEBBOU ET AL., CE-DOPED LUAG SINGLE-CRYSTAL, FIBERS GROWN FROM THE MELT FOR HIGH-ENERGY PHYSICS ACTA MATER. 67, 232 (2014),
- [5] C. DUJARDIN, E. AUFFRAY, E. BOURRET, P. DORENBOS, P. LECOQ, M. NIKL, A. N.VASIL'EV, A. YOSHIKAWA, REN-YUAN ZHU, NEEDS, TRENDS AND ADVANCES IN INORGANIC SCINTILLATORS, IEEE TRANSACTIONS ON NUCLEAR SCIENCE 65, n°8, 1977 (2018)

## Transition of Solid-phase Dynamic Alloying Behavior of Powder Particles under Repetitive Tangential Force

Project ELyT lab : COSMIC

	<i>TAKEDA Sho, Frontier Research Institute for Interdisciplinary Sciences, Tohoku University, 6- 3 Aramaki aza Aoba, Aoba-ku, Sendai, 980-8578, Japan</i>		<i>MIKI Hiroyuki Frontier Research Institute for Interdisciplinary Sciences, Tohoku University</i>		<i>FONTAINE Julien Laboratoire de Tribologie et Dynamique des Systèmes, École Centrale de Lyon, 26 avenue Guy de Collongue, 69134 Écully cedex, France</i>
	<i>GUIBERT Matthieu Laboratoire de Tribologie et Dynamique des Systèmes, École Centrale de Lyon</i>		<i>TAKEISHI Hiroyuki Chiba Institute of Technology, 2-17- 1 Tsudanuma, Narashino, 275- 0016, Japan</i>		<i>TAKAGI Toshiyuki Institute of Fluid Science Tohoku University, 2-1-1 Katahira, Aoba-ku, Sendai, 980-8577, Japan</i>

### **Abstract :**

#### **1. Introduction**

To address social demands such as resource and energy saving, developments of new materials and new methods to form materials have been actively attempted. Powder metallurgical techniques have been focusing on as the methods to answer the above demands because these methods can form materials under melting points, and are performed using less energy than other methods such as casting.

Among these methods, we focus on a novel technique, compression shearing method (COSME) [1]. COSME is the molding method in which metal powder is consolidated into a thin plate material by applying biaxial forces in ambient atmosphere and at a relatively lower temperature than sintering temperature, from room temperature to 300°C. This method not only can save energy, but also can form hard-to-sinter material, and can form composites or alloy at a relatively lower temperature than conventional powder metallurgical methods [2]. However, only a few studies have been discussed its forming mechanism of materials by COSME, and there is no report on the forming mechanism of alloy in particular. In the previous study, the bonding process of Cu powder particles by applying biaxial forces had been clarified by the unidirectional friction experiment using a tribometer [3]. Therefore, we considered that the unidirectional friction experiment could be adopted for the clarification of the forming process of the alloy during COSME.

In this study, the unidirectional friction experiment used in the previous study was performed on the uniaxially compressed sample of the mixed powder consists of pure Cu and pure Zn. By observing the microstructural change from inside to top surface of the sample cross-section, the alloying mechanism of the dissimilar materials are investigated.

#### **2. Experimentation, discussion**

The materials used in this study were powders of 99.9% purity Cu and 99.0% purity Zn. The average particle sizes of these powders were 4.8 and 5.2  $\mu\text{m}$ , respectively. A mixed powder with 50 vol.% (44 wt.%) Zn was prepared. The mixed powder was compressed under a uniaxial normal stress of 1000 MPa to get a compressed sample. The target size of a sample was  $20 \times 20 \times 0.25 \text{ mm}^3$ .

Figure 1 shows a schematic illustration of a unidirectional friction experiment. The following four steps are defined as one cycle, and this cycle was repeated. (1) The ball was placed on a sample, and a normal load was applied to the sample through the ball. (2) A tangential force was applied to the ball whilst maintaining the compressive load. The ball was sliding on the sample, and a tangential force was applied to the sample. (3) The ball was pulled off the sample. (4) The ball was moved to the initial

position of the first step. The experimental conditions were set to correspond with the forming conditions of the plate by COSME-RT apparatus (DRD-NNK-002, DIP Co., Ltd., Gunma, Japan) [2]. In order to suppress the oxidation of the sliding surface of the samples, all the tests were performed with 5.0 l/min nitrogen blowing around the contact surface. A  $ZrO_2$  ball of a half-inch diameter was chosen as a counter material. The amplitude and the sliding velocity were programmed to be 5.0 mm and 5.0 mm/min, respectively. The normal load  $P$  was set to be 27 N, which correspond to the theoretical maximum Hertzian contact pressure of 1000 MPa. The friction experiment was carried out in two stages like the actual COSME process of a CuZn plate [2]. Firstly, the friction experiment was conducted five cycles at room temperature. Then, the temperature of the sample was raised to 150°C in 28 minutes, and the other five cycles were carried out. The temperature of the sample was measured by a thermocouple placed on the sample holder.

The cross-section of the samples after the friction experiments was observed by using a scanning electron microscope (SEM) and was analysed by energy dispersive X-ray spectrometry (EDS). Figure 2 shows the SEM image of the sample cross section after the friction experiment. From Fig. 2, it was confirmed that only the powder particles near the sample surface deformed along the sliding direction by applying stress because applied stress by a spherical contact has distributed in a depth direction of a sample. In addition, the sample cross-section consisted of almost two different regions with lower and darker contrasts, and an intermediate contrast layered region had been confirmed only at a part of near the surface. From the EDS analysis, it was suggested that these three regions were  $Cu_5Zn_8$ , Cu, and CuZn, respectively. From this result, it was clarified that the alloying proceeded due to the heating even in the inner region which was not affected by a tangential stress. It appeared that the contaminations and the native oxide films which covered the particles were removed and Cu and Zn powder particles contacted enough for the atomic diffusion even only by uniaxial compressive stress.

On the other hand, most of the alloy regions of the sample were  $Cu_5Zn_8$ , and CuZn was confirmed only at near the sample surface. Furthermore, the surface regions were also mainly  $Cu_5Zn_8$ , and only the region of which thickness is relatively thin became CuZn. In this study, the concentration of Zn is 44 wt.%, and the stable alloy phase of CuZn is  $\alpha + \beta$  which shows good ductility and high tensile strength from the phase diagram. Thus, the existence of  $Cu_5Zn_8$ ,  $\gamma$  phase, which is hard and brittle appeared to indicate that atomic diffusion between Cu and Zn was not sufficient. From these results, it was suggested that Cu and Zn powder particles formed alloy region even only by applying the uniaxial compressive stress and the heating to 150°C, but these were not enough to get a stable alloy phase. To form the stable alloy phase and get a ductile and high strength material, applying shearing stress to the powder particles and forming layered structure thin enough for sufficient atomic diffusion appeared to be necessary.

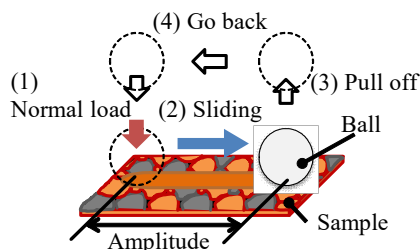


Figure 1 : Schematic illustration of unidirectional friction experiment.

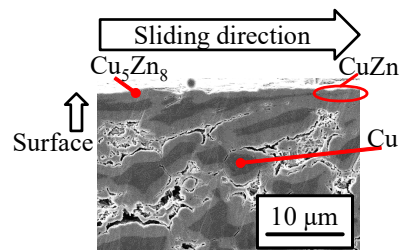


Figure 2 : SEM image of sample cross section after friction experiment

### Acknowledgements :

Extensive studies on the COSME-RT by Prof. N. Nakayama and Dr. M. Horita of Shinshu University are gratefully acknowledged. This work was partly supported by the Amada Foundation in Japan, and JSPS KAKENHI Grant Number 16H04504. Part of the work was carried out under the International Collaborative Research Project of Frontier Research Institute for Interdisciplinary Sciences, Tohoku University.

### References :

- [1] H. Miki, N. Nakayama, H. Takeishi, *Materials Science Forum*, **706-709** (2012) 1955-1960
- [2] K. Nakagoshi, S. Nagai, S. Takeda, H. Miki, T. Takagi, *48<sup>th</sup> Student Graduation Research Presentation of JSME Tohoku Branch*, March 7<sup>th</sup> (2018) 210
- [3] S. Takeda, H. Miki, H. Takeishi, T. Takagi, *Tribology Online*, **13**, **2** (2018) 43-49

## **In-flight behavior of polymeric particle during Cold-spray process**

Project ELyT lab: R6 – Resilient Polymeric cold spray coating

C. A. Bernard<sup>1,2,3</sup>, H. Takana<sup>4</sup>, G. Diguët<sup>3</sup>, K. Ravi<sup>2,3</sup>, O. Lame<sup>5</sup>, K. Ogawa<sup>2,3</sup>, J.-Y. Cavallé<sup>3</sup>



<sup>1</sup>Frontier Research Institute for Interdisciplinary Sciences, Tohoku University, Sendai, Japan

<sup>2</sup>Fracture and Reliability Research Institute, Tohoku University, Sendai, Japan

<sup>3</sup>ELyTMax, UMI 3757, CNRS—Université de Lyon—Tohoku University International Joint Unit, Tohoku University, Sendai, Japan

<sup>4</sup>Institute of Fluid Science, Tohoku University, Sendai, Japan

<sup>5</sup>MATEIS, INSA LYON, Lyon, France

### **Abstract :**

High molecular weight semi-crystalline polymers are difficult to process as coating using cold-spray because of their very long macromolecular chains and their strong viscoelastic behavior. To improve the cold-spray process for polymers, it is necessary to determine the thermal state of the particles as well the velocity of the particles before impact. Thus, a numerical model was developed to evaluate the thermal gradient and the particle velocity before impact during cold-spray process.

### **1. Introduction**

Cold-spray (CS) technology has been developed in the mid 1980's [1] where it was applied to perform metallic coating. Recently, CS was applied to other materials such as polymers and ceramics [2–4] with more or less success. During CS process, powder particles are accelerated through a convergent-divergent de Laval nozzle using a pre-heated gas flow in order to impact a substrate with a high velocity. Under the influence of the gas, the particle temperature increases leading to a thermal gradient along the particle diameter. To validate this assumption, Computational Fluid Dynamics (CFD) and Finite Element Method (FEM) simulations were coupled together to predict both the particle acceleration and the particle thermal map.

### **2. Particle acceleration and thermal gradient**

The in-flight behavior of polymeric particles during CS process was modelled using ANSYS/Fluent. The setup is composed of two convergent-divergent nozzles, 120 mm long each. The standoff distance is 10 mm. A 2D geometry was designed to investigate the evolution of the flow field and the temperature and velocity of a single particle. The flow is assumed to be (i) compressible and (ii) turbulent. Thus, four equations are governing the flow field, namely the continuity equation, Navier Stokes equation, the energy equation and the equation of state.

For an initial gas temperature of 653 K, the influence of the initial gas pressure on the in-flight behavior of a 60  $\mu\text{m}$  diameter polymer particle was investigated and reported in Figure 3. The lowest pressure does not induce any change in the particle velocity because at 0.2 MPa, the gas does not

shock again in the nozzle due to the change of the nozzle section. For higher initial gas pressures, at the intersection between the two nozzles, the flow shocks again leading to an important increase of the particle velocity. Thus, the higher the particle velocity, the lower the particle resident time inside the cold-spray nozzle. This results in an increase in temperature of the particle which is highly dependent of the nozzle geometry and cold-spray initial conditions (initial gas temperature and gas pressure). Such temperature evolution let us assume the existence of an important thermal gradient in the particle thickness.

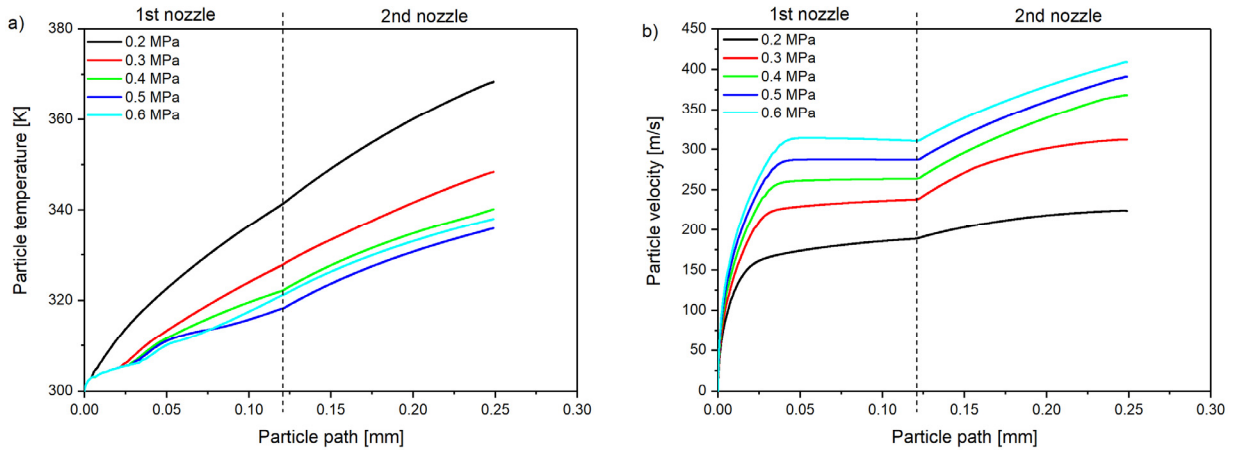


Figure 3: Evolution of the particle temperature and particle velocity in function of the initial gas pressure.

Using COMSOL Multiphysics, evolution of the particle temperature over time was investigated for an initial gas conditions of 653 K and 0.4 MPa. Accounting for the pressure and velocity evolution of the gas, its temperature is plotted in Figure 2a, until 1 ms, corresponding to the resident time of the particle inside the nozzle. The particle temperature is plotted in Figure 2b. For a 60  $\mu\text{m}$  diameter particle, a temperature gradient of about 15 K is observed for the particle with an increase of the temperature surface around 25 K for a particle initial temperature of 300 K.

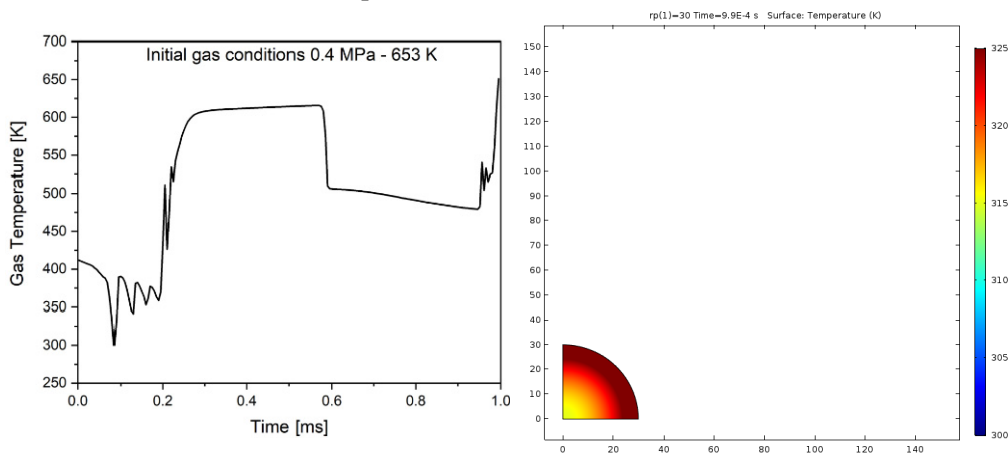


Figure 4: a) Evolution of the gas temperature and b) Thermal gradient in a 60  $\mu\text{m}$  diameter particle submitted to cold-spray experiment at 0.4 MPa and 653 K.

For polymeric particles, such temperature gradient and temperature increase should be taken into account if we wish to improve the cold-spray process for these materials.

#### References :

- [1] A.P. Alkhimov et al., Gas-dynamic spraying method for applying a coating, US Pat. (1994).
- [2] K. Ravi et al., J. Therm. Spray Technol. 24 (2015) 1015–1025.
- [3] Ravi et al., J. Therm. Spray Technol. 25 (2016) 160–169.
- [4] Ravi et al., Addit. Manuf. 21 (2018) 191–200.



---

*Monday, March 11<sup>th</sup> – Morning*  
*Session 3 – 8:40-10:20*

## **New electron microscopy techniques for ceramic materials characterization**

	<p>L. JOLY-POTTUZ<sup>1</sup>, I. ISSA<sup>1</sup>, A. KRAWCZYNSKA<sup>2</sup>, T. PLOCINSKI<sup>2</sup>, D. STAUFFER<sup>3</sup>, S. LE FLOCH<sup>4</sup>, D. MACHON<sup>4</sup>, V. GARNIER<sup>1</sup>, J. AMODEO<sup>1</sup>, T. EPICIER<sup>1</sup>, K. MASENELLI-VARLOT<sup>1</sup></p> <p>1 : MATEIS – INSA de Lyon, Campus Lyon Tech La Doua, Bât B. Pascal - 7 avenue Jean Capelle, 69621 Villeurbanne, France 2: Warsaw University of Technology, Faculty of Materials Science and Engineering, Woloska 141, 02-597 Warsaw, Poland 3: Bruker / Hysitron Inc, 9625 W 76th St., Minneapolis, MN 55344, USA 4 : Université de Lyon, UCB Lyon 1 ILM CNRS UMR5306, 69622 Villeurbanne, France</p>
---	--

### Abstract :

#### **1. Introduction**

The behavior of ceramics at the nanometer scale strongly differs from the one of the corresponding bulk material. For instance, strong plastic deformation has been reported in isolated nanometer-sized alumina nanoparticles or MgO nanocubes, when tested *in situ* in a transmission electron microscope (TEM). This plastic behavior may also occur in a powder during the compaction process, even at room temperature. Controlling plastic deformation of nanoparticles during the ceramics processing might be a way to enhance their properties or to improve the processing route (compaction and sintering steps, for instance). We develop new techniques to study the deformation mechanism of individual nanoparticles in vacuum or under environment. *In situ* TEM nanocompression of thin foils obtained from compacted powders may give interesting information of the compaction process of ceramic materials or on the deformation mechanism of bulk ceramic materials.

#### **2. Experimentation, discussion**

*In situ* TEM nanocompression tests of isolated nanoparticles were performed using a dedicated TEM (Transmission Electron Microscopy) holders equipped with force and displacement sensors [1, 2]. These tests are of great interest since it is possible to measure the mechanical properties of nanometer-sized objects and observe their structural evolution. Load–real displacements curves, obtained by Digital Image Correlation, are analyzed and these analyses were correlated with Molecular Dynamics simulations. A constitutive law with the mechanical parameters (Young modulus, Yield stress...) of the studied material at the nano-scale could be obtained [2]. *In situ* TEM nanocompression tests were performed on ceramic MgO nanocube, showing large plastic deformation (more than 50% of plastic strain without any fracture) [3]. Molecular Dynamics simulations were used to better understand the contrasts observed in the images and to define the deformation mechanisms. *In situ* TEM nanocompression is now being developed under gaseous environment by adapting the dedicated TEM holder on an Environmental Transmission Electron Microscope (ETEM). It is thus possible to compare the mechanical properties of ceramics under different environments – and not only under vacuum - and it may be useful to monitor the effects of surfaces on the mechanical properties of ceramic nanoparticles.

To go further on the compaction and sintering processes, tests on ceramic thin foils are under study. Transition alumina nanoparticles have been compacted at room temperature under different uniaxial pressures (5 GPa, 15 GPa and 20 GPa) in a diamond anvil cell or in a Paris-Edimbourg press. Thin foils of these compacted powders can be prepared by Focused Ion Beam machining (FIB) and analysed by TEM, even if the compacted powder has not been sintered. The geometry of the thin foils prepared by FIB is optimized so that these thin foils can be studied with the nanocompression TEM sample holder.

High Resolution TEM (HRTEM) observations of the thin foils after machining and diffraction patterns analyses unambiguously reveal that nanoparticles underwent plastic deformation in the compacted powder, even at room temperature [4]. A study of these HRTEM images coupled with Fast Fourier Transforms to get the associated diffraction patterns show that the deformation involves the  $\{110\}$  lattice planes, and the  $\{111\} \langle 110 \rangle$  slip system. These observations are in agreement with the deformation observed on a single nanoparticle during an *in situ* nanocompression test inside a TEM. Moreover at high pressure, phase transformation can be evidenced. In situ TEM nanocompression tests of these thin foils may give new information on the deformation mechanisms of ceramics: plastic deformation, particles movement or fracture. First results will be presented and discussed.

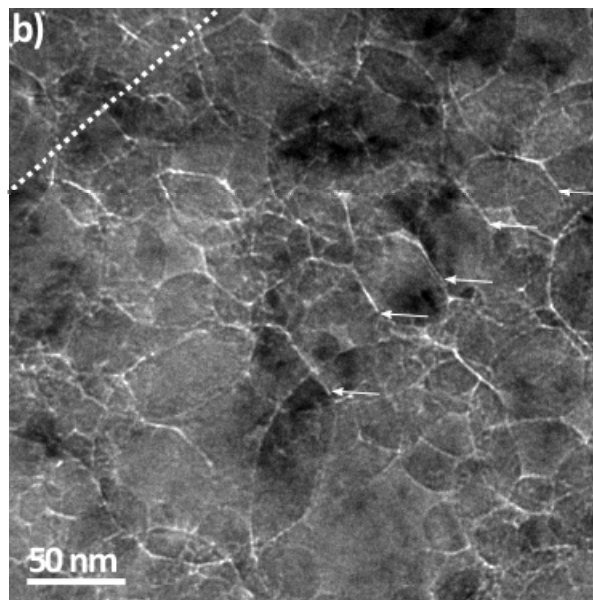


Figure 1: TEM image of alumina powder compacted at 20 GPa. A strong faceting of the nanoparticles is observed (see arrows). The long dashed line representing the normal to the solicitation direction is also shown

## References :

- [1] Q. Yu, M. Legros, A.M. Minor, MRS Bulletin 40, 62-70 (2015).
- [2] E. Calvié, L. Joly-Pottuz, C. Esnouf, P. Clément, V. Garnier, J. Chevalier, Y. Jorand, A. Malchère, T. Epicier, K. Masenelli-Varlot, J. Eur. Ceram. Soc. 32 2067-2071 (2012).
- [3] I. Issa, J. Amodéo, J. Réthoré, L. Joly-Pottuz, C. Esnouf, J. Morthomas, M. Perez, J. Chevalier, K. Masenelli-Varlot, Acta Materialia 86, 295-304 (2015).
- [4] Issa I., Joly-Pottuz L., Réthoré J., Esnouf C., Douillard T., Garnier V., Chevalier J., Le Floch S., Machon D., Masenelli-Varlot K., Acta Materialia, 150, 308-316 (2018)

## **Quantitative measurement of interfacial heat and mass transfer using high-speed phase-shifting interferometer**

	<i>Yuki Kanda</i> <sup>1</sup>		<i>Junnosuke Okajima</i> <sup>2</sup>		<i>Atsuki Komiya</i> <sup>2</sup>
<i>1. Graduate School of Engineering, Tohoku University, Sendai, Miyagi 980-8579, Japan</i> <i>2. Institute of Fluid Science, Tohoku University, Sendai, Miyagi 980-8577, Japan</i>					

### Abstract :

#### **1. Introduction**

The quantitative measurement of heat and mass transfer near a phase interface is important to understand the boundary conditions and energy balance during phase transitions, such as droplet evaporation or crystallization. For the evaluation of temperature or concentration near the interface, non-contact measurement method is useful comparing the contact method, such as a thermocouple because that disturbs the interfacial transfer due to physical contact.

The Mach-Zehnder interferometer is one of the commonly useful methods for the visualization of the heat and mass transfer. Our research team applied the phase-shifting technique with a rotating polarizer to the interferometer to improve the phase and spatial resolutions of that and succeeded to measure diffusion phenomena [1]. However, this method can only be applied to static or “slow” processes. For the “fast” transfer process, high-speed phase-shifting interferometer with an Arbaa prism was developed by our team and transient heat transfer in the liquid [2] and gas [3] phases were quantitatively measured.

In this study, we applied to this high-speed phase-shifting interferometer for the transient heat and mass transfer during methane hydrate (MH) decomposition. MH is composed of methane gas and water, and expected as a new energy resource. This hydrate is decomposed to the gas and water with endothermic reaction, however the mechanism and rate determining step have not been cleared. In our study, the heat and mass transfer near the hydrate decomposition interface was evaluated by the high-speed phase-shifting interferometer and the rate determining step was discussed.

#### **2. Experimental systems**

For the MH decomposition, a reaction cell shown in Fig. 1(a) was used. The temperature and pressure of the cell were controlled by four Peltier modules and a syringe pump. A cover glass with a hydrophilic surface treated with water vapor plasma was installed as shown in Fig. 1(b) and put 20  $\mu\text{L}$  of water for the hydrate formation. The decomposition was conducted by reducing the gas phase pressure to below the phase equilibrium point.

In the high-speed phase-shifting interferometer, a high-speed camera was installed and a He-Ne laser was used as a light source. The details of the optical components and phase-shifting algorithm can be found in our previous reports on interferometer designs [1]–[3]. In order to observe

immediately after the decomposition, the shutter of the camera was synchronized with the pressure change. The frame rate was 3000 fps and the shutter speed were set as 1/40000 s.

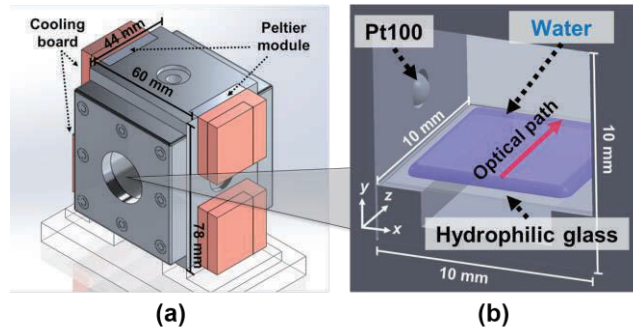


Figure 1 Schematic of (a) reaction cell and (b) interior of the cell.

### 3. Results and Discussion

The phase shifted data in the vicinity of the hydrate interface measured by the interferometer is shown in Fig. 2(a). The time shown in Fig. 2(a) is set to 0.000 s immediately before the depressurization. In this measurement, the hydrate decomposed and the interface moved when the gas phase pressure decreased from 4.3 MPa to 3.7 MPa. From the phase shifted data, immediately after depressurization, interference fringes change was observed near the interface, which is caused by the density difference of gas phase between the vicinity of the interface and the position away from the interface. Therefore, from the measurement result, the density change due to the transient heat and mass transfer was generated near the interface during depressurization.

Comparison of the density change near the interface obtained by the measurement with the numerical simulation is shown in Fig. 2(b). In the numerical simulation, the heat and mass flux were determined with activation energy of decomposition as a variable. Additionally, the adiabatic expansion effect was also considered according to the experimental conditions. As a result of the comparison, the experimental results showed a tendency close to the result when the activation energy was under 56000 J/mol. It means that the hydrate decomposition in this study was estimated as reaction rate determination rather than diffusion rate determination.

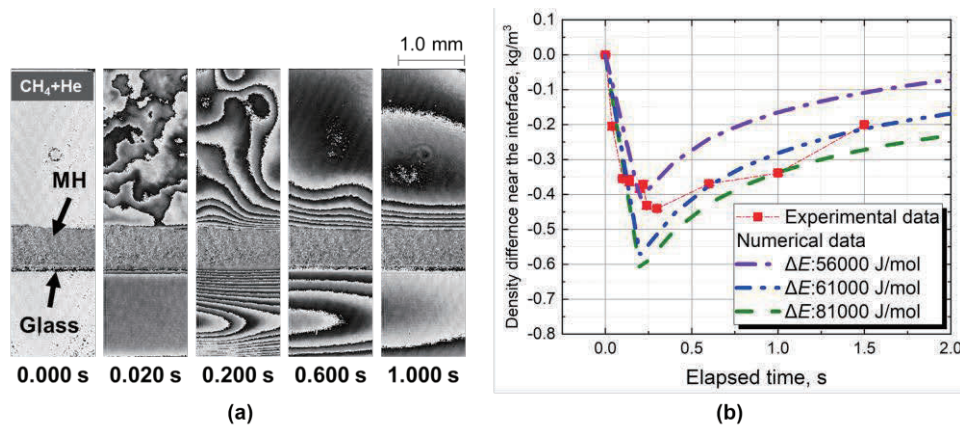


Figure 2 Schematic of (a) sequential phase-shifted data after depressurization and (b) density difference variation near the hydrate interface comparing with numerical simulation.

### References :

- [1] J.F. Torres, A. Komiya, E. Shoji, J. Okajima, S. Maruyama, Optics and Lasers in Engineering 50 (9) (2012) 1287–1296.
- [2] E. Shoji, A. Komiya, J. Okajima, H. Kawamura, S. Maruyama, Applied Optics 54 (20) (2015) 6297–6304.
- [3] Y. Kanda, E. Shoji, L. Chen, J. Okajima, A. Komiya, S. Maruyama, International Communications in Heat and Mass Transfer 89 (2017) 57–63.

## **Tribological characterization of natural bones and bone substitutes for simulating bone drilling in dry conditions.**

Project ElyT lab B6 / T:  
Development and Friction Characterization of Biomodels of Bones, BoneDrill

	Yuta MURAMOTO Graduate School of Biomedical Engineering, Tohoku University /LTDS,		Vincent FRIDRICI LTDS, Ecole Centrale de Lyon		Philippe KAPSA, LTDS, Ecole Centrale de Lyon
	Gaëtan BOUVARD, LTDS, Ecole Centrale de Lyon		Makoto OHTA ELYTMaX UMI 3757, CNRS - Université de Lyon - Tohoku University, International Joint Unit, Tohoku University		

### Abstract :

#### **1. Introduction**

Entering the super-aged society, Japan has recorded an intense increase in number of orthopedic surgeries in the last decade. For example, the number of total joint replacement of hip, knee, and shoulder operated from April 2017 to March 2018 reached 220,000, which is 28.3% larger than that of the previous year period [1]. The number of operation is estimated to continue to increase in the future.

In orthopedics and dentistry, drilling is one of fundamental surgical steps. Bone biomodel plays an important role in doctors' training or for the evaluation of medical devices such as bone screw or pin. The use of bone biomodel is preferable to natural bone, having advantages such as reproducibility and ease of handling. However, current bone biomodels can provide clinically relevant data only in limited testing methods [2]. Although a number of information is available about the mechanical properties of natural bones or bone biomodels, drilling properties of bone substitute materials have not keenly been studied yet. The purpose of this study is to extend our knowledge by performing drilling tests on bone substitutes and to compare the drilling behavior with that of natural bone specimens. Experiments were performed on previously fabricated acrylic-based composite materials for development of a new bone biomodel [3]. Providing the information of drilling behavior of natural bones and current bone substitutes is to help comparative study of the emerging performant bone biomodels.

#### **2. Materials and methods**

##### **2. 1. Sample preparation**

Porcine and canine mandible bone were provided by Prof. Viguier, a veterinary at VetAgro Sup, University of Lyon. Bone samples were taken out, cleaned, sunk in ethanol for a day, and then dehydrated at room temperature. Bone specimens were partially embedded in epoxy resin for steady fixation. 4 kinds of current bone biomodels were obtained in this study. 3 were made of polyurethane with different values of density from 20, 40, and 50 pcf (0.32, 0.64, and 0.80 g/cm<sup>3</sup>) (called PU20, PU40, and PU50 respectively) (Solid Rigid Polyurethane Foam, Pacific Research Laboratories, Inc., Vashon, WA, USA), while the rest was of epoxy resin with glass fiber reinforced (called EP-S) (Short Fiber Filled Epoxy Sheet, Pacific Research Laboratories, Inc., Vashon, WA, USA). Every sample of bone biomodels was cut into a cube 20 mm on a side for drilling tests.

## 2. 2. Drilling tests

Drilling tests were performed on a device developed by LTDS, based on a spindle Electrobroche SD 5084, Precise. The device included a system for application of thrust force, a strain gauge for measurement of friction torque, and a displacement sensor. Constant thrust force was applied by a deadweight. Work piece was fixed on the working table using double-faced adhesive tape. A twist drill (Twist drill, Nobel Biocare Japan Co., Ltd) of a diameter of 2.0 mm was used. Drilling torque and drilling displacement were recorded with a sampling rate of 200 Hz. Machining conditions were 1,000 rpm of spindle speed, 20 N of thrust force, and 5 mm of maximum displacement. Measurements were performed for 3 times, at room temperature without any addition of liquid.

## 3. Results and discussion

Figure 1 shows a representative curve of torque and displacement as a function of time for PU50. Torque was smoothed by moving average filter. Torque gradually increases along the penetration of drill-bit. Maximum value of torque was obtained slightly before reaching maximum displacement. Drilling time was defined as the time required for the drill-bit to progress until 5 mm. Figure 2 shows maximum values of torque and drilling time, averaged from 3 measurements for specimens. Polyurethane-based bone biomodels were drilled relatively shorter than epoxy-based model and natural bone specimens. EP-S and bone specimens show roughly equivalent relationship of drilling properties. It implies that specific mechanical and tribological properties of EP-S related to drilling behavior might correspond to those of natural bone specimens.

Microindentation tests were performed for elucidation of the difference of drilling properties among test specimens. The results, averaged from 10 indents, show that Porcine bone, canine bone, EP-S, and PU50 have hardness of respectively 0.639, 0.510, 0.446, and 0.121 GPa, and elastic modulus of respectively 18.5, 15.8, 11.4, and 2.05 GPa. It is likely that drilling in PU50 takes relatively shorter time than drilling in natural bones and EP-S probably due to the gap of hardness and elastic modulus. For further elucidation, classification of fracture behavior by observing cutting chips generated during drilling can be helpful.

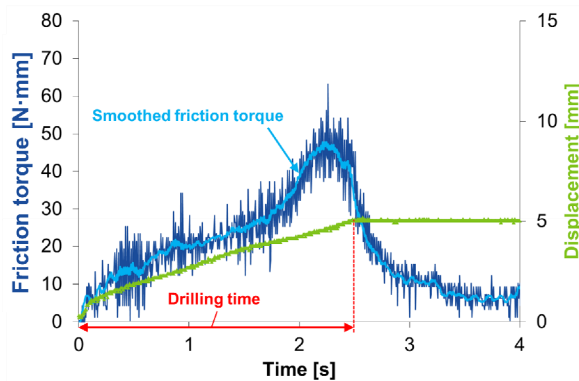


Figure 1: Representative drilling profile for PU50

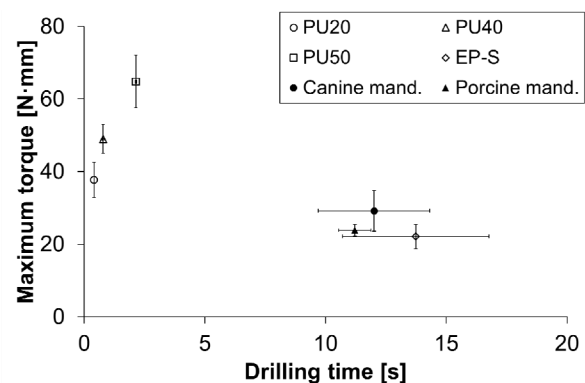


Figure 2: Relationship between maximum torque and drilling time for all the specimens

## Acknowledgement

The authors wish to thank Prof. Viguier from VetAgro Sup, University of Lyon, for kindly offering bone specimens. This work was financially supported by the JSPS Core-to-Core Program, the ImpACT Program, the Program for Leading Graduate Schools, IFS collaborative research project, the LABEX MANUTECH-SISE (ANR-10-LABX-0075) of University of Lyon, within the Program "Investissements d'Avenir" (ANR-11-IDEX-0007) operated by the French National Research Agency. LIA ELYT Global is also acknowledged.

## References :

- [1] The Japanese Society of Arthroplasty Replacement, "2017 Annual Report", 2017.
- [2] J.-T. Hausmann, *Osteo and Trauma Care*, **14**(2006) 259-264
- [3] Y. Muramoto *et al.*, ELYT Workshop 2018, La Gentilhommière, Satillieu, France

## Polymer-Metal-Fiber Adhesion Delamination Control (POMADE) by EB-Irradiation

Project ELyT lab : POMARD & COSMIC – study of Polymer-Metal-Fiber Adhesions

	<b>Yoshitake Nishi</b> , Engi-Ph.D. (TU), Prof. Emeritus [Tokai U], Director [MIF], Project Researcher (KISTEC), Hiratsuka, JAPAN. <a href="mailto:west@tsc.u-tokai.ac.jp">west@tsc.u-tokai.ac.jp</a>		<b>Helmut Takahiro Uchida</b> , Ph.D. [Göttingen U], Senior Assistant Prof. [Tokai U., Dep. Precision Engi.], Hiratsuka, JAPAN. <a href="mailto:helmutuchida@tokai.ac.jp">helmutuchida@tokai.ac.jp</a>
	<b>Masae Kanda</b> , Ph.D. (INSA Lyon), Senior Assistant Prof. [Chubu U. DAA], Nagoya, JAPAN, <a href="mailto:kanda@isc.chubu.ac.jp">kanda@isc.chubu.ac.jp</a>		<b>Michael C. Faudree</b> , Ph.D. [Tokai U.] Associate Prof. [Tokyo City Univ.], Yokohama, JAPAN <a href="mailto:faudree@tcu.ac.jp">faudree@tcu.ac.jp</a>
	<b>Kaori Yuse</b> , Ph.D. Associate Prof. [INSA Lyon, LGEF], France. <a href="mailto:kaori.yuse@insa-lyon.fr">kaori.yuse@insa-lyon.fr</a>		<b>Daniel Guyomar</b> , Ph.D. Prof. [INSA Lyon], LGEF, France. <a href="mailto:daniel.guyomar@insa-lyon.fr">daniel.guyomar@insa-lyon.fr</a>
	<b>Michelle Salvia</b> , Ph.D. Associate Prof. [LTDS, Ecole Centrale de Lyon], Ecully, FRANCE, <a href="mailto:michelle.salvia@ec-lyon.fr">michelle.salvia@ec-lyon.fr</a>		<b>Jean-Yves Cavaille</b> , Ph.D. Prof. [ELyT MaX, UdL, TU, CNRS, INSA Lyon, MATEIS], FRANCE, <a href="mailto:jean-yves.cavaille@insa-lyon.fr">jean-yves.cavaille@insa-lyon.fr</a>

**Abstract:** Our international activities of Research & Education in Japan-France collaboration have started since 1998. First of all, as the 1<sup>st</sup> project, mechanical properties of CFRPs (Carbon Fiber Reinforced Polymers), especially the one of thermo-set epoxy and of thermo-plastic polymers, have been investigated in the collaboration work between Tokai Uni. and LTDS, ECL, in order to highlight the influence of carbon fiber EBI treatment on strength with a focus on fiber/matrix interface [1-8]. As the 2<sup>nd</sup> project, electrostriction of electric conductive polymer composites has been investigated in order to use as sensors and actuators and the expansion usage as hydrogen storage was proposed. This is the collaboration work between Tokai and LGEF, INSA Lyon [9-22]. Recently, as the 3<sup>rd</sup> project, collaboration work between Tokai and MATEIS, INSA Lyon, the adhesion and strengthening of polymers induced by EBI process have been investigated [23-26].

A new method to fabricate linear connected joints of Ti (titanium) to Epoxy polymer connected by CF-plug designated here as [Ti/CFW-CFRP] was innovated to enhance safety level of airplanes, since fine carbon fibers (CFs, 6-7/1000 mm) generate extremely large friction force by their broad interface between Ti and Epoxy [Ti/Epoxy] giving strong adhesive force with high density chemical adhesion point contact. Furthermore, thermoplastic polymers (TP) with both short term of production process dominated by solidification and low materials cost have been required, although [Ti/CFW-CFRTP] joints have low strength due to easy CF pull-out from TP and delamination damage by fewer point contacts. Therefore, we first quantified the strength reduction in [Ti/CFW-CFRTP] joints (TP = ABS, PC, and PP) from that of epoxy [Ti/CFW-CFRP: Epoxy]. Based on the experimental results of ( $\frac{12[\text{Ti/Epoxy}] + [\text{Ti/CFW-CFRP}]}{13}$ ; 25 MPa), ( $\frac{12[\text{Ti/PC}] + [\text{Ti/CFW-EBCFRPC}]}{13}$ ; 21 MPa), ( $\frac{12[\text{Ti/ABS}] + [\text{Ti/CFW-EBCFRABS}]}{13}$ ; 18.5 MPa) and ( $\frac{12[\text{Ti/PP}] + [\text{Ti/CFW-EBCFRPP}]}{13}$ ; 8.0 MPa), as well as ( $\frac{12[\text{Ti/ABS}] + [\text{Ti/CFW-CFRABS}]}{13}$ ; 8.5 MPa), ( $\frac{12[\text{Ti/PC}] + [\text{Ti/CFW-CFRPC}]}{13}$ ; 7.0 MPa) and ( $\frac{12[\text{Ti/PP}] + [\text{Ti/CFW-CFRPP}]}{13}$ ; 3.5 MPa), the tensile strength  $\sigma_b$  of [Ti/CFW-CFRTP: ABS; 55 MPa], [Ti/CFW-CFRTP: PC; 30 MPa] and [Ti/CFW-CFRTP: PP; 9.5 MPa] joints were found to be far below, ~20, 14 and 3% that of Epoxy matrix CFRP [Ti/CFW-CFRP: Epoxy; 283 MPa][1,27,28]. As expected, Epoxy has higher resistance to CF pullout by its superior chemical adhesion point contact by its oxygen groups at CF/Epoxy interface. Therefore, to help remedy the typically weak TP/CF adhesion, we employed the novel process of Polymer-Metal-Fiber

Adhesion Delamination control (POMADE) by low voltage EB-irradiation. After the CF half-length of the joint was already welded to and wrapped by Ti, the bare CF half-length was treated by optimal dose of EB prior to dipping in their respective TP molten resins (ABS, PC, and PP), enhancing the  $\sigma_b$  of [Ti/CFW-EBCFRTP] samples over that without EB, [Ti/CFW-CFRTP]. Although the TP joints were not improved over that of the Epoxy, the  $\sigma_b$  of [Ti/CFW-EBCFRABS; 140 MPa], [Ti/CFW-EBCFRPC; 195 MPa], and [Ti/CFW-EBCFRPP; 68 MPa] were improved, respectively, at 50, ~60 and 25% that of Epoxy matrix CFRP [Ti/CFW-CFRP; 283 MPa] compared to the untreated at ~20, 14 and 3%  $\sigma_b$  of the Epoxy [1,27,28]. Improvements are attributed to the action of the EB increasing the nucleation frequency of hard segments (crystalline) of TPs at nucleation surface sites of the CFs. For [Metal/Polymer] joints, we provide a hierarchy of tensile strength of the above data included with a summary of our team's research:

CF/Epoxy (Full contact more than 5 mm CF wrapped by Epoxy glue) > CF [29] > Ti [30]  
 > [Ti/NiCFW-CFRP; 413 MPa] = [Ti/NiCFW; 413 MPa] (5 mm Ni coated CF dipped in Ti)  
 > [Ti/CFW-CFRP; 283 MPa] = [CFW/Ti; 283 MPa with 5 mm CF covered dipped in Ti]  
 > [Ti/CFW-EBCFRPC; 195 MPa] = [EBCFRPC; 195 MPa with 5 mm active CF dipped in PC]  
 > [Ti/CFW-EBCFRABS; 140 MPa] = [EBCFRABS; 140 MPa with 5 mm active CF dipped in ABS]  
 > ([Ti/CFW-EBCFRPP]; 68 MPa) = [EBCFRPP; 68 MPa with 5 mm active CF dipped in PP]  
 > [Ti/CFW-CFRABS; 55 MPa] = [CFRABS; 55 MPa; 55 MPa with 5 mm CF dipped in ABS]  
 > PC (60MPa) [31] > Epoxy (50 MPa) [32]  
 > [Ti/CFW-CFRPC; 30 MPa] = [CFRPC; 30 MPa with 5 mm CF dipped in PC]  
 > [Ti/CFW-CFRPP; 9.5 MPa] = [CFRPP; 9.5 MPa with 5 mm CF dipped into PP]  
 > [Ti/ABS; 4 MP] [27] > [Ti/Epoxy; 3.5 MPa] [28] > [Ti/PP; 3 MPa] [28] > [Ti/PC; 1 MPa] [1]

Finally, authors would like to thank Mr. A. Mizutani, H. Hasegawa, R. Nomura, S. Ishii, A. Takahasi, D. Kitahara, N. Tsuyuki and Y. Miyamoto, as well as Profs. A. Tonegawa, H. Kimura, N. Inoue and Y. Matsumura for their useful help.

## References:

- [1] H.H., M. C. Faudree, Y.E., S.T., H.K., A.T., Y.M., I.J., M. Salvia, Y. Nishi, Mater. Trans. 58-11 (2017) 1606-1615.
- [2] Y. Nishi, R. Ourahmoune, M. Kanda, J.H. Quan, M.C. Faudree, M. Salvia, Mater. Trans. 55-8 (2014) 1304-1310.
- [3] H. Takei, M. Salvia, A. Vautrin, A. Tonegawa, Y. Nishi, "EBI-elasticity-CFRP-PEEK," Mater. Trans. 52-4(2011) 734-739.
- [4] Y. Nishi, H. Takei, K. Iwata, M. Salvia, A. Vautrin, "EBI-impact-CFRTP-Phenol", Mater. Trans. 51-12(2010) 2259-2265.
- [5] Y. Nishi, H. Takei, K. Iwata, M. Salvia, A. Vautrin, "EBI-impact-CFRPEEK", Mater. Trans. 50-12 (2009) 2826-2832.
- [6] Y. Nishi, H. Kobayashi and M. Salvia, "EBI-Impact-GFRP", Materials Trans. 48-7 (2007) 1924-1927.
- [7] Y. Nishi, K. Inoue and M. Salvia, "Impact strengthening of CFRP by EBI," Mater. Trans. 47-11 (2006) 2846-2851.
- [8] H. Kobayashi, M. Salvia and Y. Nishi, "Effects of EBI on impact value of CFRP," J. Japan Inst. Met, 70-3 (2006) 255-257.
- [9] N.T.A.T.S.T.D.K., M. Kanda, N.I., K. Yuse, D. Guyomar, A.T., Y.M., Y. Nishi, Mater. Trans. 59-3 (2018) 450-455.
- [10] Y. Nishi, J. O., M. C. Faudree, M. Kanda, K. Yuse, D. Guyomar, H-H. Uchida, Mater. Trans. 59-1 (2018) 129-135.
- [11] M. Kanda, K. Yuse, B. Guiffard, L. Lebrun, Y. Nishi, D. Guyomar, Mater. Trans. 56-12 (2015) 2029-2033.
- [12] M. Lallart, J.-F. Capsal, A. K. Mossi Idrissa, J. Galineau, M. Kanda, D. Guyomar, J. Appl. Phys, 112 (2012) 094108.
- [13] M. Kanda, K. Yuse, B. Guiffard, L. Lebrun, Y. Nishi, D. Guyomar, Mater. Trans. 53 (2012) 1806-1809.
- [14] M.L., J.F.C., M. Kanda, J.G., D. Guyomar, K. Yuse, B. Guiffard, Sensors & Actu. B: Chemical, 171-172(2012)739-746.
- [15] D. Guyomar, P.-J. C., L. L., C.P., K. Yuse, M. Kanda, Y. Nishi, Polym. Adv. Technol, (2011) DOI 10.1002/ pat. 1993.
- [16] D. Guyomar, K. Yuse and M. Kanda, Sensors and Actuators A, 168 (2011) 307-312.
- [17] K. Yuse, D. Guyomar, M. Kanda, L. Seveyrat and B. Guiffard, Sensors and Actuators A, 165 (2011) 147-154.
- [18] D. Guyomar, K. Yuse, P.-J. Cottinet, M. Kanda and L. Lebrun, J. Applied Physics, 108 (2010) 114910.
- [19] J. Okawa, M. Kanda, K. Yuse, H-H. Uchida, D. Guyomar and Y. Nishi, Mater. Trans., 51 (2010) 994-1001.
- [20] Y. Nishi, Y. E., N.K., M. Kanda, K.I., K. Yuse, B. Guiffard, L. Lebrun, D. Guyomar, Mater. Trans. 51 (2010) 1437-1442.
- [21] Y. Nishi, N. Kunikyo, M. Kanda, L. Lebrun and D. Guyomar, Mater. Trans., 51 (2010) 165-170.
- [22] Y. Nishi, S.O., M. Kanda, AS., RS., YE., DK., H.H. Uchida, K. Yuse, D. Guyomar, Mater. Trans. 50 (2009) 2460-2465.
- [23] ST., H.T. Uchida, AY., M. Kanda, OL., J.Y. Cavaille, YM., Y. Nishi, PE/PET-EB-Glue, Mater. Trans. 58-7(2017)1055-1062.
- [24] C. Kubo, M. Kanda, O. Lame, J.-Y. Cavaille, Y. Nishi, "HLEBI-adhesion-PE/18-8," Mater. Trans., 57-3 (2016) 373-378.
- [25] M. Kanda, T. D., O. L., Y. Nishi, J.-Y. Cavaille, "EBI-Strengthening UHMWPE", Mater. Trans., 56-9 (2015) 1505-1508.
- [26] Y. Nishi, M. Kanda, K.S., S.I., M.U., S.I., M.C. Faudree, O.L., J.-Y. Cavaille, "EBI-TMMW-PE", unpublished data.
- [27] H. H., M.C. Faudree, Y.M., I. J., Y. Nishi: Ti/CFRABS joint strength by EBI-CF: Mater. Trans. 57-7 (2016) 1202-1208.
- [28] Y. Nishi, H.T. Uchida, M.C. Faudree, S. K., H. K., CF-plug Ti/TPs joints; Proc. ICKEM2019, March, 29<sup>th</sup>-April 1<sup>st</sup>, in press.
- [29] Y. Nishi, A. Mizutani, A.K., T. T., K. Oguri, A. Tonegawa, EBI-strengthened CF, J. Mater. Sci. 38 (2003) 89-92.
- [30] ASM Inter. Handbook Committee, (1990), "Properties and Selection: Nonferrous Alloys and Special-Purpose Materials, Vol. 2", ISBN: 9780871703781.
- [31] T. Takahashi, T. Morishita, Y. Nishi, "Strength of EBI PC", J. Japan Institute of Metals, 69-8 (2005) 759-762.
- [32] A. Mizutani and Y. Nishi, "Improved Strength in CFRP by EBI", Materials Transactions. 44-9, (2003) 1857-1860.

## Magneto Rheological Elastomers and energy harvesting



Gildas Diguët<sup>1</sup>, Gaël Sebald<sup>1</sup>, Masami Nakano<sup>1,2</sup>, Mickael Lallart<sup>3</sup>, Jean-Yves Cavaillé<sup>1</sup>  
<sup>1</sup>ELyTMaX UMI 3757, CNRS-Université de Lyon-Tohoku University International Joint Unit, Tohoku University, Sendai, Japan  
<sup>2</sup>New Industry Creation Hatchery Center, Tohoku University, Sendai, Japan  
<sup>3</sup>Univ. Lyon, INSA-Lyon, LGEF EA682, F69621 Villeurbanne, France

**Abstract:** This study reports the use of MagnetoRheological Elastomers (MREs) for mechanical to electrical energy conversion. Based on magnetic particles dispersed in an elastomer matrix, it is shown that the dependence of the magnetic properties on applied mechanical strain allows obtaining a pseudo-Villari effect.

### 1. Introduction

MRE are composite materials based on a soft elastomer matrix (silicone rubber) and ferromagnetic particle (carbonyl iron particles). As the mixture was cured, a magnetic field was applied to induced column of particles along the magnetic flux lines. Such structured MREs possess magneto-elastic coupling giving rise to the magnetically-tuned elastic modulus. In this study, the converse effect, namely the elastically tuned magnetic permeability is used to convert a mechanical excitation (as a shear deformation of the MRE) into an electrical signal [1,2].

The device is schematically presented in Fig.1a. A primary coil (excitation coil) is inducing a magnetic flux ( $\Phi=BS$ , where  $B$  is the magnetic flux density and  $S$  is the magnetic circuit cross section) within the magnetic core which flows along the magnetic circuit (core and MRE); then the time variation of the permeability  $\Delta\mu(t)$  yields a time dependent contribution to the magnetic flux density induction  $\Delta B(t)$ . This time dependent flux therefore induces a voltage on the secondary (or pick-up) coil.

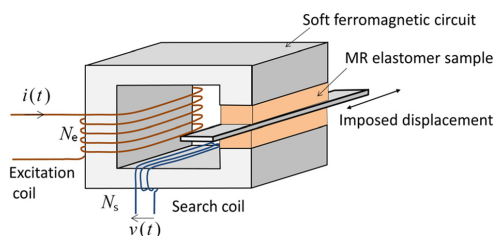


Fig.1a: harvesting device [1]

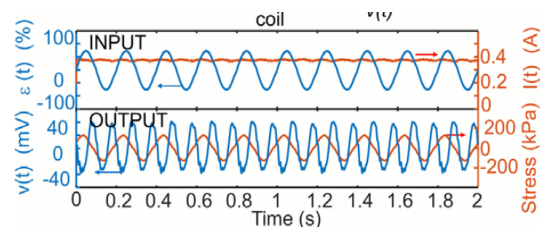


Fig.1b: Experimental condition and results [2]

### 2. Experimentation, discussion

The result is presented in Fig.1b, showing the electrical current injected in the excitation coil and the applied shear strain as INPUT and the measured stress and voltage at the pick-up coil as OUTPUT.

A model that combine analytical expressions and FEM model has been built. The time dependent shear strain is supposed to be a sinusoidal excitation expressed as  $\gamma(t)=A\sin(2\pi\nu t)$ , where  $A$  refers to the oscillation amplitude and  $\nu$  to the frequency of the oscillation.

An analytical expression for magnetic relative permeability of the composite has been derived as [3]:

$$\mu_r(\gamma) = 1 + \frac{3\phi}{1-(\phi-2D)} - \frac{\gamma^2}{\gamma^2+1} \left[ \frac{3\phi}{1-\left(\phi+2D\frac{1}{(\gamma^2+1)^{3/2}}\right)} - \frac{3\phi}{1-\left(\phi-D\frac{1}{(\gamma^2+1)^{3/2}}\right)} \right] \quad 1$$

Where  $\phi$  is the composite filling factor and  $D$  refers as a structure coefficient. As  $D=0$  for isotropic material this leads to the well-known Maxwell Garnett expression  $\mu_{MG}=(1+2\phi)/(1-\phi)$ . As the shear strain  $\gamma(t)$  increases, the magnetic permeability is reduced. For example, the permeability without shear ( $A=0$ ) and with a shear ( $A\neq 0$ ) are plotted in Fig 2. As a result, without shear ( $A=0$ ), the magnetic flux density is constant and there is no voltage at the pick-up coil, while in the case where a shear is applied ( $A\neq 0$ ), the magnetic induction is varying and a voltage is generated across the pick-up coil.

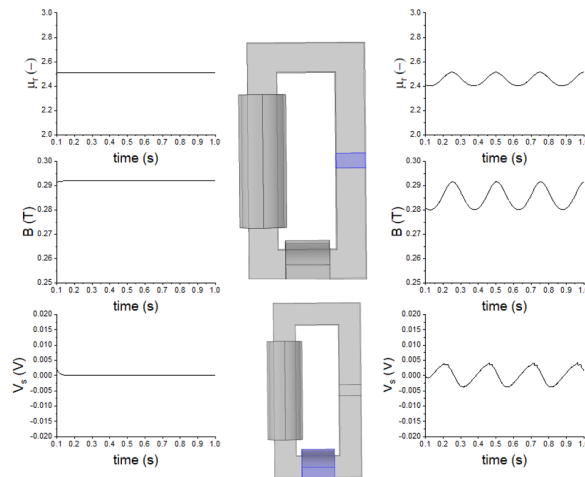


Figure 5 : The time dependency of the MRE permeability induces a voltage in the secondary coil.

Left  $A=0$  and right  $A=0.3$

Effect of (i) material properties such as the filling factor or magnetic saturation, (ii) external condition such as the amplitude of the applied magnetic field and shear strain will be discussed.

### 3. Conclusion

This study exposed the use of MRE for mechanical to electrical energy conversion. While such materials are usually used for mechanical stiffness tuning, this work showed that using a bias magnetic field permits of disposing of a pseudo-Villari effect, hence opening brand new application fields.

### References:

- [1] Mickael Lallart, Gael Sebald, Gildas Diguët, Jean-Yves Cavaille and Masami Nakano. *J. Appl. Phys.* 122, 103902 (2017).
- [2] Gael Sebald, Masami Nakano, Mickael Lallart, Tongfei Tian, Gildas Diguët, Jean-Yves Cavaille. *Science and Technology of Advanced Materials*, 2017 Vol. 18, No. 1, 766–778
- [3] Gildas Diguët, Gael Sebald, Masami Nakano, Mickael Lallart, Jean-Yves Cavaille, *J. Magnet Magnet Mat*, **revised**



---

*Monday, March 11<sup>th</sup> – Morning*  
*Session 4 – 10:40-12:20*

---

**Possibilities of the Gleeble machine at MATEIS laboratory**



Abstract :

Since more than 10 years, the laboratory MATEIS at INSA-LYON masteries a Gleeble. A Gleeble is a dynamic testing machine that can simulate a wide variety of thermal/mechanical metallurgical situations. Starting with the basic treatment of metals to obtain specific structure and proceeding through the testing of specimens taken from finished products, the Gleeble can simulate and provide test data on almost any thermal/mechanical exposure the material sees during its life. After a short presentation of the Gleeble, I'll present some results obtained at MATEIS.



## **Advancement of acoustic emission inspection using system invariant analysis technology**

Project NEC & IFS Joint research

	<p><i>Tomoya SOMA</i> <i>NEC Solution Innovator</i> <i>Tohoku brunch</i></p> <p><i>t-soma@cq.jp.nec.com</i></p>		<p><i>Toshiyuki TAKAGI</i> <i>Institute of Fluid Science,</i> <i>Tohoku University</i></p> <p><i>takagi@wert.ifs.tohoku.ac.jp</i></p>
	<p><i>Tetsuya UCHIMOTO</i> <i>Institute of Fluid Science,</i> <i>Tohoku University</i></p> <p><i>uchimoto@wert.ifs.tohoku.ac.jp</i></p>		<p><i>Shichao CAI</i> <i>Graduate School of Engineering,</i> <i>Tohoku University</i></p>

### Abstract :

#### **1. Introduction**

The acoustic emission (AE) test is used as a method of non-destructive inspection in industry. In this technique, a crack occurs in a structural material such as a pipe, and when a crack propagates in the structure, it receives a signal of an elastic wave generated by energy released to judge the presence or absence of abnormality. Therefore, it can be collected by a sensor fixed to the surface of the structure. However, in an actual examination, it is very difficult to capture a target abnormality with many environmental noises. In recent years, AI technology and big data analysis method are rapidly growing. It is also beginning to be used in the field of non-destructive inspection. System invariant analysis technology (SIAT) can process various data sets to discover hidden patterns, unknown relationships and other useful information [1]. When such technology is used for AE inspection, various effects including improvement of inspection accuracy can be expected. The purpose of this research is to apply the SIAT method to evaluate the feasibility of SIAT as a tool for processing AE data of fatigue test and monitoring the health of structures. For that purpose, we collect the AE signal in the fatigue test of aluminum alloy and evaluate the result processed by SIAT.

#### **2. What is System Invariant Analysis Technology (SIAT)**

Invariant analytical technology is a machine learning technique that comprehensively extracts relationships between time series of numerical values obtained as system performance information and plant sensor information 1). By using the relationship between the learned sensor information as an operation model of the target system and monitoring the time and place where the relationship changed at real time, it is possible to detect abnormal symptoms at an early stage (Fig.1)

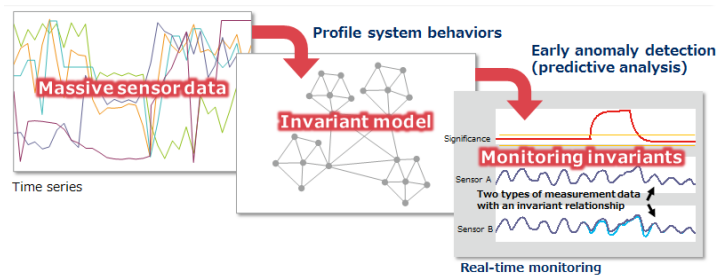


Fig. 1. System Invariant Analysis Technology(SIAT) Overview

In anomaly detection, the value of the corresponding sensor (y term) is predicted by substituting the current process value into the x term of the model expression of invariant learned and extracted automatically. When this predicted value and current value deviate from the "usual range" learned at the time of model creation, detection is made as abnormality.

## 2. Application to AE inspection

In order to verify the applicability of the SIAT system, test data of crack specimens and crackless specimens were obtained respectively. Figure.2 is an abnormal score obtained as a result of processing the AE signal measured during the fatigue test of the intact test piece by SIAT. Overall, it can be seen that the value of the abnormal score stably fluctuates in the range of 100 to 300.

Next, the abnormality score calculated by SIAT is shown in Fig. 4 using the data during the fatigue test of the crack specimen. The abnormal score at the initial stage is low. Over time, abnormal scores show an upward trend, the maximum value exceeds 800. It decreased suddenly after reaching the peak in about 30 minutes. Subsequently, the value of the abnormal score falls to a much lower initial stage. This is due to the broken specimen.

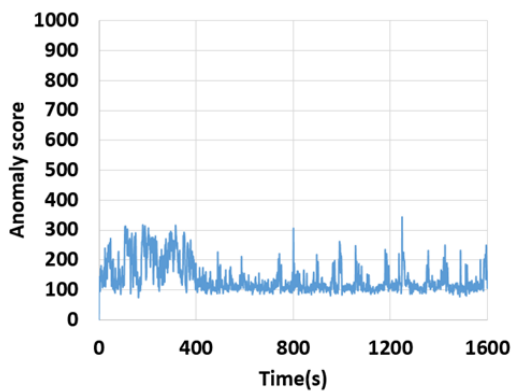


Figure.2 Anomaly score of intact specimen

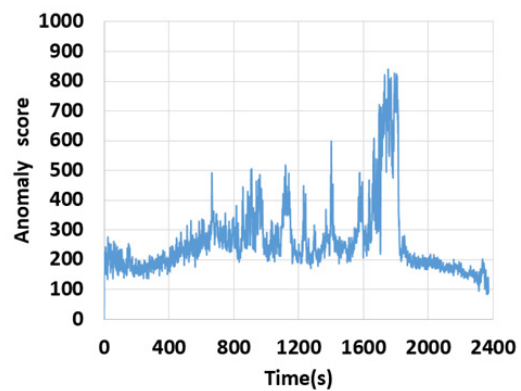


Figure.3 Anomaly score of cracked specimen

In this way, it was possible to make the AE signal difficult to recognize with human eyes by processing with SIAT to make it easy to see. This seems to indicate that even a small inexperienced examiner can do a certain degree of examination.

References :

- [1] Guofei Jiang, Haifeng Chen, Kenji Yoshihira, Discovering likely invariants of distributed transaction systems for autonomic system management, Cluster Comput. (2006) 9:385–399 DOI 10.1007/s10586-006-0008-1

## Future prospects in the MISTRAL (Miniature-Scale Energy Generation by Magnetic Shape Memory Alloys) project

Project ELyT lab : **MISTRAL** (MIniature-Scale Energy GeneraTion by Magnetic Shape MemoRy Alloys)

	<p><i>MIKI Hiroyuki, Assoc. Prof. Frontier Research Inst. for Interdisc. Sci. (FRIS), Tohoku University, Aramaki asa Aoba 6-3, Aoba-ku, Sendai, Japan</i></p>		<p><i>KOHL Manfred, Prof. Institute of Microstructure Technology (IMT), Karlsruhe Institute of Technology (KIT), Hermann-von-Helmholtz-Platz 1 76344 Eggenstein-Leopoldshafen</i></p>
	<p><i>LALLART Mickaël, Assoc. Prof. Univ. Lyon, INSA-Lyon, LGEF EA 682, F-69621, VILLEURBANNE, FRANCE</i></p>		<p><i>YAN Linjuan, Adj. Assist. Prof. Univ. Lyon, INSA-Lyon, LGEF EA 682, F-69621, VILLEURBANNE, FRANCE</i></p>

**Abstract:** In order to address the issue of delicate thermal interfacing of conventional thermoelectric generators, the MISTRAL project addresses a breakthrough approach relying on ferromagnetic materials. This allows disposing of a miniature heat engine providing mechanical vibrations from a thermal gradient, which can then be harvested using electromechanical coupling devices. In the framework of JSPS fellowships starting from Sept. 2019, potential research prospects are presented.

### 1. Introduction

The spreading of autonomous wireless sensor networks (for instance in the framework of IoT) has raised an important issue regarding their power supply. Over the last decades, using surrounding energy sources has emerged as an interesting alternative, leading to the concept of “energy harvesting” ([1]). More specifically, thermal source is of particular interest as it is widely available. Unfortunately, conventional devices using thermoelectric modules show very low conversion efficiency due their high thermal conductivity. Recently, the use of phase transition materials has raised the possibility of disposing of small-scale heat engines able to convert a heat flux into mechanical vibrations ([2, 3]) opening possible technological and scientific breakthroughs for the conversion of thermal gradients into electrical form. MISTRAL addresses such a possibility, with the originality of using materials featuring both ferromagnetic behavior and shape-memory effect (*e.g.*, Ni-Co-Mn-In or Ni-Mn-Ga).

The general objective of upcoming investigations lies in the following three axes:

1. The use of multiphysic phase transitions (mechanical and magnetic - “MultiPhysic Memory Alloys” (MPMA) - Figure 6) to enhance heat engine performance (incoming energy optimization).
2. The use of several combined conversion effects and design of the associated multisource energy extraction electrical interface (enhancement of the conversion abilities).
3. Analysis of the energy path and transfers to ensure the best combination of the different energy sources to the associated energy conversion material (global optimization).

## 2. Enhance active part within the system

Previous collaborative works between Tohoku FRIS laboratory and KIT IMT have developed a micro heat engine consisting in a cantilever beam vibrating at high frequency from a thermal gradient (Figure 7 - [3]). The first objective will be to extend this concept by including other conversion effects (piezoelectric and/or pyroelectric for instance) in order to dispose of a maximum of active parts within the device. This part will also raise the issue of multi-effect energy harvesting, for which a dedicated electronic interface (for instance based on nonlinear circuit [4, 5]) will be developed.

## 3. New structure design

Still aiming at a microgenerator that exhibits the largest active parts (relatively speaking), a new device that will take directly advantage of the multiphysic nature of the MPMA will be considered. For example, using such materials in the shape of a coil that would also have a spring behavior, the energy could be converted thanks to Lenz law of induction through electromagnetic coupling hence providing an all-in-one device. This multiphysic design will be preceded by a characterization phase of the multiphysic spring, through the consideration of the thermomechanical, thermomagnetic and, finally, thermo-magneto-mechanical effects.

## 4. Towards MultiPhysic Memory Alloys

Characteristic identification of the multi-physical couplings will be carried out, including the thermomechanical, thermomagnetic, and hybrid thermo-magneto-mechanical effects. This will permit setting up a model of the MPMA to predict the phase transitions, based on experimental observations, ultimately allowing quantification of the performance of the heat engine and optimization routes. Additionally, MPMA benefits to other fields (control or actuation) will be envisioned.

## 5. Funding opportunities and insights

The research concepts will be developed in the framework of one long-term JSPS Invitational Fellowship (1 call/year, typ. August) and one Standard JSPS Postdoctoral Fellowship managed by CNRS (2 calls/year, typ. November and April). Future considered supports to the MISTRAL project consist in JSPS BRIDGE program (for JSPS alumni), PHC Sakura and ANR-DFG for instance.

## 6. Conclusion

MISTRAL project proposes an innovative approach for addressing the issue of limited efficiency of conventional thermal to electrical energy converters and harvesters. Based on the combination of the expertise of the three partners (FRIS, IMT and LGEF), it is forecasted that a complete global approach allowing the mastering of each elementary stages and their interfaces will enable the development of an efficient device for converting thermal gradients into electricity.

### References :

- [1] K. V. Selvan and M. S. M. Ali, *Renew. Sustain. Energy Rev.* **54**(2016) 1035-47.
- [2] M. Gueltig, H. Ossmer, M. Ohtsuka, H. Miki, K. Tsuchiya, T. Takagi and M. Kohl, *Adv. Ener. Mater.* **4**(2014) 751-758
- [3] M. Gueltig, F. Wendler, H. Ossmer, M. Ohtsuka, H. Miki, T. Takagi, M. Kohl, *Adv. Energy Mater.* **7**(2017) 1601879
- [4] D. Guyomar, G. Sébald, S. Pruvost, M. Lallart, A. Khodayari and C. Richard, *J. Intel. Mat. Syst. Struct.* **20**(2009) 609-624
- [5] M. Lallart, *Energy Conv. Mag.* **133**(2017) 444-457

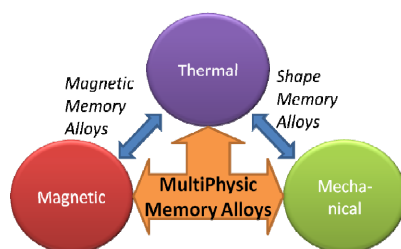


Figure 6 : MPMA concept

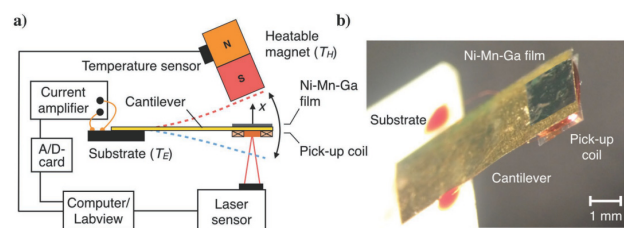


Figure 7 : Current heat engine ([3])

## **Polymer-Metal-Fiber Adhesions DELamination control**

Project ELyT lab: R32 – POMADE

	<i>OLLIVIER-Lamarque Lucas, IFS - ELyTMaX MARY Nicolas, ELyTMaX UCHIMOTO Tetsuya, IFS - ELyTMaX</i>		LIVI Sebastien, IMP@INSA YUAN Sheng, MATEIS MARCELIN Sabrina, MATEIS TER-OVANEISSIAN Benoit, MATEIS NORMAND Bernard, MATEIS
--	---	--	---

### **Abstract:**

Polymer materials are one solution to protect material against aggressive environment. However, new chemical regulation needs to consider new hardener instead of diamine used nowadays. A previous based on electrochemical characterizations shown high hydrophobicity and low diffusion kinetic of water in ionic liquid epoxy resin compared to epoxy amine. Since performance of new epoxy resin were highlighted, new investigations were performed based on nondestructive evaluation technique. Polymer capacitance as a function of immersion time in a saline solution were quantified and values of water uptake were compared to gravimetric measurements. Both electrochemical and NDE capacitance measurements shown the same trend in term of water uptake behavior and quantity of adsorb water for two kind of epoxy resin.

### **1. Introduction**

Corrosion is one of big concerns for metal based materials in our industrial society. Polymer coatings are used to prevent from corrosion. They are easy to apply and cost efficient. But water uptake in polymer layer is responsible of substrate corrosion. That is why in transportation and industries, there is a need to control the evolution of water uptake process before degradations become critical.

According to European Chemicals Agency (ECHA), diamine should be removed in coating fabrication process. New anti-corrosion coating has been developed using ionic liquid (IL) instead of diamine. These coatings have better water protection properties and IL are less toxic than diamine so they are good candidates to replace the diamine [1].

Non-Destructive Evaluation (NDE) is a widely used method to seek defects in structures. Capacitor sensor is chosen for its locally measurement of permittivity feature in thin volume.

The objectives of this study are the investigation of electromagnetic properties of coating and implementation of NDE method to be able to monitor the water uptake in the polymer layer. At first electromagnetic properties of polymer like permittivity are measured for different ionic liquid concentrations in the polymer. Then a sensor is developed for coating evaluation application. In parallel, values are compared thanks to gravimetric measurements.

## 2. Experimentation, discussion

In order to find a correlation between measured capacitance and water uptake, immersion tests have been performed with samples of different concentration of IL. During fabrication process, IL is mixed with BADGE epoxide. Four samples have been studied with different IL concentrations: 30 phr, 20 phr, and 10 phr. The fourth sample does not contain IL but diamine as hardener.

Capacitance measurements of polymer samples were performed by impedance analyzer as shown in Fig.1. Capacitance value of the coating was first evaluated in dry condition before immersion. Then, samples were immersed in water solution with concentration of 0.1 mol.L<sup>-1</sup> of sodium chloride at room temperature. From the capacitance spectroscopy, the value at 10 kHz is extracted and the evolution is monitored as shown on Fig.2.

When water diffuses in polymer layer, electric properties of the layer are changing. The relative dielectric constant water is much higher ( $\epsilon_r=80$ ) than the permittivity of ionic liquid composite polymer ( $\epsilon_r\approx 4$ ). The value of the dielectric constant of the overall coating gives information about water uptake because capacitance is proportional to the dielectric constant. In this way, the capacitance value changes according to the variation of permittivity. Water uptake of the coating can be locally evaluated with appropriate sensor.

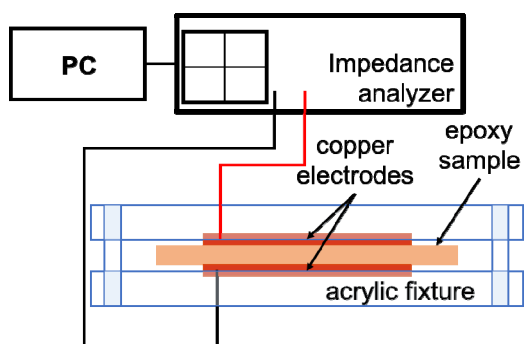


Fig.1: Impedance analyzer experimental setup.

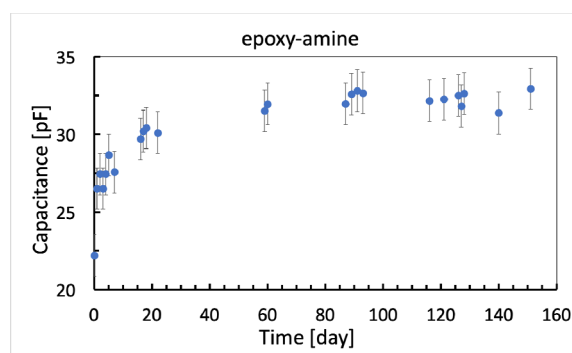


Fig.2: Time evolution of capacitance for epoxy-amine specimen

For all specimens, it was shown that capacitance is increasing quickly as the water diffuses in the material during the beginning of immersion. Then saturation phenomenon is observed. Regarding the water uptake values given by the Brasher Kingsbury relationship [2], it was shown that epoxy-IL10 phr polymer is the most appropriate for corrosion protection. In the other hand, epoxy-diamine has a faster and higher water uptake rate. It means the degradation of the polymer is more important.

With another batch of specimens, gravimetric measurements were performed after immersion tests. Immersion conditions were the same as described previously. Mass variation is measured with a precision weight scale. By assuming the mass variation is only due to the water uptake, specimens are sorted and epoxy-diamine shows the highest relative mass variation (2.5%). On the opposite, epoxy-IL specimens show better hydrophobic properties with less than 1% of relative mass variation.

### References:

- [1] C.Banciu, S.Joly-Marcelin, B. Ter-Ovanesian, S.Livi, "Préparation et caractérisation des propriétés anticorrosion de revêtements époxydes à base de liquides ioniques", INSA Lyon, Matis, Master report, June 2017
- [2] D. M. Brasher and A. H. Kingsbury, « Electrical measurements in the study of immersed paint coatings on metal. J. Appl. Chem., vol. 4, no 2, pp. 62-72, 1954

## **Effect of wettability of carbon fiber on interfacial shear stress on PP/PA polymer blend**

Project ELyT Global: DESign of Interface structure of fiber-Reinforced polymer blEnd

	<p><i>KOSUKEGAWA, Hiroyuki</i> <i>Institute of Fluid Science,</i> <i>Tohoku University</i> <i>2-1-1 Katahira Aoba-ku,</i> <i>980-8577 Sendai, Japan</i></p>		<p><i>DALMAS, Florent</i> <i>MATERiaux: Ingénierie et</i> <i>Science - CNRS UMR5510</i> <i>INSA-Lyon</i> <i>7, avenue Jean Capelle,</i> <i>69621 Villeurbanne cedex,</i> <i>France</i></p>
	<p><i>TAKAGI, Toshiyuki</i> <i>Institute of Fluid Science,</i> <i>Tohoku University</i> <i>2-1-1 Katahira Aoba-ku,</i> <i>980-8577 Sendai, Japan</i></p>		<p><i>CAVILLE, Jean-Yves</i> <i>ELyTMax UMI 3757, CNRS –</i> <i>Université de Lyon – Tohoku</i> <i>University, International</i> <i>Joint Unit, Tohoku University</i> <i>MaSC, room 502, 2-1-1</i> <i>Katahira, Aoba-ku, 980-8577</i> <i>Sendai,</i></p>

### Abstract :

#### **1. Introduction**

Carbon fiber reinforced thermoplastic (CFRTP), which is a composite made of carbon fibers embedded in a thermoplastic matrix, has been studied for the applications to mass-production industries. CFRTP has some problems for practical applications. One problem is that adhesion between fiber and matrix can be weak, depending on the polymer matrix. For example, polypropylene (PP), which is generally used as the matrix of composites, cannot be bonded well with carbon fiber because of hydrophobicity of PP [1]. Therefore, to improve this compatibility, the use of a hydrophilic polymer such as polyamide (PA) has been studied. However, PA has disadvantages such as high hygroscopicity, high melting point and viscosity which make the material handling difficult.

The other problem of CFRTP is that impact resistance, and strength of thermoplastic materials are generally incompatible. The use of polymer blends (made of two or more kinds of polymers) as a matrix for CFRTP has attracted attention in order to combine two properties of component polymers at the same time. When blended polymers are immiscible, it is known that the polymer blend has a phase separation structure such as sea-island structure. The control of this phase separation structure can change the physical properties of the polymer blend. To reach properties for the polymer blend better than those of each polymer component, a compatibilizer is used to form stable phase structures. Even though hydrophobic PP and hydrophilic PA are incompatible, adding a compatibilizer makes the diameters of the dispersed phase in PP/PA polymer blend smaller and stable, and also improves the mechanical properties of the blend. In the case of PP/PA polymer blend, maleic anhydride grafted polypropylene (MAGPP) is often investigated as a compatibilizer.

The purpose of this project is to evaluate whether CFRTP based on PP/PA polymer blend can be applied to a commercial product and to design the optimum interface structure of fiber/ polymer blend in CFRTP. To make CFRTP practicable, it is necessary to optimize the interfacial shear strength (IFSS) between fiber and resin matrix. The value of IFSS means the transfer performance of the stress which should be transferred from resin to fiber during use. IFSS can be influenced by several factors such as

compression force, mechanical anchor effect, and electrostatic force. The electrostatic force is discussed as work of adhesion between fiber and resin. Since the surface of commercial carbon fiber is smooth, anchor effect may not be contributed to IFSS. We investigate the work of adhesion of carbon fiber and polymer blend and discuss the effect of work of adhesion on IFSS. The work of adhesion of fiber/resin is calculated with the surface free energy of carbon fiber and PP/PA polymer blend.

## 2. Experimentation

PP/PA polymer blends which have different concentration of PA were prepared by using a kneader (HAAKE Rheomix 600p, Thermo Scientific Inc.). All specimens have 10 wt% of MAgPP as a compatibilizer. PP/PA polymer blends were processed into thin films with a thickness of 100~200  $\mu\text{m}$  by using a hot press (AH-203, AS ONE Co.). Three kinds of carbon fibers with different surface characteristics were prepared as follows: sizing reagent on commercial carbon fiber (T700SC, Toray Industries Inc.) was removed with a mixture of acetone and methyl-ethyl ketone (50/50, v/v), and the desized fiber was reduced by the reduction treatment by referring Gao's method [2]. Sized polar fiber (commercial one) and reduced nonpolar fiber are respectively named as "sCF" and "hCF".

Surface free energy of sCF and hCF was measured by the Wilhelmy method with a dynamic contact angle tester K100SF (KRÜSS GmbH). One fiber was carefully fixed on a fiber holder, and a stage on where a bath filled with liquid was set and moved up toward the fiber so that the fiber immersed into the liquid vertically. When the fiber was wet with the liquid, advancing or receding tension force  $F$  was loaded on the fiber. The contact angle  $\theta$  was determined by the following equation [3] :

$$\cos \theta = \frac{F}{\pi d \gamma_L} \quad (1)$$

where  $d$  is the diameter of the fiber and  $\gamma_L$  is the surface free energy of the liquid. With two or more kinds of liquids, the dispersive ( $\gamma_S^d$ ) and polar components ( $\gamma_S^p$ ) of the surface free energy of the fiber are decided by the following Owens-Wendt equation :

$$\gamma_L(1 + \cos \theta) = 2(\gamma_S^d \gamma_L^d)^{1/2} + 2(\gamma_S^p \gamma_L^p)^{1/2} \quad (2)$$

Distilled water and diiodo methane were employed as the liquid;  $\gamma_L^d$  and  $\gamma_L^p$  are 21.8 mN/m and 51.0 mN/m for water, 49.5 mN/m and 1.3 mN/m for diiodo methane, respectively.  $F$  was measured with high-precision load cell which has 30  $\mu\text{g}$  in resolution. The dipping speed of the fiber was 6 mm/min. The advance contact angle was adopted for determining  $\cos\theta$ .

The surface free energy of PP/PA polymer blend was measured with contact angle tester (DM501, Kyowa Interface Science Co.). Since the surface of PP/PA polymer blend film is often segregated with PP [5], the contact angle on the inside of the film was measured for determining the surface free energy of PP/PA polymer blend and work of adhesion with carbon fiber.

The work of adhesion  $W$  between carbon fiber (sCF, hCF) and PP/PA polymer blend was calculated by the following equation :

$$W_{FP} = 2(\gamma_F^d \gamma_P^d)^{1/2} + 2(\gamma_F^p \gamma_P^p)^{1/2} \quad (3)$$

where the indicators of F and P are "fiber" and "plastic" respectively.

A single filament of carbon fiber was embedded in molten PP/PA polymer blend film at 200°C by using a hot press and then cooled to room temperature. Uniaxial tensile test of the single carbon fiber embedded films was conducted by a displacement of 1 mm, and the length of fragments of the broken fiber in the film was measured by using an optical microscope. The values of IFSS of the specimens were calculated by the Eq. (4) :

$$\tau = \frac{3d\sigma_f}{8L_a} \quad (4)$$

where  $\tau$  is IFSS (Pa),  $\sigma_f$  is the strength of the fiber,  $L_a$  is the mean length of the fragments (m) [6].

### 3. Results and Discussion

To determine the surface free energy of sCF and hCF, the contact angle against water and diode methane was measured with the Wilhelmy method. The advancing tension force was measured by the force-displacement curve (Fig. 1), and the contact angle was calculated by Eq. (1). Subsequently, the surface free energy of sCF and hCF was obtained by Eq. (2). The surface free energy of PP/PA polymer blend was also measured by contact angle tester as well. The work of adhesion of the respective setting was calculated by Eq. (3).

The IFSS of carbon fiber and PP/PA polymer blend was measured by fragmentation test by Eq. (4). The tendency of IFSS according to the concentrations of PA in polymer blend was different depending on the surface characteristics of carbon fiber as shown in Fig. 2. IFSS of sCF, which is polar fiber, increases according to the concentrations of PA and reached about 12 MPa at 100wt% of PA. On the other hand, IFSS of hCF, which has a nonpolar characteristic, becomes the maximum at 40wt% of PA showing about 12 MPa. This result indicates that the use of nonpolar fiber is sometimes more suited in terms of the adhesion between fiber and polymer blend matrix than polar fiber.

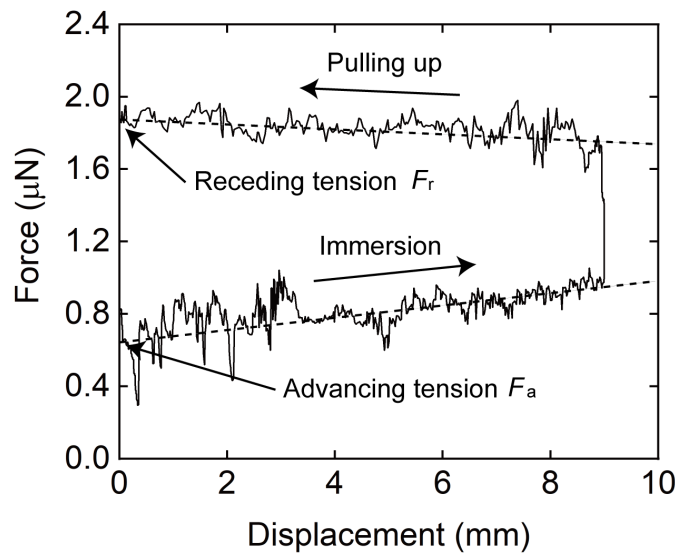


Figure 1 Measurement of advancing and receding tension of sCF in water.

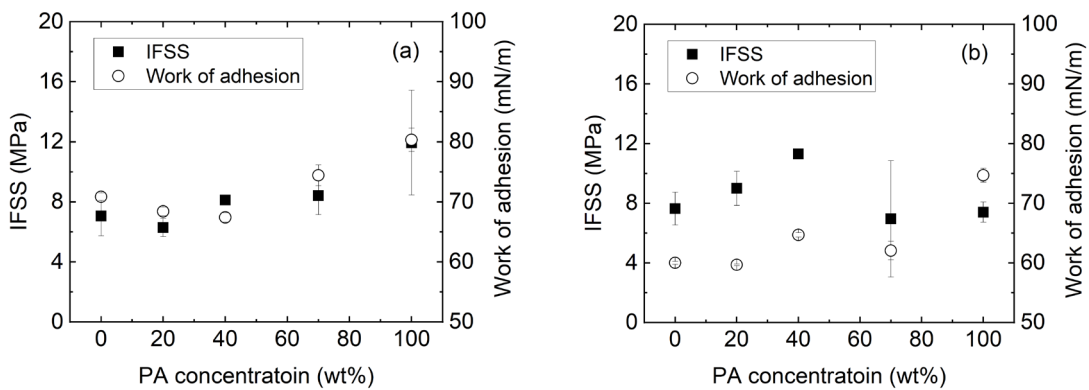


Figure 2 Relationship of IFSS and work of adhesion for PA concentration of PP/PA polymer blend : (a) sCF, (b) hCF.

The work of adhesion on carbon fiber and PP/PA polymer blend has a similar tendency to IFSS for PA concentration. In the case of polar fiber, work of adhesion increases according to the PA concentration, whereas it shows the maximum value at 40 wt% of PA concentration in the case of nonpolar fiber (with the exception of PA 100 wt%). These results indicate that IFSS can be determined by the surface free energy of both surfaces of carbon fiber and polymer blend. In other words, normal adhesive force originated from electrostatic coupling between the surface of carbon fiber and polymer blend is dominant on IFSS.

To improve and control the IFSS of fiber and PP/PA polymer blend of CFRTP, it is required to adjust the surface chemical characteristics of fiber. In addition, considering that the value of IFSS of carbon fiber and epoxy resin, which is the combination used in aircraft industry, is more than 20 MPa [4], it is needed to improve IFSS of CFRTP more for practical applications.

### Acknowledgement

This work was partly supported by a JSPS KAKENHI Grant-in-Aid for Young Scientists (B) Grant Number 15K18219 and the JSPS Core-to-Core Program, A. Advanced Research Networks, “International research core on smart layered materials and structures for energy saving”.

### References :

- [1] N. Hirano, H. Muramatsu, T. Inoue, *J Japan Soc Composite Mater*, **39** (2013) 113-119.
- [2] W. Gao, et al., *Nature Chemistry*, **1** (2009) 403-408.
- [3] B. B. Sauer and W. G. Kampert, *J Colloid and Interface Science*, **199** (1998) 28-37.
- [4] A. Kelly and W. R. Tyson, *J Mech Phys Solids*, **13** (1965) 339-350.
- [5] K. Tanaka, et al., *Hyomen Kagaku*, **28** (12) (2007) 688-697 in Japanese.
- [6] Y. Sawada and Y. Nakanishi, *Tanso*, **140**(1989) 248-254.



---

*Monday, March 11<sup>th</sup> – Afternoon*  
*Session 5 – 14:00-16:10*

---

## **Team Science and Interdisciplinary Research in Lyon**

Project ELyT lab: Building scientific collaboration between France, the US, and Japan



### Abstract:

#### **1. Introduction**

The eleven laboratories of excellence that just had funding renewed for five years in the Lyon-St. Etienne region provide new opportunities for Team Science and interdisciplinary research. Arizona State University's Decision Theater (DT) provides the kind of environment and support system that can be mobilized for such work. In this talk, I first present the interest of the field of Science of Team Science. Then, I describe Lyon's project for a space similar to Arizona's Decision Theatre. Finally, I give examples of research contexts where Lyon could benefit from sophisticated data visualization of complex processes in order to facilitate their interpretation and support decision-making within varied stakeholder groups.

#### **2. Studying Science and the Science of Team Science**

Different academic communities have studied science from a variety of perspectives. The history of science examines how our understanding of the natural world has changed over the centuries whereas the philosophy of science is concerned with the foundations and purpose of science, as well as its implications (1, 2). Science, Technology, and Society studies focus on society's role in developing science and technology, framing these three domains in a complex systems framework (3). The Social Studies of Science explores the dynamics of science including its relationship to politics, society, and culture. Scientometrics measures and analyzes science, focusing for example on impact of science through bibliometrics (4) or through mapping of fields of inquiry or the scientific work of particular institutions (5). More recently the Science of Team Science has developed a commitment to critically examine how scientific teams work together. This field's objective is to understand and improve how scientists collaborate and integrate theories and methods across disciplinary, institutional, and professional boundaries (6, 7, 8, 9).

#### **3. Knowledge Decision Confluence in Lyon<sup>1</sup>**

---

<sup>1</sup> The Knowledge Decision Confluence structure is currently being developed within a multidisciplinary and diverse stakeholder task force, comprised of Pierre Borgnat, David Coeurjolly, Mariétou Diagne, Alessandro Farne, Aurélien Garivier, Gilles Gesquiere, Sebastian Grauwin, Clément Jourdan, Jean-Philippe Lachaux, Kristine Lund, Marion Nicolas, François Pellegrino, Charlotte Tardy, Patrick Vincent, and Romain Vuillemot. The text in this section comes from this group.

The KDC (Knowledge Decision Confluence) platform is a device for addressing complex and multidisciplinary societal, technological or scientific issues by enabling the presentation of multidimensional data and modeling to facilitate data analysis and the understanding of complex processes, to illuminate decision-making and knowledge exchange between stakeholders of various profiles (scientists, policy makers, general public, etc.).

In this conceptual stage, operational devices such as Decision Theater (Arizona State University) or immersive visualization (CAVES) inspire the platform project. In the future, KDC will be a technological platform centered around a Decision Theater venue and mobile data representation devices (typically via virtual reality headsets), implemented by a dedicated technical team. This paper presents a roadmap to analyze the feasibility and initial conditions necessary to deploy the platform. The objectives and intended uses are briefly presented as well as the actions to be implemented, based on a valuation of pre-existing skills and capacities on the Lyon Saint-Étienne site (LSE) and the implementation of demonstrators articulated around several real case studies.

The KDC project results from the meeting between proposals from researchers on the LSE site and the desire to govern the IDEXLYON project on the one hand and Greater Lyon on the other hand to promote initiatives to develop skills and attractiveness of the site around the theme of artificial intelligence and the use of digital data. In autumn of 2018, two meetings initiated by the IDEXLYON project confirmed the interest and potential of such a platform. A task force was formed in early 2019 to develop a shared vision. In parallel, informal exchanges with several partners of the International Alliance of the University of Lyon (Canada and Japan in particular) suggest a strong potential for cooperation around this platform and perhaps a more ambitious project aiming at the interconnection of platforms allowing for an elaborate form of tele-presence at these sites.

Targeted stakeholders are researchers, small and large businesses, associations, non-governmental organizations, political decision-makers, interest groups, & the general public. General goals include:

- Establishing a platform open to the entire LSE ecosystem, ensuring high visibility at both national and international levels;
- Promoting innovation around complex issues and massive and / or multidimensional data to meet a variety of needs;
- Collaborating with policymakers;
- Encouraging exchanges between researchers from different disciplines;
- Promoting the know-how of our researchers to the world of business;
- Facilitating the dissemination and appropriation of complex issues by the general public.

### 3. Interdisciplinary Hotbeds in the Lyon St. Etienne ecosystem

Thanks to the structuring power of the IDEXLYON project, the scientific landscape of LSE has succeeded in organizing into large interdisciplinary projects. Fig 1 illustrates each of their visual identities and Tab 1 links each acronym with its title.



Fig. 1: Eleven of twelve of Lyon's laboratories of excellence were renewed for five more years of funding.

There are three human and social sciences labex and eight from the exact sciences. Currently ASLAN, COMOD, and IMU are exploring a joint project around data representation and the time is ripe for exploring additional collaborations around a Knowledge Decision Confluence) platform in Lyon.

Tab.1: Acronyms & names of the Labex in Lyon

<b>Labex Acronym</b>	<b>Labex Name</b>
ASLAN	Advanced Studies on Language Complexity
CeLyA	Lyon Acoustics Centre
COMOD	Constitution of modernity: reason, politics, religion
CORTEX	Construction Cognitive Function and Rehabilitation of the Brain
DEVWECAN	Development Cancer and Targeted Therapies
IMU	Urban Worlds Intelligences
IMUST	Institute for Multi-scale Science and Technology: from Fundamental Physics and Chemistry to Engineering in New Material and Processes and Eco-technologies
LIO	Lyon Institute of Origins
MANUTECH-SISE	Surface Interface Science Engineering
MILYON	Community of mathematics and fundamental computer science in Lyon
PRIMES	Physics, Radiobiology, Medical Imagery and Simulation

More specific examples of current interdisciplinary collaborations will be given at the workshop. These will center around, for example, the visualization of complex temporal and spatial pathways, urban territorial problems, visualization of the human brain, and networks of scientific cooperation, amongst other topics.

## References

- [1] M. Hollis, (1994). *The Philosophy of Social Science: An Introduction*. Cambridge. ISBN 978-0-521-44780-5.
- [2] T. Kuhn, (1962). *The Structure of Scientific Revolutions* (Edition 1970). Chicago: The University of Chicago Press.
- [3] P. Sasvari, in “The Effects of Technology and Innovation on Society”. *Bahria University Journal of Information & Communication Technology* **5**,1 (2012) 1-10
- [4] K. Lund, H. Jeong, S. Grauwin, & P. Jensen in « Une carte scientométrique de la recherche en éducation vue par la base de données internationales Scopus » *Les Sciences de l'éducation - Pour l'Ère nouvelle*, **50**, 1 (2017) 67-84
- [5] S. Grauwin, G. Beslon, E. Fleury, S. Franceschelli, C. Robardet, JB. Rouquier, P. Jensen, Complex systems science: dreams of universality, reality of interdisciplinarity. *Journal of the American Society for Information Science and Technology, ASIS&T* (2012)
- [6] K. Börner, *Atlas of science: visualizing what we know*: The MIT Press, Cambridge, MA/London, UK, 2010,
- [7] Stokols D, Misra S, Moser RP, Hall KL, Taylor BK. The ecology of team science: Understanding contextual influences on transdisciplinary collaboration. *Am. J. Prev. Med.* 2008;35(suppl.): S96–S115.
- [8] Fiore SM. Interdisciplinarity as teamwork—How the science of teams can inform team science. *Small Group Res.* 2008; 39:251–277.
- [9] Stokols D, Hall KL, Taylor BK, Moser RP. The science of team science: Overview of the field and introduction to the supplement. *Am. J. Prev. Med.* 2008;35(suppl.):S77–S89



---

## **Collaborative Decision Making in a Visualized, Data Driven Environment**



*Jon Miller is the Director, Arizona State University Decision Theater and leads efforts to model, simulate, and visualize complex problems leading to informed policy discussions through better understanding and the ability to forecast decision outcomes before they are made.*

### Abstract:

#### **1. Introduction**

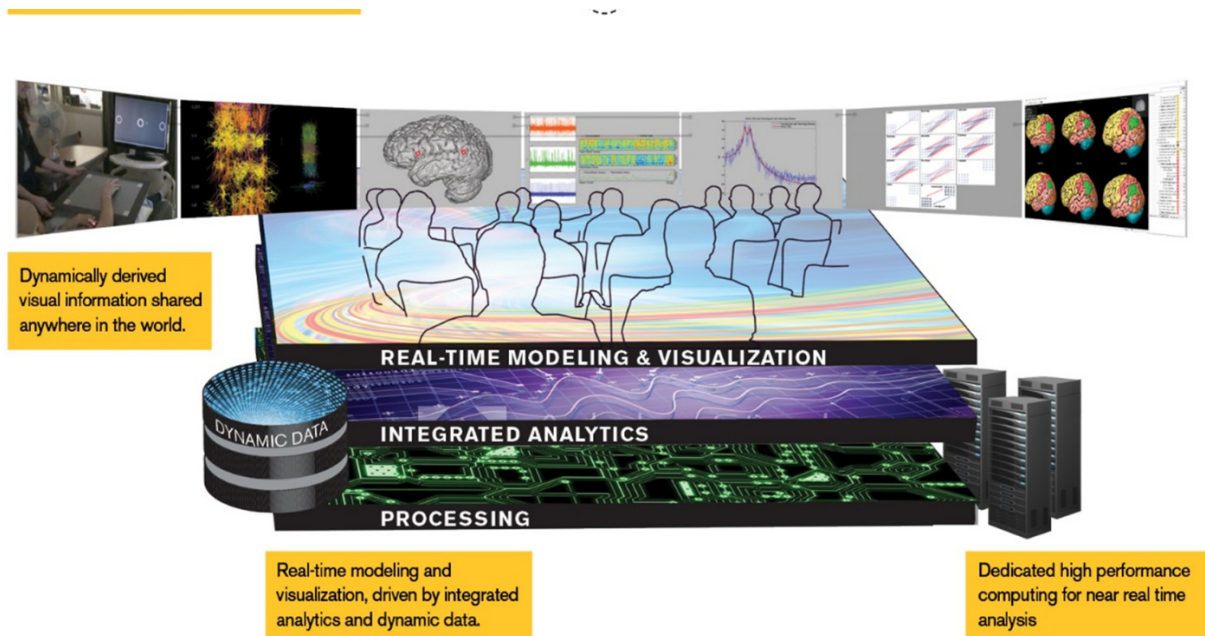
Arizona State University's Decision Theater (DT) brings together relevant parties and stakeholders to better understand and forecast decision outcomes to complex, cross-disciplinary problems in an immersive, visualized environment. A 26-foot circular room is used to present multiple integrated and interactive models across a 270-degree display of seven panoramic High Definition monitors. The environment's intimate and explorative nature immediately engages participants' curiosity and facilitates new and better informed conversations. Data visualization, predictive modeling, and expert analytics are used to enhance all stages of the decision making process. The result is more informed decision making, made by more informed decision makers, in complex and ambiguous environments.

DT connects people, processes, and technologies to facilitate informed discussions and develop solutions to cross-disciplinary complex problems. The nature of the problems we address typically require the collaborative effort, resources, capabilities and expertise of multiple organizations. DT provides mechanisms to bring together organizations to explore problems, share, analyze, and visualize data, and evaluate solutions from multiple perspectives, across disciplines and locations. ASU DT fuses Team and Decision Sciences with a variety of technical capabilities while partnering with subject matter experts drawn from over 3,000 research professionals on ASU campuses. We also work extensively with external subject matter experts.

Decision Theater actively partners with researchers and leaders to visualize solutions to complex problems. DT staff and facilities provide the latest expertise in collaborative, computing, gaming, and display technologies for data visualization, modeling, and simulation. DT's cross-disciplinary local, national and international issues are explored by drawing on Arizona State University's diverse academic and research capabilities as well as through partnerships with external subject matter experts.

Because our capabilities, skills and processes are problem agnostic, we are able to partner topic specific researchers and organizations to work across a range of complex issues including combating and preventing wildlife crime, implementing smart cities technology interventions, improving academic attainment, economic and workforce development and environmental sustainability issues. We have partnered with relief organizations to develop tools for humanitarian relief, governments and interest groups negotiating international trade agreements, the energy generation industry and a host of other activities where data driven models exist, or can be created to represent complex multi-faceted problems.

As depicted in the figure below, Decision Theater is not just a facility or a building. It is an organization with prototyping tools and processes in computation, analytics, visualization, and facilitation. Our objective is better decisions, made by better informed decision makers, using the best available expertise, —wherever it is found.



## 2. Experimentation, discussion

DT is a boundary object. “Boundary objects are mediating artefacts that have interpretive flexibility and can be an important means of achieving collaboration, promoting the sharing of knowledge between diverse groups.”[1] This is an intentional placement of DT and its capabilities. DT prides itself in its factual and complete representation of issues and the varied, and often competing, perspectives. DT works here to create and maintain an environment that is welcoming, non-threatening and accessible to participants from all areas of expertise, education levels, life experiences and political leanings. Our approach leads to a cooperative approach data sharing and to modeling and data visualization that is truly objective and data driven. DTN allows the data to speak for itself, albeit in a visually immersive and enrapturing way.

DT’s approach includes a variety of methods, such as Team Science (the study of convening people and facilitating productive engagements), Decision Science (the study of how decisions are made and how to facilitate the best decision making process), Data

Science and Focus Stacking (the ability to look at a complex problem from multiple scopes).

What truly allows DT to distinguish itself as a boundary object and be problem agnostic is its place as a university entity.

DT is part of ASU's Office of Knowledge Enterprise Development, the Research wing of Arizona State University. This means that DT is not under the direction of a single college or school within ASU. Rather, it can partner as needed access the campus and with many of the leading experts across a wide range of study as mentioned earlier.

The work at DT is not confined to regional issues affecting only Arizona. While we do partner with local institutions and effect change locally, our work involves issues effecting the United States as well as global challenges. This is facilitated by the Decision Theater Network (DTN), a global network of facilities and partners with our team located on our Tempe, Arizona campus. For example, in Washington DC, just steps from the White House, Arizona State University maintains a presence. This includes an extension of our DT immersive visualization facilities. In this facility, we reach out to and engage Washington based influencers and decision makers. While projects are developed at the Tempe, Arizona ASU campus, our DTN leverages our tools, projects, and capabilities. DTN allows interested partners to build on our capabilities to provide informed dialog and decision making on a global scale while addressing issue unique to them.

Ultimately, DTN lowers the barrier to entry for data analytics, predictive modeling, and data driven decision making in a visualized, immersive environment. DTN relies on knowledge sharing within the university and with global partners to ensure necessary data, complete background knowledge, and informed engagements. DTN's process allow partner organizations to join minimal facility investment while grown human capacity to do work within the demonstrated successful Decision Theater framework. Existing ASU teams, and our technology shelf of capabilities, including data ready models allows partners to focus on the resolution of the challenges they face. As ASU's Decision Theater continues to grow our capabilities and partnerships, we are mindful to tailor each Decision Theater Network node to the unique characteristics of our partners, their institutions, and the intended use of their Decision Theater Network node. With that in mind, no two Decision Theaters are, or should, be the same. What does remain constant across members of the DTN is a collaborative, information sharing culture demonstrating flexibility and a commitment to the creation of better, more informed decision makers informed in a fact based, data driven decision making environment .

#### References:

- [1] Barrett, M., & Oborn, E. (2010). Boundary object use in cross-cultural software development teams. *Human Relations*, 63(8), 1199–1221.
- Referencing: Sapsed J, Salter A (2004) Postcards from the edge: Local communities global programs and boundary objects. *Organization Studies* 25(9): 1515–1534



## Study on composite materials in NARITA laboratory

<http://www.material.tohoku.ac.jp/~fukugo/en/>

	<p><b>NARITA Fumio</b> Professor</p> <p>Department of Materials Processing</p> <p>Graduate School of Engineering</p> <p>Tohoku University</p>		<p><b>KURITA Hiroki</b> Assistant Professor</p> <p>Department of Materials Processing</p> <p>Graduate School of Engineering</p> <p>Tohoku University</p>
---	---	--	--

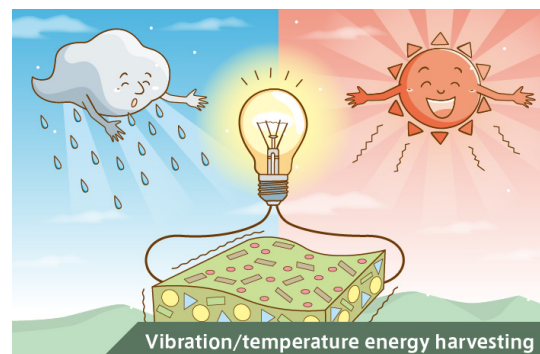
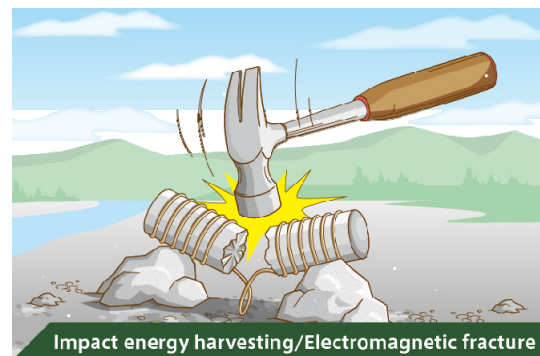
### Abstract :

We are performing the following studies on fracture and deformation of material systems in electromagnetic devices (macro-, micro-, and nano-systems) from both a theoretical and experimental point of view at some meso-scopic level. We have a high motivation to accept foreign (especially French) students in our laboratory. We have accepted 2 French students from University of Technology of Troyes.

### 1. Piezoelectric and Magnetostrictive composites

We focus on the development of a novel group of polymer-based nanocomposites incorporating magneto-strictive fibers or particles for sensing, energy harvesting, and bone conduction applications. Multi-functional coatings and composites of magnetostrictive elements will be designed and fabricated. During our studies, mixed-mode fracture test and finite element analysis on cracked magnetostrictive materials will be carried out.

Our another interesting is to employ computer simulations to clarify complex microstructure-electromechanical property correlations from cryogenic to high temperatures in novel nanostructured materials based on lead-free ferroelectric ceramics. Potential applications of such materials will include multi-energy (e.g. vibration, temperature) harvesting and IoT-based mobile services. New ferroelectric thin flexible films and inorganic-organic hybrids will be designed, fabricated, and characterized in terms of their mechanical, electrical, and other functional properties.



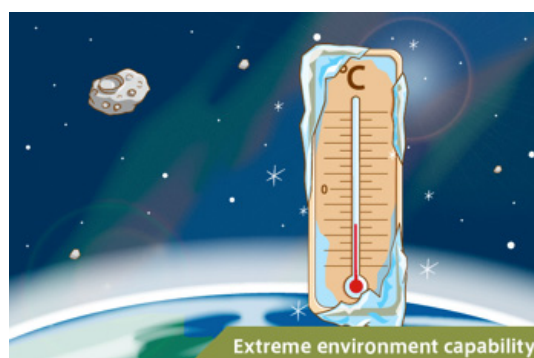
## 2. Metal and Ceramic Matrix Composites

Metal and ceramic matrix composites are increasingly applied within the aerospace and automotive industries, due to the combination of high specific modulus and yield strength. Our research line focuses on the development of such metal matrix nanocomposites with high mechanical strength and without any detrimental degradation of the damage tolerance properties. More fundamental work is then carried out to investigate fracture and deformation from room to high temperatures.

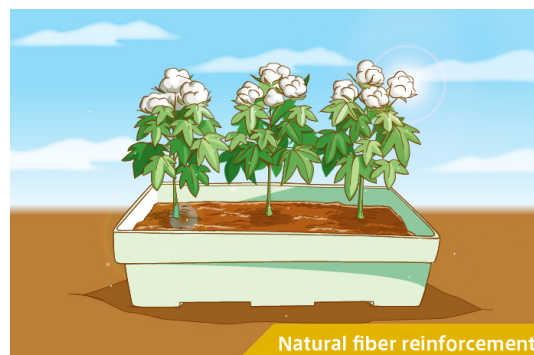


## 3. Fiber reinforced Plastics and Natural fiber composites

Our research interests are focused on the mechanical behavior of novel materials, such as single-layer triaxially carbon fiber reinforced polymer (CFRP) composites, triaxially CFRP composites with ferroelectric nanoparticles, for space probes. We design and develop these novel materials for a wide range of structural and functional applications (e.g., damping, energy harvesting). In our work, we make extensive use of state-of-the-art cryogenic and high temperature mechanical characterization techniques, in combination with computational modeling to gain insights into fundamental structure-property relationships of complex triaxially CFRP composites.



In Tohoku, cotton have been planted in farmlands no longer suitable for growing rice due to the tsunami. This is one of the activities being done with an aim to restore farming and industry. Plants such as trees and bamboos are materials which possess both strength and flexibility. In our lab, we grow cotton and bamboo and strive to create eco-friendly composite materials derived from plants. We also use cellulose nanofibers to reinforce polymers. We are conducting research with a new theme of "Let's create the best biodegradable composite!"



## Promotion du laboratoire de Narita

Nous proposons un stage (ou un échange universitaire) d'une durée indéterminée\* dans notre laboratoire sur l'un de nos sujets. Vous aurez, non seulement, l'occasion d'en apprendre plus dans le domaine des matériaux, mais aussi d'appliquer vos connaissances de chimie et de physique. Tout en vous plongeant dans une culture riche et atypique qui est la culture Japonaise. Pour toutes questions, veuillez contacter, Hiroki KURITA, à l'adresse suivante : [kurita@material.tohoku.ac.jp](mailto:kurita@material.tohoku.ac.jp)

\*Pour ce qui est de la durée du stage cela dépend, si je ne m'abuse, principalement de vous et de la formation (du site de votre école : "Trois stages d'une durée cumulée de 12 mois"). Il est à savoir que nous pouvons proposer des stages de 3, 6 ou 12 mois. Et des échanges dès 1 semestre.

## Piping system, risk management based on wall thinning monitoring and prediction

Project ELyT lab : PYRAMID

	<i>Toshiyuki TAKAGI</i> <i>Institute of Fluid Science</i> <i>Tohoku University</i>		<i>Philippe GUY</i> <i>Laboratoire Vibrations Acoustique</i> <i>INSA de Lyon</i>
---	--	--	--

### Research Members:

Yutaka WATANABE, Hiroshi ABE, Shinji EBARA, Tetsuya UCHIMOTO, Takayuki AOKI, Fumio KOJIMA, Mitsuo HASHIMOTO, Ryoichi URAYAMA, Hongjun SUN (Tohoku University), Thomas MONNIER, Jérôme ANTONI, Bernard NORMAND (INSA-Lyon), Nicolas MARY (INSA-Lyon/TU/ELyTMaX), Ryo MORITA, Shun WATANABE (Central Research Institute of Electric Power Industry, Japan), Atsushi IWASAKI (Gunma University, Japan), Hiroyuki NAKAMOTO (Kobe University), Pierre CALMON, Christophe REBOUD, Edouard DEMALDENT, Vahan BARONIAN, Xavier ARTUSI, Sylvain CHATILLON, Alain LHEMERY (CEA-LIST)

### Abstract :

In the decommissioning of Fukushima Daiichi Nuclear Power Station, a flow with a high concentration debris of various kinds (concrete, corrosion, metallic etc.) occurs in piping when removing fuel debris. Pipe wall thinning by Slurry Flow induced Corrosion (SFC) under solid-liquid two-phase has been anticipated. The location where wall-thinning is the most severe and maximum wall-thinning rate are revealed by experiments and numerical simulations. We aim at developing new tools and techniques to quantify pipe wall thinning, and provide a risk management system based on prediction-monitoring of pipe wall thinning due to SFC in piping systems. Corrosion modes and rate will be predicted by numerical simulations at any position for actual layouts of piping systems. These predictions will be validated by electrochemical experiments under controlled mass transfer coefficient. From the previous results, ultrasonic guided modes EMAT (Electromagnetic Acoustic Transducer) networks and EMAR (Electromagnetic Acoustic Resonance) systems will be designed. Their performance will be investigated in laboratory corrosion facilities and an adequate risk management system based on Bayesian approach will be developed.

### **1. Introduction**

The performance of the flow damage of carbon steel pipes in power plants has caused considerable concern. Carbon steels are the principle coolant pipe materials in nuclear and fossil fuel power plants. Erosion-corrosion induced wall thinning of pipe bores by the high temperature, velocity and pressure water flow has required structural evaluation of these pipes to allow integrity of these piping systems to be maintained [1]. In the decommissioning of Fukushima Daiichi Nuclear Power Station, a flow with a high concentration of debris of various kinds (concrete, corrosion, metallic etc.) occurs in piping when removing fuel debris. Pipe wall thinning by Slurry Flow induced Corrosion (SFC) under solid-liquid two-phase has been anticipated. Locations with most severe wall-thinning and maximum wall-thinning rates may be revealed by experiments and numerical simulations. We aim at developing new tools and techniques to quantify pipe wall thinning, and provide a risk management system based on prediction-monitoring of pipe wall thinning due to SFC in piping systems[2].

## 2. Description of the research

### 2.1. Clarification of wall-thinning for SFC by experiment and numerical simulations

Pipe wall thinning by SFC under solid-liquid two-phase has been anticipated. Therefore, the mechanism of accelerating corrosion due to disturbance of concentration boundary layer by repeated contact of particles must be understood (Fig.1). Moreover, the particle behaviors in flow and the corrosion rate considering interaction with particles should be evaluated by experiment and numerical analysis. Wall-thinning model based on the wall-thinning rate evaluation in consideration of a mass transfer coefficient evaluated under solid-liquid two-phase flow is developed. SFC is elucidated with experiment using water-circulation loop due to the disturbance of concentration boundary layer by repeated contact of particles, the reaction rate evaluation, and the tribo-corrosion effects. The effects of solid particles on fluid factor of flow accelerated corrosion in water piping with numerical flow simulation is elucidated. As a result, the location where wall-thinning is the most severe and maximum wall-thinning rate are revealed by the experiments and the numerical simulations.

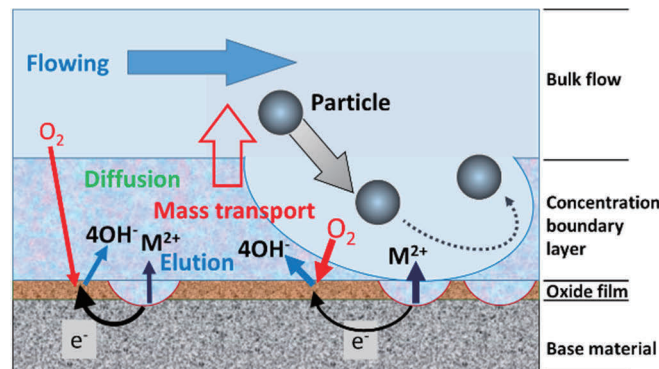


Fig. 1. Pipe wall thinning phenomena induced SFC

### 2.2. Development of EMAT Monitoring System

A system that can monitor pipe wall thinning by SFC with high accuracy and high resistance to environment is developed. The electromagnetic acoustic transducer (EMAT) and electromagnetic acoustic resonance (EMAR) methods are used. The EMAT increases the spatial resolution by focusing the ultrasonic wave. Moreover, ultrasonic guided modes EMAT networks will be designed.

### 2.3. Evaluation of Engineering Risk

A quantitative evaluation method for engineering risks associated with SFC in power plant is proposed. Specifically, PoF (Probability of Failure) evaluation in consideration of the various errors (inspection / damage progress and applied force) is achieved by means of Bayesian inference. Moreover, the reasonable plan by integrative evaluation of factors using a risk matrix is obtained.

## Acknowledgement

This study is the result of “Piping System, Risk Management based on Wall Thinning Monitoring and Prediction”, carried out under the Center of World Intelligence Project for Nuclear S&T and Human Resource Development by the Ministry of Education, Culture, Sports, Science and Technology of Japan, and ANR of France.

## References

- [1] R.J.K. Wood, Erosion-corrosion interactions and their effect on marine and offshore materials, *Wear*. 261 (2006) 1012-1023. doi: 10.10
- [2] T. Takagi et. al., Piping system, risk management based on wall thinning monitoring and prediction –PYRAMID, Short paper for 4<sup>th</sup> ICMST-Tohoku 2018, I-2, (2018).

Recent advances in PYRAMID project :

EMAT experimental results for corrosion characterization

	<i>Philippe Guy Laboratoire Vibrations Acoustique INSA de Lyon</i>		<i>Pr. Bernard Normand MATEIS INSA de Lyon</i>
	<i>Hiroyuki NAKAMOTO, Graduate School of System Informatics, Kobe University (1-1 Rokkodai-cho, Nada, Kobe 657-8501, Japan)</i>		<i>Pr. Toshiyuki Takagi Center for Fundamental Research on Nuclear Decommissioning, Tohoku University Tohoku University Institute of Fluid Science</i>
	<i>Dwaipayyan Mallick MATEIS INSA de Lyon</i>		

**1. Introduction**

As presented in the 2018 ElyTWorkshop, the PYRAMID project is an International Collaborative Research Project (PRCI), which involves French public laboratories (MATEIS and LVA at INSA Lyon, and CEA-LIST), an International Joint Unit (ELyTMax), Japanese public laboratories (IFS, and GSE at Tohoku University, GSST at Gunma University), and the Nuclear Technology Research Laboratory at CRIEPI a non profit research foundation, supported by the electrical Japanese industries. aim to develop new tools and techniques to detect and quantify wall thinning due to Flow Assisted Corrosion in piping systems. Corrosion modes and rate will be predicted by numerical simulations at any position for actual layouts of piping systems. These predictions will be validated by electrochemical experiments under controlled mass transfer coefficient.

We will briefly describe hereafter the work that have been initiated during the first year of PYRAMID, mainly by MATEIS and LVA in collaboration with IFS. Three aspects will be developed. First, we have determined the physical and acoustical properties of the carbon steel representative of actual structures. Then we will describe the experiments taht have been carried out to identify the corrosion process and measure the wall thinning online by ultrasonic measurements. Finally, we will present the very first experiments with guided waves.

**2. Materials characteristics**

Carbon steels are the principle coolant pipe materials in nuclear and fossil fuel power plants. We have several samples, two pipes of 2m long and two elbows.

As explained during ELYTWorkshop 2018, in the PYRAMID project, simulations carried out by CRIEPI for the tribo-chemical aspects and CEA for the EMAT NDT system using guided waves, will play a great role in the experimental validation and in the optimization of the inspection device.

The geometrical, ultrasonic and magnetic (Figure 1) properties of the carbon steel used in the piping system have been determined and shared between all the project partners.

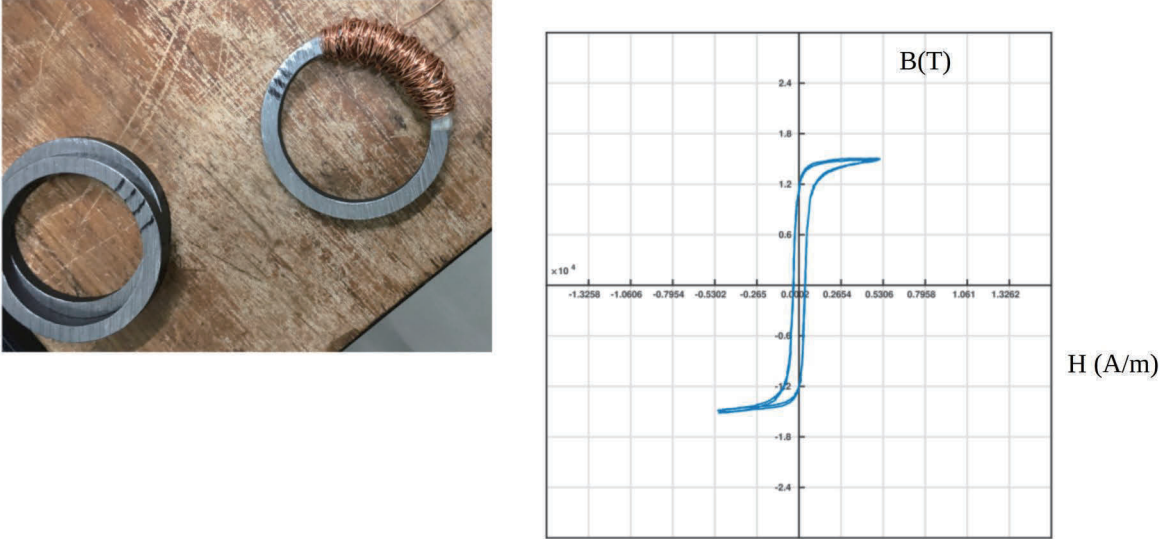


Figure 1: Magnetic characterization of the carbon steel

**3. Wall thinning monitoring**

A special corrosion cell has been developed by MATEIS team in order to control an accelerated corrosion process on carbon steel samples. The samples were square 40\*40mm<sup>2</sup> plates of 20mm in thickness. This cell was instrumented with an EMAT probe allowing to measure the thickness at any time, by means of a normal beam of bulk SH waves emitted from the outside face of the sample and reflected by the face in contact with the corrosion solution. The electrolyte was a Na<sub>2</sub>SO<sub>4</sub> stirred solution with addition of H<sub>2</sub>SO<sub>4</sub> till the pH is 1, and the potential was maintained to 0.2V during 28 hours.

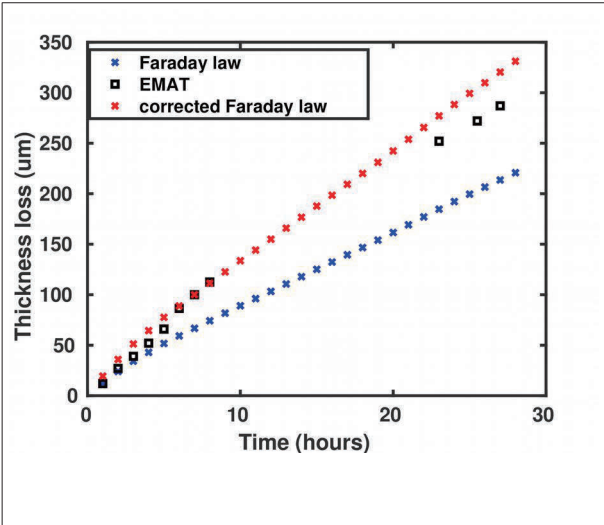


Figure 2: Thickness loss evaluation

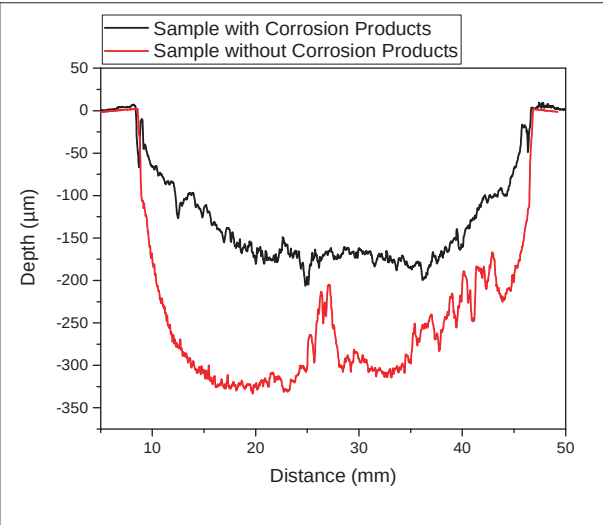


Figure 3: Corroded sample profilometry

On Figure 2, are compared the thickness losses measured by EMAT and deduced from Faraday law (blue crosses). Up to 6 hours the agreement between Faraday law and EMAT values are in quite good agreement, but after the discrepancy increases. This is probably because Faraday law assumes a uniform thickness loss all over the corroded surface, and deduces the thickness loss from the mass loss. This assumption is not really valid as it can be seen on the measured profiles of Figure 3. We plotted a modified Faraday law assuming the same mass loss with a parabolic profile of the corroded area (red crosses on Figure 2). After 28 hours this corrected law is much closer to the EMAT measurements, and to the profile obtained after the corrosion products have been removed. The ultrasonic wave seem to be reflected by the modified interface between the corrosion solution and the bulk of carbon steel. New experiments are currently carried out and should confirm the good ability of the ultrasonic SH waves to monitor the wall thinning online.

#### 4. Guided waves

Preliminary experiments involving guided waves have been carried out and showed promising potential in the detection of through thickness holes in steel pipes, both in transmission and pitch-catch configuration. The experimental setup is depicted on Figure 4.

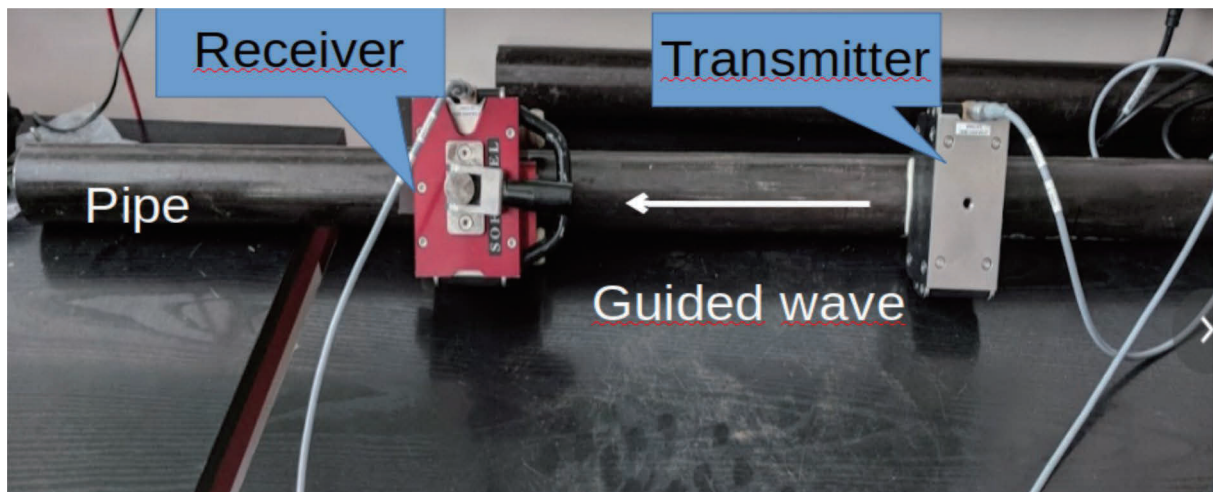


Figure 4: Guided waves experimental setup : transmission case

#### 5. Concluding remarks

The first results already obtained in the wall thinning continuous monitoring by SH bulk waves as well as for the damage detection of through thickness holes are very encouraging. At this moment, two post doc researchers have been recruited, one by MATEIS team and one by LVA, and will work full time on the project.

#### Acknowledgement

This work was realized in the framework of the PYRAMID project (Piping sYstem, Risk management based on wAll thinning MonItoring and preDiction) which is supported by the French National Agency of Research. (ANR-17-CE08-0046) and carried out under the Center of World Intelligence Project for Nuclear S&T and Human Resource Development by the Ministry of Education, Culture, Sports, Science and Technology of Japan. Part of the work was carried out under the Collaborative Research Project of the Institute of Fluid Science, Tohoku University.



## Advanced simulation tools for nondestructive assessment of corrosion affecting steel pipes

Project ELyT Max: PYRAMID



### Abstract:

CEA LIST participates to the French and Japanese PYRAMID research project (Piping System, Risk Management based on Wall Thinning Monitoring and Prediction) aiming at monitoring corrosion processes affecting complex tubular structures in a decommissioning context. This communication presents contributions made by CEA LIST regarding the development of dedicated models for the efficient simulation of ultrasonic inspections in view of corrosion detection and wall-thinning monitoring. Simulation tools introduced in the CIVA platform will help partners to design adapted EMAT sensors and provide model-based data to feed risk management analyses.

### 1. Introduction

Within the research project PYRAMID, jointly supported by Agence Nationale de la Recherche in France and the Japan Science and Technology Agency in Japan, many French and Japanese research teams collaborate in order to develop new tools and techniques to detect and quantify wall thinning due to Slurry Flow induced Corrosion (SFC) in piping systems. Simulation plays an important role in this project, as it is intensively used to support, firstly, probe design in order to optimize their performance, and, secondly, to complement experimental data used as inputs in risk management analyses, in particular. CEA LIST mainly contributes to the simulation aspects of the project, with a focus on two particular inspection configurations, illustrated in Figure 1, namely the guided wave ultrasonic inspection of tubes with complex parts like elbows [1], in collaboration with LVA laboratory of INSA Lyon, and the thickness measurement of pipes by means of electromagnetic acoustic resonance (EMAR) [2].

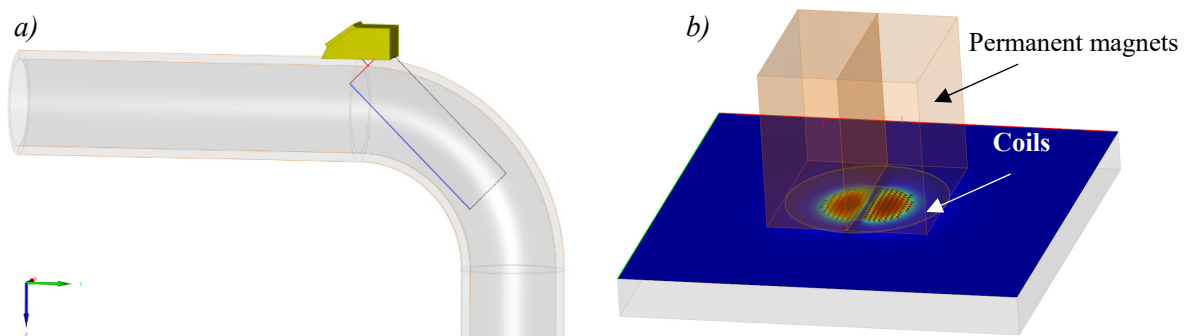
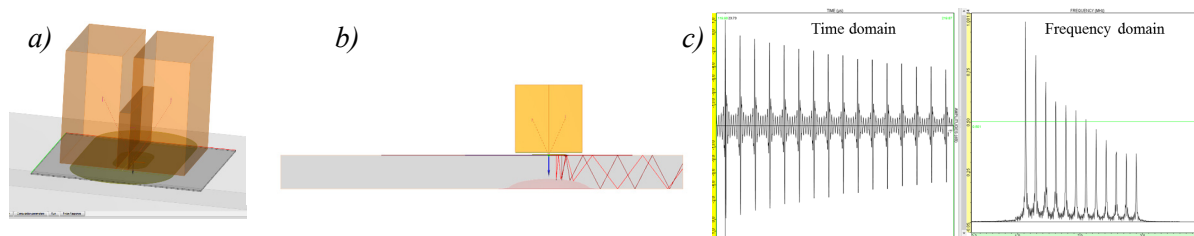


Fig. 1. a) Typical configuration of interest: inspection of a pipe elbow for wall thinning due to SFC.  
b) Simulation of the EMAR technique in the CIVA software.

## 2. Simulation of the EMAR technique

Typical EMAR configurations of interest, developed at University of Tohoku [3,4], involve two coils and a set of two or three permanent magnets. The Lorentz force distribution generated in transient regime yields an ultrasonic shear wave propagation in the piece [5]. A dedicated post-processing in spectral domain enables to accurately estimate the piece thickness from a set of measurements carried out for different frequencies of the sine burst excitation signal.



*Fig. 2. a) Illustration of the 3 magnet EMAR configuration modelled in CIVA. b) Perturbation of the UT paths in a corroded area of the piece. c) Example of time signals and spectrum obtained in the nominal case of a non-corroded plate.*

The complete inspection process has been simulated in the CIVA platform by jointly using the electromagnetic and ultrasonic modules. In addition, other coils designs like the point focused EMAT [6] are also under investigation.

## 3. model-based data to feed risk management analyses

Parametric studies carried out in simulation enable to generate representative set of synthetic signals, from which thickness estimations can be derived. The comparison between such estimations and the actual profile of corroded parts yields a distribution of measurement error that will be used in the risk management study carried out by Gunma University within the PYRAMID project.

### Acknowledgement:

This study is the result of “Piping System, Risk Management based on Wall Thinning Monitoring and Prediction”, carried out under the Center of World Intelligence Project for Nuclear S&T and Human Resource Development by the Ministry of Education, Culture, Sports, Science and Technology of Japan, and ANR of France.

### References:

- [1] V. Baronian, A-S. Bonnet-Ben Dhia S. Fliss and A. Tonnoir, Iterative methods for scattering problem in isotropic and anisotropic elastic waveguide - *Wave Motion* (2016)
- [2] M. Hirao, H. Ogi, in *Electromagnetic Acoustic Transducers*, 2nd Edition, Springer, 2016, Chapter 5
- [3] R. Urayama, T. Uchimoto, T. Takagi, S. Kanemoto, “Quantitative Evaluation of Pipe Wall Thinning by Electromagnetic Acoustic Resonance”, *E-Journal of Advanced Maintenance*, Vol. 2, No. 1, pp. 25–33 (2010/2011)
- [4] R. Urayama, T. Takagi, T. Uchimoto, S. Kanemoto, T. Ohira, T. Kikuchi (2013). Implementation of electromagnetic acoustic resonance in pipe inspection. *E-Journal of Advanced Maintenance*, 5(1), 25-33.
- [5] B. Clause and A. Lhémy, Transformation of body force generated by non-contact sources of ultrasound in an isotropic solid of complex shape into equivalent surface stresses, *Wave Motion* (2016)
- [6] A. Tezuka, H. Sun, R. Urayama, T. Uchimoto, T. Takagi, Development of thickness gauging method for pipe wall thinning inspection with Point Focusing EMAT, *The 23rd International Workshop on Electromagnetic Nondestructive Evaluation (ENDE2018)*



---

*Monday, March 11<sup>th</sup> – Afternoon*  
*Session 6 – 16:30-18:30*

## Molecular Simulation Analysis for Adhesion Mechanisms Involved in Polyethylene Processed by Cold Spray

	<p><i>Yukie Ishizawa<sup>1</sup></i> <i>New Industry Creation</i> <i>Hatchery Center</i> <i>(NICHe), Tohoku</i> <i>University</i></p>		<p><i>Ryuji Miura<sup>1</sup></i> <i>New Industry Creation</i> <i>Hatchery Center</i> <i>(NICHe), Tohoku</i> <i>University</i></p>
<p>Ai Suzuki<sup>1</sup>, Naoto Miyamoto<sup>1</sup>, Nozomu Hatakeyama<sup>1</sup>, Akira Miyamoto<sup>1</sup>, Chrystelle Bernard<sup>2,3</sup>, Jean-Yves Cavaille<sup>2</sup>, Kesavan Ravi<sup>2</sup>, Kazuhiro Ogawa<sup>2</sup>, <sup>1</sup>New Industry Creation Hatchery Center (NICHe), Tohoku University, 6-6-10, Aoba, Aramaki, Aoba-ku, Sendai 980-8579, Japan <sup>2</sup>ELyTMax UMI 3757, CNRS – Université de Lyon – Tohoku University, International Joint Unit, Tohoku University, 2-1-1, Katahira, Aoba-ku, Sendai 980-8577, Japan <sup>3</sup>Frontier Research Institute for Interdisciplinary Science (FRIS), Tohoku University, 6-3, Aoba, Aramaki, Aoba-ku, Sendai 980-8578, Japan</p>			

**Abstract:** To study the adhesion atomistic behavior between Ultra-high molecular weight polyethylene (UHMWPE) and nano-alumina particles during Cold Spray process, molecular simulation model of polyethylene molecule and OH terminated gamma-alumina surface is developed. Molecular Dynamics simulation is performed on these interface with various initial velocity of polyethylene molecule for impact to alumina surface. It shows the difference of temperature after impact between polyethylene molecule with and without hydroxyl group.

### 1. Introduction

Ultra-high molecular weight polyethylene (UHMWPE) is a semi-crystalline polymer with long macromolecular chains exhibiting strong viscoelastic behavior. Thus, it is difficult to process it by classical techniques such as extrusion or injection molding. One alternative technique is the Cold Spray (CS) process, which consists of propelling powder at solid state onto a substrate to form a coating. Using native polyethylene powder, no adhesion can be observed between UHMWPE particles during CS. In presence of nano-alumina particles added to UHMWPE powder, new bounds are created and allow thick but porous coating [1,2]. From these experimental observations, numerical approaches are needed to better understand the interface adhesion mechanisms to improve coating performances.

In this work, the bonding properties between alumina and polymer particles are investigated from a chemical viewpoint. Atomistic scale simulations, such as Molecular Dynamics are applied to quantify the bounding energy between particles with the assumption of Van der Waals and hydrogen bond interactions.

### 2. Method

We used our original classical molecular dynamics (MD) simulation program “New-RYUDO” [3,4]. In this study, we use a following equation for inter atomic potential:

$$E_{ij} = \frac{q_i \cdot q_j}{r_{ij}} + D_{ij} \{ \exp[-2\beta_{ij}(r_0 - r_{ij})] - 2 \exp[-\beta_{ij}(r_0 - r_{ij})] \} + E[\sigma_0 - \sigma_{ij}] + E[1 + s \cdot \cos(n \cdot \psi - \psi_0)] + \left( \frac{A_{ij}}{r_{12}} - \frac{B_{ij}}{r_0} \right) \quad (1)$$

Here, the first term means the Coulombic interaction, the second term means the Morse potential for covalent bond, the third term means the 3-body angle potential, the fourth term means 4-body torsion potential, and the last term means Lennard-Jones (LJ) potential for Van der Waals interactions.

The 3-dimensional periodic boundary condition was used to simulate the cell. The Verlet algorithm was adopted to solve the equation of motion, and the Ewald method was used to compute the long-range Coulombic interactions.

We constructed a simulation model with pure polyethylene (PE) molecule as a preliminary UHMWPE model and a modified PE in which 10 hydrogen atoms were replaced by 10 hydroxyl groups in the expected impact region.

### 3. Results and Discussion

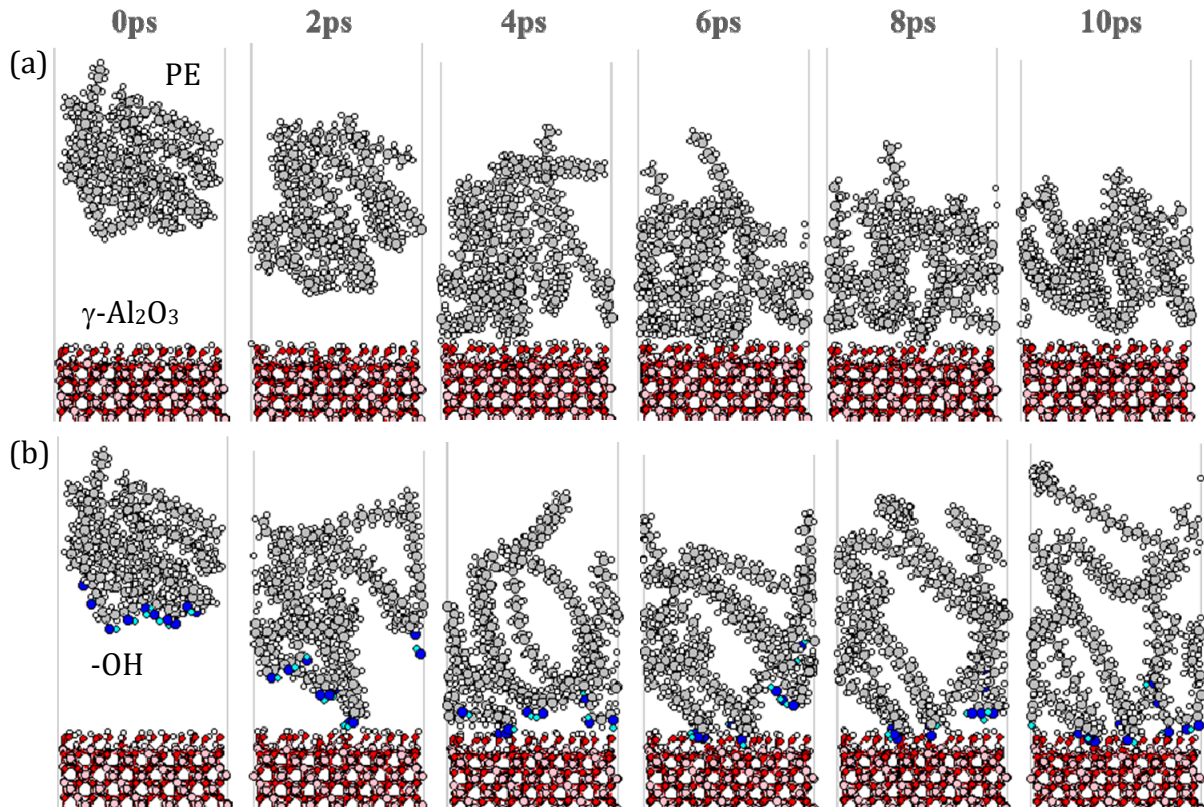


Fig.1 Collision Behavior of (a) PE (b) PE with 10 OH on  $\gamma$ -alumina surface

During MD simulation, PE molecules collide with  $\gamma$ -alumina surface with velocities of 100, 150 and 200 m/s (Fig.1). The structure of  $\gamma$ -alumina surface remains unchanged and PE sticks on it after the impact. PE with 10 OH groups shows larger deformation than PE without hydroxyl groups. Fig.2 shows the temperature of PE molecule after the impact and we can see that the PE with OH groups increases more the temperature than without OH, while the impact velocity dose not change it much.

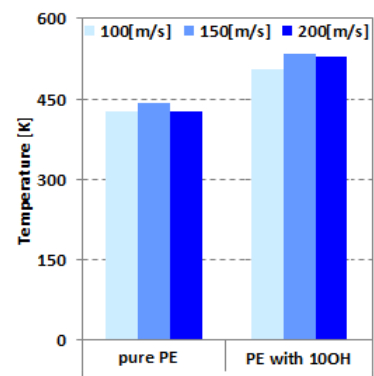


Fig.2 Temperature of PE after impact

#### References:

- [1] K. Ravi, Y. Ichikawa, K. Ogawa, T. Deplancke, O. Lame, J.Y. Cavaille, *J. Therm. Spray Technol.*, 25 (2016), 160–169.
- [2] K. Ravi, Y. Ichikawa, T. Deplancke, K. Ogawa, O. Lame, J.Y. Cavaille, *J. Therm. Spray Technol.*, 24 (2015), 1015–1025.
- [3] U. Mart, C. Jung, M. Koyama, M. Kubo, A. Miyamoto, *Appl. Surf. Sci.*, 244 (2005), 640-643.
- [4] T. Onozu, I. Gunji, R. Miura, S. S. C. Ammal, M. Kubo, K. Teraishi, A. Miyamoto, Y. Iyechika, T. Maeda, *Jpn. J. Appl. Phys.*, 38 (1999), 2544-2548.

## **Transonic buffet phenomenon by optimized extraction of transient structure based on physical sensitivity**



### Abstract :

#### **1. Introduction**

A self-excited pressure oscillation occurs when the aircraft fly at high speed, due to the complicated interaction between the shock wave and the separation vortex in downstream. This is called the Buffett phenomenon, the problem for safe flight. That elucidation, prediction and control of it is one of significant engineering tasks. High precision numerical fluid simulation in the transonic speed is not easy, from the viewpoint of the computation cost. However, as long as we identify such a characteristic structure that governs the self-excited oscillation, it is possible to set the resolution according to it, design the computation model.

In response to such engineering problems, we are considering taking advantage of new knowledge from the viewpoint of data science. Large-scale numerical calculations that captured the transonic buffet phenomenon by the wall model LES in recent years (Fukushima and Kawai (2018)[1]). In this report, we analyze transonic Buffett phenomenon which is an unsteady flow. Firstly, we deal with statistics with a spatial average in the spanwise direction of two-dimensional wings.

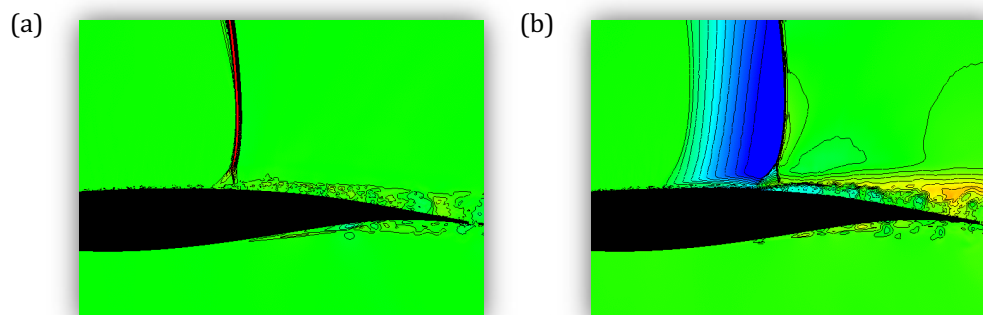


Fig.1: Instantaneous visualization of pressure fluctuation,  $p'$ , around an airfoil at transonic speed:

(a)  $Ma = 0.715$  without Buffet, (b)  $Ma = 0.73$  with Buffet [1].

## 2. Procedure

The characteristic structure of the unsteady flow is defined as the eigenvector of the self-adjoint operator and the initial value,  $\mathbf{A}^*(\tau)\mathbf{A}(\tau)\mathbf{u}(0)$ , in which the kinetic energy is amplified as an operator  $\mathbf{A}(\tau)$  for advancing the initial value  $\mathbf{u}(0)$  for a time  $\tau$ . In this research,  $\mathbf{A}(\tau)$  is not be determined as a normal operator, and diagonalization using orthogonal matrices is also allowed for non-normal operators, so singular value decomposition is applied.  $\mathbf{u}(\tau)$  is reconstructed from the singular value decomposition of  $\mathbf{A}(\tau)\mathbf{u}(0)$  as follows:

$$\mathbf{u}(\tau) = \mathbf{A}(\tau)\mathbf{u}(0) = \mathbf{U}\Sigma\mathbf{V}^* \quad 1$$

Here, the eigenvalues of  $\mathbf{A}^*(\tau)\mathbf{A}(\tau)\mathbf{u}(0)$  correspond to the kinetic energy of each mode and are the same as the squares of the singular values  $\sigma_k$  of  $\mathbf{A}(\tau)\mathbf{u}(0)$ . In the process of structure extraction, in order to be able to handle pressure and density as the same variable as speed, it is necessary to allow negative cases. Therefore, all the variables of the flow field are assumed to be fluctuation components obtained by subtracting the time average value. In this report, by using the results of iterative computation up to a certain time  $\tau$ , let  $n$  steps as a time step  $\Delta t$  be a sequence, and obtain the variance component of  $(m, n)$  matrix.

$$[ \mathbf{u}(0) \quad \mathbf{A}(\Delta t)\mathbf{u} \quad \mathbf{A}(\Delta t)^2\mathbf{u}(0) \quad \dots \quad \mathbf{A}(\tau)\mathbf{u}(0) ] \quad 2$$

In this study, we analyzed the data extraction of the transonic Buffett phenomenon obtained with wall model LES by Fukushima & Kawai (2018)<sup>[1]</sup> as an unsteady flow field. The Reynolds number is  $Re_c = 3.0 \times 10^6$ , the angle of attack is 3.5 [deg], the OAT 15 A supercritical airfoil shape, the Mach number is compared in the case of  $Ma = 0.715$  in which the Buffet phenomenon is not occurring,  $Ma = 0.73$  in which the Buffet is occurring (Fig. 1(a), (b)). The target is two-dimensional spanwise spatial-averaged, one cycle data set of the Buffett phenomenon. Grid point numbers are (4505, 1, 130) in the streamwise, the spanwise, and the wall-normal direction. Time period is  $\tau = 0.225$  in one cycle, with time step of  $\Delta t = 1.5 \times 10^{-3}$ , 150 instantaneous data. As a result, a matrix of formula Eq. 2 of 585,650 rows and 150 columns was constructed for each variable of pressure, density and speed, and singular value decomposition was applied. For one variable, the real time required for the calculation was about two minutes.

By applying the position evaluation method based on observability in data assimilation (Kang *et al.*, (2012))<sup>[2]</sup>, we computed the sensitivity of the physical quantity for each position and extracted mode, and search for a characteristic structure that governs self-excited oscillation. Here, a Gram matrix for evaluating the physical sensitivity is constructed from the  $Y$  matrix having the time series data such as the equation 2 using the fluctuation of the physical quantity  $y$  expressed by the following equation.

$$\Delta y_{k,j}(\lambda) = [y_k(x_0 + \delta x_{0,j}, \lambda) - y_k(x_0, \lambda)] \quad 3$$

In the  $Y$  matrix, 150 data per cycle, which is time direction information are arranged in the vertical direction, and  $n$  columns are arranged in the horizontal direction.

$$Y = \begin{pmatrix} \Delta y_{1,1} & \Delta y_{1,2} & \dots & \Delta y_{1,mode} \\ \vdots & \ddots & \ddots & \vdots \\ \Delta y_{step,1} & \Delta y_{step,2} & \dots & \Delta y_{step,mode} \end{pmatrix} \quad 4$$

$$G_0 = YY^T.$$

The Gram matrix is a symmetric. Therefore, the singular value analysis and the eigenvalue analysis are the same here. In this report, we focus on the temporal change of pressure  $\partial p/\partial t$  as a physical quantity and the result of the sensitivity analysis.

### 3. Results and discussion

At  $Ma = 0.73$  where the transonic Buffett phenomenon occurs, the flow direction velocity fluctuates greatly in the vicinity of the shock wave and the wall boundary layer, and the position of the shock wave also moves greatly back and forth on the blade surface. On the other hand, at  $Ma = 0.715$ , the position of the shock wave does not move and the speed fluctuation range remains small. When shock waves are generated at the transonic speed, it is believed to cause an unsteady Buffett phenomenon due to the interaction of it with the boundary layer developing near the wall (Pearcey *et al.* (1968))<sup>[3]</sup>.

In this study, this sensitivity was evaluated for each position and mode using the temporal change of pressure  $\partial p/\partial t$  as an index. For each of the four modes of the singular values corresponding to the square root of the kinetic energy obtained in the previous section, a gram matrix (Eq. 4) is constructed for each position. As a result, when considering all four singular value decomposed modes, the maximum eigenvalue became distribution as shown in Fig.2. The pressure change due to the interference of the shock wave with the boundary layer developed near the wall can be seen in the figure as the maximum eigenvalue is large.

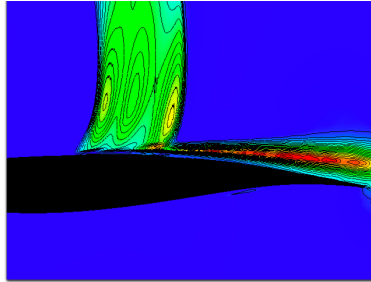
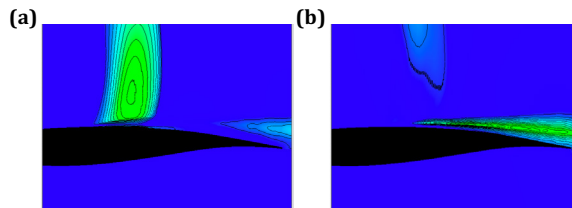


Fig.2: The maximum eigenvalue of pressure gradient Gramian consisting of four unsteady modes

In order to ascertain how this pressure change was caused, the maximum eigenvalue was calculated for each of the four modes, in order from the top of the singular value corresponding to the square root of the kinetic energy (Fig. 3 (a) - (d)). As a result, it was found that the mode leading to a large pressure change near the wall as seen in Fig. 2 is due to the fourth mode (d). In other words, it has been found that there is a possibility of obtaining a better understanding of the flow field by selecting a specific physical quantity sensitive mode.



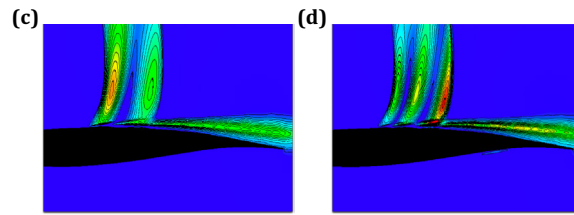


Fig.3: The maximum eigenvalue of pressure gradient Gramian consisting of four unsteady modes

## References :

- [1] Fukushima, Y. and Kawai, S., "Wall-Modeled Large-Eddy Simulation of Transonic Airfoil at High Reynolds Number", *AIAA Journal*, Vol. 56, No. 6, pp. 2372 - 2388 (2018).
- [2] Kang, W. and Xu, L., *Tellus A: Dynamic Meteorology and Oceanography*, **64**, 17133 (2012).
- [3] Pearcey, H. H., Osborne, J. and Haines, A. B., *Transonic Aerodynamics*, AGARD Conference Proceedings 35, paper number 11 (1968).

## **A new device based on a unique 6-axis force sensor for environment-controlled tribological and mechanical experiments**



*Julien FONTAINE, Matthieu GUIBERT, Jules GALIPAUD, Thierry LE MOGNE,  
Thibaut DURAND*

LTDS, UMR 5513 CNRS / ECL / ENISE / ENTPE  
36 avenue Guy de Collongue  
69134 Ecully cedex – France

### Abstract :

Tribology, the science of contact, friction, wear and lubrication, is a highly pluri-disciplinary field: the involved phenomena may be related to mechanics, physics, chemistry, etc. Moreover, these phenomena may take place simultaneously and affect each other. The effect of environment on the tribological behavior is thus very interesting, not only on an application point of view, but also on a more fundamental side, to study the coupling of chemical, mechanical and even physical phenomena.

LTDS has developed for 30 years an environment-controlled analytical tribometer, combining tribological experiments in an ultra-high vacuum chamber with surface analysis by X-ray Photoelectron Spectroscopy (XPS). Over the years, several versions of the XPS have been installed and several versions of the tribometer have been developed. Drastic effects of the environment on the tribological response of materials have been revealed thanks to this device. For instance, MoS<sub>2</sub> or hydrogenated amorphous carbon coatings may exhibit friction coefficients below 0.01. For such low values, it is rather challenging to have a good accuracy on the force measured: for 1 N normal force, we need to measure a tangential force lower than 10 mN. The main challenge then to measure such low friction coefficients inside a vacuum chamber is to have a perfect alignment between the actual tangential and normal forces applied on the contact and the corresponding measuring sensors.

So far, the way to solve this issue was to operate in linear reciprocating motion, with 2 force sensors placed on shafts that were stiff in the measured force direction but relatively compliant in a perpendicular direction. With such design, the range for normal force was from 1 to 5 N, and due to the low signal to noise ratio for small tangential forces, it was difficult to measure accurately friction coefficients in the millirange (below 0.01, corresponding to forces lower than 10 mN). Furthermore, the compliance of the system could also lead to non-linear displacement of the contacting bodies for high friction coefficients.

In order to improve the accuracy of our tribometer, we have thus decided to use a 6-axes force transducer, allowing the measurements of all forces and torques between the two counterfaces. Since the sensor has to operate in a vacuum vessel and under relatively small forces, no commercial sensors could fit in our system, and we had to design our own sensor. It is based on the elastic deformation between two plates attached by several stages of wires, the relative displacements being measured by 6 capacitive sensors placed in 6 different directions. The stiffness of the sensor is thus much higher, and the signal to noise ratio is much better. Also, the wires stages allow to have a hollow sensor, allowing electrical and thermal feedthrough. This design being unique, it has been patented.

Thanks to this new sensor, the range of operation could be drastically improved, the maximum force being about 20 N, while the accuracy is about 1 mN. Thanks to electrical and thermal feedthrough, we can control the temperature of the specimen placed on the sensor in the range from -120°C to +600°C. So far, the counterpart is attached to a 2 axes manipulator allowing vertical displacement (to apply the load) and rotation (to generate relative motion), allowing to perform rotating pin-on-disc experiments, continuous or reciprocating. The upper specimen can also be controlled in temperature thanks to an electrical slip ring, with a range from room temperature to 600°C.

Nevertheless, thanks to the six axes force transducer, it is possible to use any kind of motion of the counterpart. It is also possible to perform not only tribological experiments, but also mechanical ones. In order to explore the possibilities of this new sensor, we have performed indentation, scratch and fracture experiments. Indentation experiments were performed on several materials, with maximum loads down to 10 mN, and on steel from room temperature up to 500°C, showing the loss of hardness at high temperature, as expected. For fracture experiments, we have used silica samples, broken under ultra-high vacuum and under 25 hPa of water vapor, showing the lower toughness of silica in the presence of water vapor.

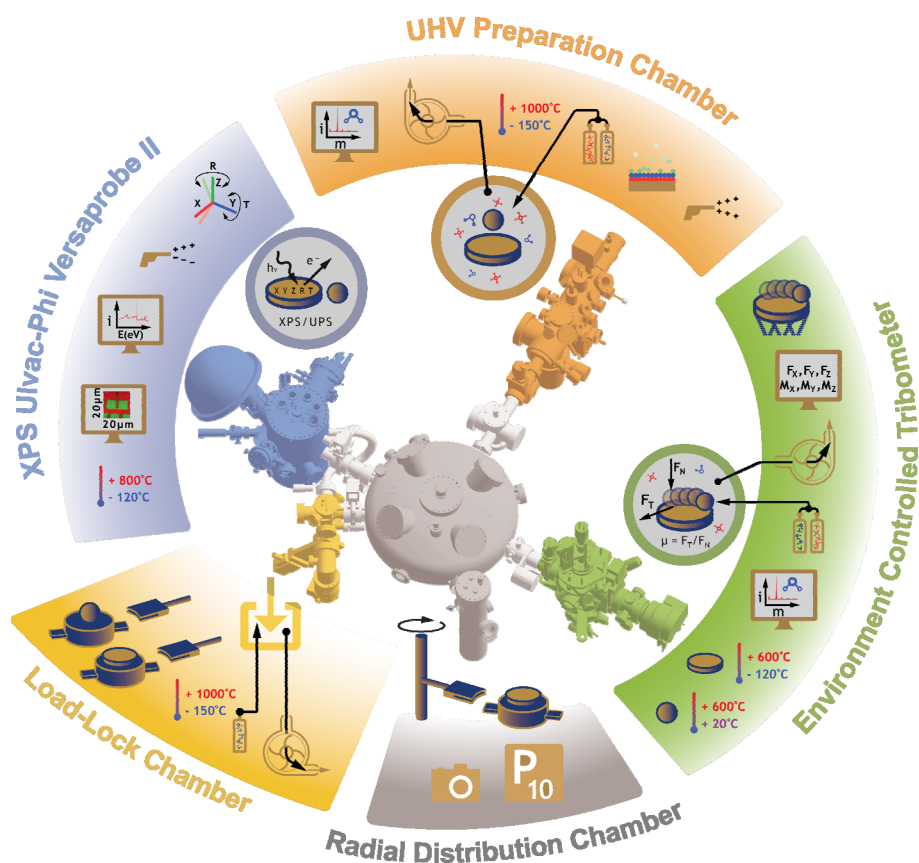


Figure 1: schematic of the environment controlled analytical tribometer developed at LTDS.

## **Modelisation and simulation of nanoscale phenomena**

	<p><i>Takashi Tokumasu Tohoku University Institute of Fluid Science Quantum nanoscale flow laboratory</i></p>		<p><i>Patrice Chantrenne Université de Lyon Institut National des Sciences Appliquées de Lyon MATEIS Laboratory</i></p>
---	---	--	---

### Abstract :

#### **1. Introduction**

Physic for Engineers is used to describe phenomena that can be observed and handle at usual scales. It leads to laws (Newton's law for classical mechanic, Fourier's law for heat transfer, Fick's law for mass transfer...) and properties (young modulus, viscosity, thermal conductivity...) avoiding the description of the matter at the atomic scale and fundamental interactions. However, with the development of nanotechnologies new questions arise meanwhile new research tools are available. Since several years, computers became so efficient that it is possible to simulate the matter at the atomic scale and to study properties of nanostructures and nanostructured materials.

As professors T. Tokumasu and P. Chantrenne are responsible of the Modeling and Simulation axe of ELyT Global, their aim is to develop collaborations between Tohoku University and Université de Lyon in the field of atomic scale modelling. Two main directions are considered: the development of collaboration between the different institutions of Tohoku University and Université de Lyon and the development of collaborations between their laboratories (Quantum nanoscale flow laboratory and MATEIS).

#### **2. Institutional relationships**

Modeling and simulation is a part of almost all research activities. However some researchers are dealing with simulation using large scale simulation facilities. We would like to favor collaborations inside this community. In Lyon, these researchers are gathered within the 'Fédération Lyonnaise de Modélisation and Simulation Numérique' (FLMSN). As Professor T. Tokumasu will come in Lyon as Invited professor in June and July 2019, meetings will be organized to present the research activities within the FLMSN to Professor T. Tokumasu.

Also, main part of the research is done thanks to master and PhD students. It is quite difficult to hire good students who are interested and have abilities in the atomic scale modeling and simulation field. So, a school on atomic scale simulation will be organized. This school will gather students and teacher from Tohoku University and Université de Lyon.

## 2. Research projects

Two main projects are considered for collaborations. For these projects, four researchers are involved in MATEIS: Pierre-Antoine Geslin (who already spent one year in Tohoku University) and Jonathan Amodéo, Associate CNRS Researchers, Julien Morthomas, Associate Professor and Professor Patrice Chantrenne. Professor T. Tokumasu already involved one Postdoctoral fellow (W. Goncalves). Also one PhD student and post graduate and under graduate students came in Lyon for a visit in November 2018.

### 2.1 Silica aerogels

Development of new material for insulation is of great importance for building renewing and insulation application that require a high ratio between performance and volume. As an example, in France, a significant part of the buildings should be renovated in order to decrease their energy consumption without decrease the usable space in the houses.

Silica aerogel are good candidate for such applications. Their highly porous (more than 90% porosity) nanostructure is responsible for the low thermal conductivity (lower than air thermal conductivity), however, this is at the expense of the mechanical properties.

Understanding the link between the nanostructure and the thermal and mechanical properties is fundamental since it would allow optimizing the material processing.

Previous studies devoted to the prediction of thermal and mechanical properties of pure silica aerogel using atomic scale simulations. However, during the elaboration, the material surface is functionalized. As the surface to volume ratio is huge, these simulations might not be realistic although they gave interesting results.

This aim of this project is to study the influence of the chemical treatment that is used during the material processing (hydrophobic treatment) on the thermal and mechanical properties. It is then important to adapt the simulation methodology (inter atomic potential, coarse grain technique). The collaboration between IFS and MATEIS is necessary in order to gather the abilities in ab initio simulation and molecular dynamics simulation to get realistic simulation.

### 2.2 Carbon electromigration in Iron

Carbon based iron alloys (steels) are widely used for various applications. New treatments are under development to increase the variety of properties. Among them, electromigration allows increasing C diffusion in the direction of the electric field. This might be used to get non isotropic microstructures and mechanical properties or to decrease the duration of the thermal treatment.

The description of the physical phenomena leading to the drift velocity of C in Fe under the influence of an electric field has been proposed by Nernst Einstein. However this has been done only for single phase systems. In this project, C concentration profile and temperature level induce a phase change and the use of the drift velocity predicted by the Nernst Einstein Theory to predict the phase change front propagation is not relevant.

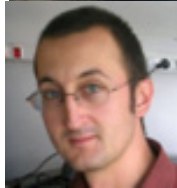
This project is organized on three stages :

- simulation of C electrodiffusion at the atomic scale, first in single phase system to correlate the simulation results to the classical results
- simulation of the solid phase change in Iron due to C diffusion
- simulation of the solid phase change in Iron due to C electrodiffusion.

The two latter stages requires a preliminary accurate study of the interatomic potential using ab initio calculations in order ensure that phase change might be simulated using MD.

## Robust Shape optimization under mechanical stability criteria

Project ELyT lab : R7 – Robust Multi Objective optimization design approaches

	<p>Koji SHIMOYAMA Institute of Fluid Science Tohoku University Sendai, Japan</p>		<p>Sébastien BESSET</p>
	<p>Pradeep MOHANASUNDARAM Double degree PhD student</p>		<p>Frédéric GILLOT</p> <p>Laboratoire de Tribologie et Dynamique des Systèmes École Centrale de Lyon Écully, France</p>

**Abstract :**

The main aim of the project is to optimise the structures involved in braking system for vibro-acoustic properties arising from friction induced vibration, commonly known as squeal noise. The complex nature of the problem demands an efficient optimisation strategy considering the computation cost. This problem is addressed through defining the expensive evaluation of the Stability criteria (representing the magnitude of the squeal noise) with the meta-model and using the Efficient Global Optimisation (EGO) search algorithms. The multi-objective definition of the optimisation results in pareto-optimal solutions obtained through genetic algorithm for the considered shape parameters. The work in progress of invoking the Isogeometric discretisation for its many advantage against classic finite element is also briefly described.

**1. Introduction**

The brake squeal noise is considered to be a very challenging problem since there is no stand-alone mechanism to explain the behaviour, though there are many mechanisms which explains in their own respective sense. This makes it hard to define the criteria for squeal noise to be considered for optimisation. But one of the methods which has proven to be efficient is complex eigenvalue analysis which gives a measure of instability which is efficient to be considered for optimisation. This is achieved through classic finite element discretisation with the setting for optimisation. Due to the expensive computation cost of the criteria evaluation, the method of EGO is used to efficiently search the design space. EGO balances the search of the design points where we could minimise/maximise the criteria, exploiting the region and also to explore the design space which is more uncertain. The meta-model updated through EGO is used to optimise the multi-objective problem through NSGA-2 algorithm which leads to pareto-optimal solutions.

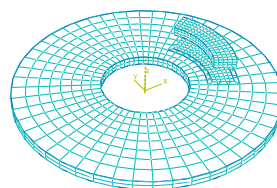


*Figure 1 : Classic FEA model of the brake system*

While the classic finite element discretisation works well with polynomial shape functions, the Isogeometric discretisation provides a large advantage in shape optimisation due to the utilisation of the same functions to define the geometry and analysis. Using the same function means to avoid the bottle neck of communication between the original geometry and the discretised version, also while defining the geometry through NURBS provides a very good scope for shape optimisation to be directly done on control points rather than the parameters, to look for unconventional shapes which can be more efficient. The achievement is made until a good comparison of matching the modal analysis results between the two discretisation. Current work in progress is done on contact and friction description with the Isogeometric elements.

## 2. Achieved results

The results from classical finite element model used for optimisation is detailed below. Initial sampling through latin hypercube shows that a large number of design points with in the considered design space show a considerable squeal noise represented through stability criteria. Further to understand the effect of the parameters a sensitivity study is performed through Variance decomposition. And then using the EGO, the new design points are added to the initial sampling and the meta-model is also updated with the new parameters. Finally, multi-objective optimisation using genetic algorithm is performed using the meta-model to find the course towards minimising the squeal noise with maximising the area of contact for effective braking. The results of the pareto-optimal solutions obtained through NSGA-2 are shown below.

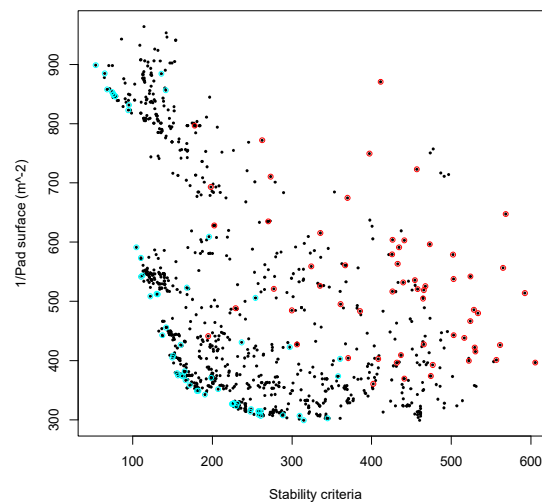


*Figure 2 : Results showing the pareto-optimal solutions, with red representing the initial generation and cyan for the final generation*

## References :

- [1] L. Nechak, F. Gillot, S. Besset, J.-J. Sinou, *Sensitivity Analysis and Kriging based Models for Robust Stability Analysis of Brake Systems*, Mechanics Research Communication, vol. 69, pp. 136-145, 2015
- [2] R. Troian, K. Shimoyama, F. Gillot, S. Besset, *Methodology for the design of the geometry of a cavity and its absorption coefficients as random design variables under vibroacoustic criteria*, Journal of Computational Acoustics, Accepted 03 October 2015

## The Eddy Current Magnetic Signature (EC-MS) non-destructive micro-magnetic technique - Simulation

Project ELyTGlobal BENTO

	MATSUMOTO Takanori Graduate School of Engineering, TohokuUniversity		DUCHARNE Benjamin <i>Université de Lyon, INSA-Lyon, LGEF EA682</i>
	UCHIMOTO Tetsuya - ELyTMaX UMI 3757, CNRS - Université de Lyon - Tohoku University, International Joint Unit - Institute of Fluid Science, Tohoku University		GUPTA Bhaawan - ELyTMaX UMI 3757, CNRS - Université de Lyon - Tohoku University, International Joint Unit, - Université de Lyon, INSA-Lyon, LGEF EA682
	TAKAGI Toshiyuki - ELyTMaX UMI 3757, CNRS - Université de Lyon - Tohoku University, International Joint Unit - Institute of Fluid Science, Tohoku University		SEBALD Gael ELyTMaX UMI 3757, CNRS - Université de Lyon - Tohoku University, International Joint Unit, Tohoku University

### Abstract:

Residual stresses inevitably occur in metallic components due to industrial machining or heat treatment processes. These local micro-residual stresses affect real-life performance of industrial parts. Measurements and analysis of residual stresses are necessary for quality assurance and maintenance anticipations.

Local magnetization processes are highly dependent on the distribution of the residual stresses. Consequently, the use of micro-magnetic techniques such as the Magnetic Barkhausen Noise (MBN) [1][2] or the Magnetic Incremental Permeability (MIP) [3][4] has increased exponentially in the industrial field. In [5][6], authors propose a new micro-magnetic technique called Eddy Current Magnetic Signature (ECMS) particularly effective for the mapping of these residual stresses. The ECMS experimental setup is similar to the MIP's one.

The ECMS method consist of plotting the evolution of the real versus imaginary part of the EC probe impedance during minor loop situation.

The industrial use of the micro-magnetic characterization techniques is very empirical: based on experimental data obtained from well-known samples, operators set thresholds of validation. Once rejected, the targeted samples are destroyed and no extra investigations are done to determine the origin of the defects. In this field, the demand for simulation tools are particularly important. Up to now, they are almost inexistent. Numerical simulations could improve highly the aging behavior

understanding and associated to experimental results detect by anticipation possible failures in structural steel components.

Developing such simulation tools have been the motivation of this work. Indeed, in this study, a lump phenomenological scalar model of EC-MS has been developed. We observed that the only way to get correct simulation results is to consider a dynamic contribution product of a  $B$  dependent variable  $\rho$  to the time derivation of the Induction field. In previous work focusing on dynamic hysteresis,  $\rho$  always exhibits constant values [7][8]. It is established that  $\rho$  depends on the tested component's geometry and electrical conductivity. From a physical point of view, it seems obvious that the electrical conductivity will not be modified during the magnetization process. As a consequence, the geometry of the treated area is the only remaining parameter. On the EC-MS experiment setup, there is no way to correctly define the geometry of the scanned area but we know that its depth will depend on the frequency and on the magnetization level. To give a  $B$  dependence to  $\rho$  is then necessary and consistent with this property.

The model developed in this study shows no mechanical stress consideration. Up to now, we have just been focusing on a correct simulation of the experimental results obtained for a free to move virgin sample. The next step will be to include a mechanical property dependence and try to understand why EC-MS is so residual stress sensitive.

#### References:

- [1] B. Ducharne, B. Gupta, Y. Hebrard, J. B. Coudert, "Phenomenological model of Barkhausen noise under mechanical and magnetic excitations", IEEE Trans. on. Mag, vol. 99, pp. 1-6, 2018.
- [2] B. Ducharne, MQ. Le, G. Sebald, PJ. Cottinet, D. Guyomar, Y. Hebrard, "Characterization and modeling of magnetic domain wall dynamics using reconstituted hysteresis loops from Barkhausen noise", J. of Mag. And Mag. Mat., pp. 231-238, 2017.
- [3] G.Dobmann, I.Alt peter, B.Wolter, R.Kern, Industrial applications of 3MA– Micromagnetic multi parameter microstructure and stress analysis, Stud. Appl. Electromagnet. Mechan. Vol. 31, pp. 18-25, 2018.
- [4] G. Dobmann, I. Altpeter, B. Wolter, R. Kern, "Industrial applications of 3MA – Micromagnetoc multiparameter microstructure and stress analysis", Elec. Nondestr. Eval. (XI), IOS Press, 2008.
- [5] T. Matsumoto, B. Ducharne, T. Uchimoto, "Numerical model of the Eddy Current Magnetic Signature (EC-MS) non-destructive micro-magnetic technique", AIP Advance, under minor revision, 2019.
- [6] T. Matsumoto, T. Uchimoto, T. Takagi, G. Dobmann, B. Ducharne, S. Oozono, H. Yuya, "Investigation of Electromagnetic Nondestructive Evaluation of Residual Strain in Low Carbon Steels Using the Eddy Current Magnetic Signature (EC-MS) Method", J. of Mag. And Mag. Mat., vol. 479, pp. 212-221, 2019.
- [7] M. A. Raulet, B. Ducharne, J.P. Masson, and G. Bayada, "The magnetic field diffusion equation including dynamic hysteresis: a linear formulation of the problem", IEEE Transactions on Magnetics, vol. 40, n° 2, pp. 872 – 875, 2004.
- [8] B. Ducharne, G. Sebald, D. Guyomar, G. Litak "Dynamics of magnetic field penetration into soft ferromagnets", Journal of Applied Physics, pp. 243907, 2016.



---

*Tuesday, March 12<sup>th</sup> – Morning*  
*Session 7 – 8:30-9:50*

## Computational fluid dynamics for perfusion MRI simulation

	<p><i>Méghane DECROOCQ</i></p> <p><i>Master Student INSA de Lyon</i></p>		<p>Makoto OHTA <i>ELyTMaX UMI 3757, CNRS – Université de Lyon – Tohoku University, International Joint Unit, Tohoku University</i></p>
	<p><i>Carole FRINDEL</i></p> <p><i>CREATIS INSA Lyon</i></p>		<p>Guillaume LAVOUE  LIRIS  INSA Lyon</p>

### Abstract :

#### **1. Introduction**

Dynamic-susceptibility Contrast (DSC) Magnetic Resonance Imaging (MRI) is an imaging modality which provides information about blood perfusion in brain tissues by injecting a contrast agent. The imaging process is dynamic: after injection, several MRI acquisitions are recorded in time. DSC-MRI is used in clinical routine to confirm ischemic stroke diagnosis, determine the extent of damages and choose appropriate treatment. Many processing steps are required to obtain interpretable parametric maps from original images, including deconvolution of the arterial input function (AIF), which describes the arrival of the contrast agent in the brain [1]. However, validation of deconvolution algorithms remains problematic due to the absence of ground truth.

To cope with this problem, in-silico validation is a possible approach. French laboratory CREATIS recently implemented a DSC-MRI simulator to produce validation material for such algorithms [3]. This simulation tool involves realistic lesion shapes and considers different sources of variability to model perfusion MRI signal. For every class of pixels (white matter, gray matter, lesion), hemodynamic parameters are selected from specific statistical distributions in order to shape the microcirculation signal locally. Then, a global AIF is convoluted and noise added to produce simulated images.

However, if the simulator can be qualified as statistically realistic, it still lacks physical realism. More particularly it has been shown that arterial input function tends to be delayed or dispersed along arteries, phenomenon which is not considered in the current simulations. Therefore, the use of local arterial input functions is investigated. As delay and dispersion of arterial input function mainly depends on the shape of artery, geometry of the vascular tree and pathology, computational fluid dynamics offers a suitable way to obtain realistic local AIFs [2].

## 2. Experimentation

The objective of this work is to increase the realism of images generated by the existing DSC-MRI simulator by integrating contrast flow simulation in a realistic vascular tree model. For this purpose, we propose to create patient-specific meshes of brain arteries from MR angiography images and to run computational fluid dynamics simulations using OpenFOAM software [4]. Numerical simulations yield high resolution local arterial input functions which can be used to quantify delay and dispersion effects and to input into the simulator.

## Acknowledgement

This work was made possible by COLABS exchange program of Tohoku University, and Institute of Fluid Science. INSA of Lyon, especially CREATIS and LIRIS laboratories are also to be thanked.

## References :

- [1] Fernando Calamante. Arterial input function in perfusion mri: A comprehensive review. *Progress in Nuclear Magnetic Resonance Spectroscopy*, 74:1–32, 2013.
- [2] Fernando Calamante, Peter J. Yim, and Juan R. Cebral. Estimation of bolus dispersion effects in perfusion mri using image-based computational fluid dynamics. *NeuroImage*, pages 341–353, 2003.
- [3] Mathilde Giacalone, Carole Frindel, Marc Robini, Frederic Cervenansky, Emmanuel Grenier, and David Rousseau. Robustness of spatio-temporal regularization in perfusion mri deconvolution: An application to acute ischemic stroke. *Magnetic Resonance in Medicine*, 2016.
- [4] H. G. Weller, G. Tabor, H. Jasak, C. Fureby, A tensorial approach to computational continuum mechanics using object-oriented techniques, *COMPUTERS IN PHYSICS*, VOL. 12, NO. 6, NOV/DEC 1998.

## On the potential of materials with a high elastic limit and moderate plasticity for dental implants

	<p><b>LIENS Aléthéa,</b></p> <p><i>Laboratoire MATEIS, UMR CNRS 5510, 20 Avenue Albert Einstein, 69621 Villeurbanne Cedex, France</i></p>		<p><b>TER OVANESSIA N Benoit,</b></p> <p><i>Laboratoire MATEIS, UMR CNRS 5510, 20 Avenue Albert Einstein, 69621 Villeurbanne Cedex, France</i></p>		<p><b>KATO Hidemi,</b></p> <p><i>Institute for Materials Research, Tohoku University, Sendai, Japan</i></p>		<p><b>FABREGUE Damien,</b></p> <p><i>Laboratoire MATEIS, UMR CNRS 5510, 20 Avenue Albert Einstein, 69621 Villeurbanne Cedex, France</i></p>
	<p><b>REVERON Helen,</b></p> <p><i>Laboratoire MATEIS, UMR CNRS 5510, 20 Avenue Albert Einstein, 69621 Villeurbanne Cedex, France</i></p>		<p><b>COURTOIS Nicolas,</b></p> <p><i>Anthogyr SAS, 2237 avenue A. Lasquin F- 74700 Sallanches, France</i></p>		<p><b>CHEVALIER Jérôme,</b></p> <p><i>Laboratoire MATEIS, UMR CNRS 5510, 20 Avenue Albert Einstein, 69621 Villeurbanne Cedex, France</i></p>		

### Abstract :

#### **1. Introduction**

Titanium Ti-6Al-4V alloy (Ti-6Al-4V) has been traditionally used for many years to design implants and other medical devices [1]. However, this alloy has reached a *plateau* in terms of mechanical properties, which can be detrimental as the down-sizing of implants has become one of the major issues in modern medicine. On the other hand, 3mol%-Yttria Stabilized Tetragonal Zirconia (3-YTZP) ceramic has gained an increase interest in dental implantology. However, this material is known to suffer from Low Temperature Degradation (LTD), a negative phenomenon which may have negative effects on the implants [2-4]. In this context, the need to develop new biomaterials with excellent mechanical properties, perfect biocompatibility, the absence of toxic elements and a very good corrosion resistance has become crucial for dental implantology. For these reasons, the potential of two materials - a Ti-based Ti<sub>40</sub>Zr<sub>10</sub>Cu<sub>36</sub>Pd<sub>14</sub> Bulk Metallic Glass (BMG) [5-8] and a new ceria-doped zirconia based composite [9, 10] - has been investigated in this study. These materials have the advantage to exhibit very high elastic limits. They are also perfectly biocompatible and corrosion-resistant. Moreover, the ceramic shows an unneglectable esthetical advantage over its metallic counterparts. However, these two materials are generally thought to present

limited or no plasticity. Our goal, within this study, is to ensure the potential of these two materials for the development of innovative dental implants.

## **2. Experimentation, discussion**

BMGs alloys have been elaborated in the laboratory of Professor Kato, at the Institute for Materials Research in Sendai. The alloys with nominal composition of  $Ti_{40}Zr_{10}Cu_{36}Pd_{14}$  (at %) were prepared by arc melting the pure elements with purities above 99.9% in a high purity argon atmosphere. The bulk metallic glasses' rods with diameter of 5 mm were prepared by copper mold-tilt casting, in a purified argon atmosphere. Mechanical properties were analyzed by compressive tests, tensile tests and static and fatigue tests on dental implant-abutment assemblies. Resistance to sterilization was assessed. Electrochemical measurements were conducted in a three electrode cell in saline solution (0.9% NaCl, pH: 7.4, following the ISO 10271 standard), at 37 °C. Direct cytotoxicity tests were carried out using MG63 osteoblasts and Human Dermal Fibroblasts cells to evaluate the cells' proliferation and adherence after 3, 6 and 10 days of culture.

Ce-TZP composite (84vol%  $ZrO_2$  with 11mol%  $CeO_2$ , 8vol%  $Al_2O_3$  and 8vol%  $SrAl_{12}O_{19}$ ) provided by Doceram (Dortmund-Germany) was fully characterized. Samples with diameter and machining conditions comparable to those applied in dental implants, have been turned by CNC lathe (Computer Numerical Control). Static and dynamic mechanical properties were analyzed by tensile and rotative bending fatigue tests and compared to 4-point bending and biaxial flexural tests results. Evaluation of the load to failure and fatigue limit on narrow diameter dental implants were estimated following the specifications of ISO 14801 standard. Load-unload tests were conducted in 4-point bending (4PB) and tensile tests.

Results show that the BMG exhibits excellent mechanical properties, superior to that of Ti-64 (compressive strength of 2GPa, hardness of 5.5 GPa and a toughness of  $56 \text{ MPa}\sqrt{\text{m}}$ ) and a very good corrosion resistance (corrosion potential of -0.07 V/SCE and corrosion current density of  $6.0 \text{ nA/cm}^2$ ). The alloy is unaffected by sterilization. The two materials show a perfect biocompatibility on both osteoblast and fibroblasts cells. The zirconia composite shows the advantage of not suffering from LTD, it exhibits a very high Weibull modulus (30) and it is not sensitive to fatigue (fatigue limit of more than 90% of the tensile strength) which gives it an unneglectable advantage over the well-known 3-YTZP material.

Moreover, the two materials have shown some plasticity (~1% in tension for the ceramic and 0.7% in compression for the BMG) and the results on real-sized dental implants are more than promising (load to failure of dental implants 1.5 times higher than Ti-64 and a fatigue limit 30% higher than Ti-64 for the BMG).

This study has shown that the newly developed BMG and zirconia based materials appear as viable alternatives to both Ti-64 and 3YTZP materials for the development of innovative dental implants.

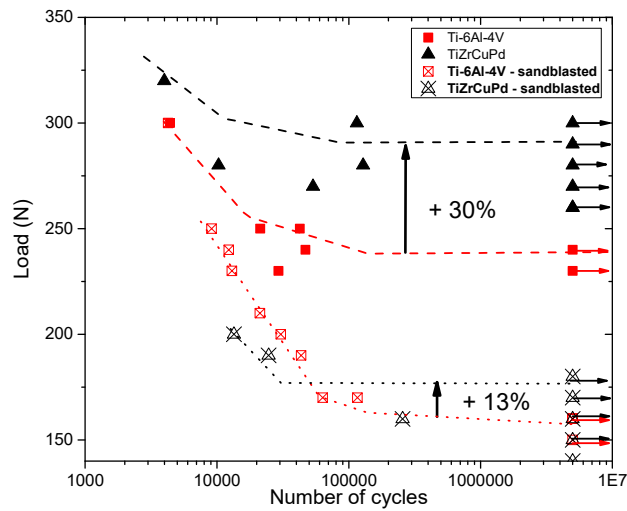


Fig.1: Wöhler curve (load as function of the number of cycles) of the Ti40Zr10Cu36Pd14 metallic glass compared to the Ti-6Al-4V with and without sandblasting.

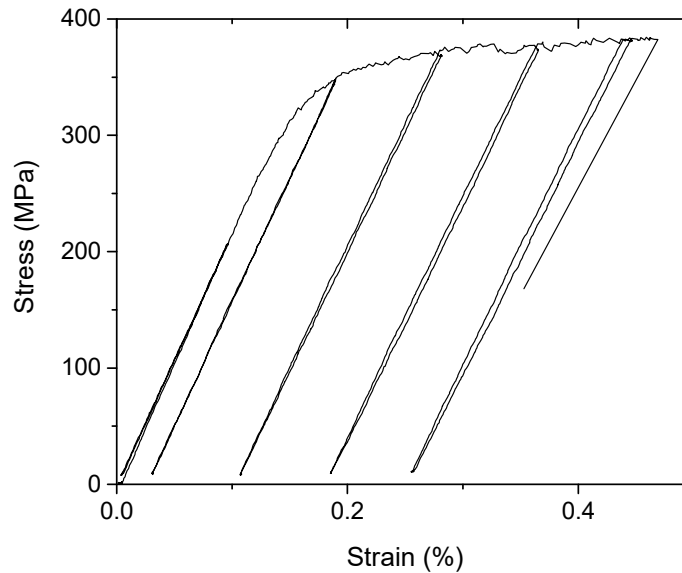


Figure 2: Stress-strain load-unload curve of a ZA8Sr8C11-1450°C composite during a tensile test, exhibiting a significant amount of plasticity before failure.

## References :

- [1] Metallic Materials, J.R. Davis (Ed.), Handbook of Materials for Medical Devices, ASM International, Materials Park, Ohio, 2003, pp. 21-50.
- [2] J. Chevalier, Biomaterials 27, 2006.
- [3] J. Chevalier, L. Gremillard, S. Deville, Annu. Rev. Mater. Res., 2007.
- [4] J. Chevalier, L. Gremillard, A. V. Virkar, D. R. Clarke, J. Am. Ceram. Soc., 2009.
- [5] S.L. Zhu, X.M. Wang, F.X. Qin, A. Inoue, A new Ti-based bulk glassy alloy with potential for biomedical application, Mater. Sci. Eng. A 459 (2007) 233-237.
- [6] F.X. Qin, X.M. Wang, A. Inoue, Effect of annealing on microstructure and mechanical property of a Ti-Zr-Cu-Pd bulk metallic glass, Intermetallics 15 (2007) 1337-1342.
- [7] F.X. Qin, M. Yoshimura, X. Wang, S. Zhu, A. Kawashima, K. Asami, A. Inoue, Corrosion behavior of a Ti-based Bulk Metallic Glass and its crystalline alloys, Mater. Trans. Vol. 48, No.7 (2007) 1855-1858.
- [8] S.L. Zhu, X.M. Wang, F.X. Qin, A. Inoue, A new Ti-based bulk glassy alloy with potential for biomedical application, Mater. Sci. Eng. A 459 (2007) 233-237.
- [9] P. Palmero, M. Fornabaio, L. Montanaro, H. Reveron, C. Esnouf, J. Chevalier, Biomaterials, 2015.
- [10] H. Reveron, M. Fornabaio, P. Palmero, T. Fürderer, E. Adolfsson, V. Lughì, A. Bonifacio, V. Sergio, L. Montanaro, J. Chevalier, Acta Biomater., 2016.



## Understanding Creep Phenomenon in High Chromium Steel Samples: Characterisation and Modelling

Project ELyTGlobal BENTO

	<p><i>GUPTA Bhaawan</i> - <i>ELyTMaX UMI 3757, CNRS - Université de Lyon - Tohoku University, International Joint Unit, - Université de Lyon, INSA-Lyon, LGEF EA682</i></p>		<p><i>DUCHARNE Benjamin</i> <i>Université de Lyon, INSA-Lyon, LGEF EA682</i></p>
	<p><i>UCHIMOTO Tetsuya</i> - <i>ELyTMaX UMI 3757, CNRS - Université de Lyon - Tohoku University, International Joint Unit - Institute of Fluid Science, Tohoku University</i></p>		<p><i>SEBALD Gael</i> <i>ELyTMaX UMI 3757, CNRS - Université de Lyon - Tohoku University, International Joint Unit, Tohoku University</i></p>
	<p><i>TAKAGI Toshiyuki</i> - <i>ELyTMaX UMI 3757, CNRS - Université de Lyon - Tohoku University, International Joint Unit - Institute of Fluid Science, Tohoku University</i></p>		

**Abstract:** Creep phenomenon is an important feature to assess in high temperature applications, although the correlations with microstructure and magnetic behaviour remain unclear. In this work, 12%Cr-Mo-W-V creep test samples (used in thermal power plants) are investigated using three electromagnetic inspection techniques. Magnetic parameters based on the results are then evaluated in comparison to the microstructure. Additionally, a modified Jiles-Atherton model has been used to numerically reproduce experimental results from Magnetic Incremental Permeability (MIP), Magnetic Barkhausen Noise (MBN) and standard B(H) measurements. All the three techniques exhibit different responses in understanding creep and the modelling parameters derived from the adapted Jiles-Atherton Model parameters are then correlated to the microstructure information. Some suitable parameters are then shortlisted according to the application technique.

### 1. Introduction

In ferromagnetic materials, magnetic domain walls interact with microstructure over similar mechanisms as dislocations do [1, 2, and 3]. This fundamental observation is the basis of micro-magnetic materials characterization. Coupling between the stress and magnetic field is the main and important feature of the ferromagnetic materials consisting of various small magnetic domains in its microstructure [4]. Conventional Eddy current testing has been extensively used for the ferromagnetic materials characterization but when it comes to creep damage detection, it becomes difficult to distinguish between the changes caused by the actual creep damage and from the signals generated by other sources like, cracks, surface roughness, hardness etc.

In this research three different electromagnetic techniques are applied to the 12 different samples from three different categories with different temperature and stress treatments. Magnetic Incremental

Permeability (MIP) is used to investigate samples as it is highly sensitive to stress. On the other hand, Magnetic Barkhausen Noise being sensitive to the mechanical changes in the materials, is also used to analyse the samples in addition to standard B(H) curve measurements. Finally, ferromagnetic hysteresis models such as dry friction quasi static model, Preisach model, Jiles-Atherton model, which are based on magnetic induction B versus applied magnetic field strength H, are implemented to get the simulated data based on experiments. All these models will be presented along with their limitations which are majorly the accommodation and the congruency issue (particularly in the case of MIP). For instance, MIP technique is related to the dynamic permeability of the material when applying a bias excitation field, and the resulting ferromagnetic minor loop modelling requires advanced modelling techniques. Having a physical interpretation, the J-A model [5] is chosen to derive some modelling parameters which are then evaluated against the microstructure of the test samples. Finally, experimental data on MIP applied to creep samples are presented, and the relevant ferromagnetic model is given. It is shown that using appropriate model, it is possible to assess model parameters directly from MIP signals. The objectives of these simulations are to improve magnetic signatures interpretations in co-relation to microstructure. Using Jiles-Atherton model, it is shown that 3 out of 5 parameters can be obtained from the magnetic curves. Their correlation to microstructure information is discussed. Such parameters are foreseen to constitute indicators of damaging independent of the experimental setup.

## 2. Results

Experimental results based on three techniques will be presented in detail and how the models are adapted to a particular method will also be presented. While fitting to the experimental data, the 5 J-A parameters can be used as degrees of freedom in the simulation process. Fig. 1(a) below shows evolution of one of the J-A parameters ‘K’ vs. Precipitation number for differently treated samples. It is quite evident that the energy required (K) to break the pinning site is larger in case of higher number of precipitates. After the determination of these parameters, Pearson correlation coefficient is evaluated against different mechanical and microstructural parameters. Fig. 1(b) shows the Pearson correlation coefficient of ‘K’ in case of Magnetic Barkhausen Noise.

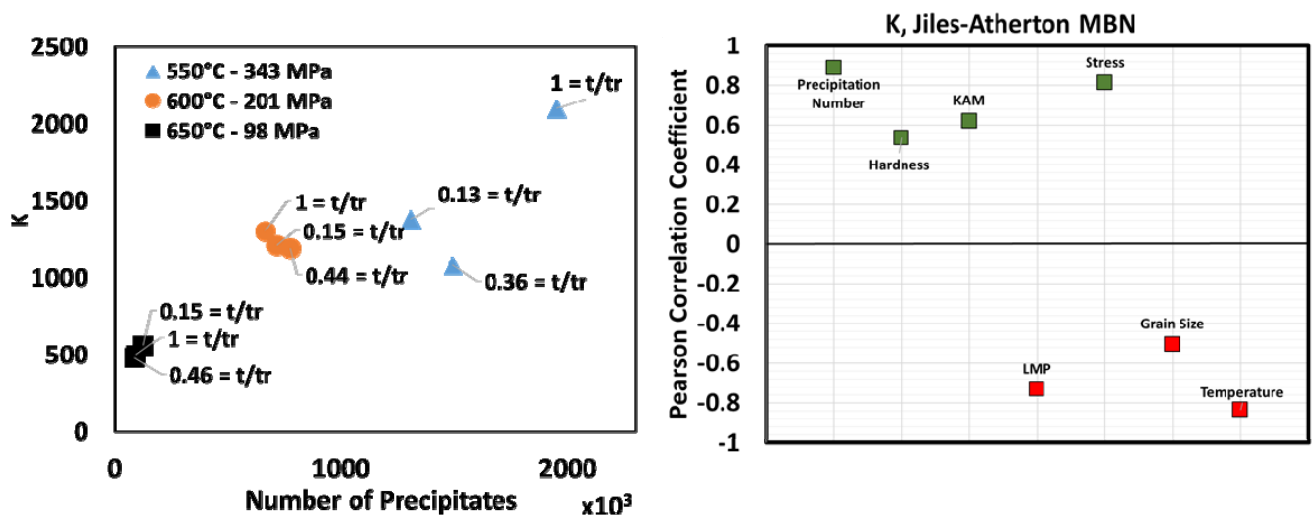


Figure 1(a): Evolution of J-A parameter ‘K’ vs. Precipitations

Figure 1(b): Pearson correlation coefficient for evolution of ‘K’ vs. different microstructural and mechanical parameters

## References :

- [1] Bozorth R.M.; Ferromagnetism. Van Nordstrand, Princeton. 1951.
- [2] Cullity B. D.; Introduction to magnetic materials. Addison-Wesley. 1972.
- [3] Jiles D.; Introduction to magnetism and magnetic materials. Chapman and Hall.1991.
- [4] Schull P.J.; Non-destructive evaluation: theory, techniques and applications. New York. Marcel Dekker,Inc.2002.
- [5] D. C. Jiles and D. L. Atherton, *J. Magn. Magn. Mater.*, vol. 61, no. 1–2, pp. 48–60, Sep. 1986.

**Low and ultralow friction of microcrystalline diamonds films**  
*towards smart and tribo-resistant coatings*

Project lofDIAMS

ELyT Global  
**Surface and interfaces**  
**Materials and structure design**

	<p><b>Dr. Hiroyuki MIKI</b></p> <p>Frontier Research Inst. for Interdisc. Sci. (FRIS), Tohoku University Aramaki asa Aoba 6-3, Aoba-ku, Sendai, Japan</p>		<p><b>Michel BELIN</b></p> <p>LTDS, CNRS Ecole Centrale de Lyon 36 avenue Guy de Collongue, 69134 Ecully cedex, France</p>
--	---	---	--

### 1. Introduction

In the field of tribology, the low and ultra-low friction is one of the most challenging subject [1, 2]. Different kinds of tribosystems are expected to exhibit low friction performances. One of them is some hard coatings, and especially the carbon-based coatings under dry lubrication. Interesting results have been reported previously, obtained on partly polished CVD diamond-films. Very low friction has been reached in air [3]. The authors have shown that the friction results were strongly influenced by contact conditions, especially the sliding speed and surface profile. These results are very promising, but not fully understood yet.

Starting from that point, we are running a research program, dealing with low- and ultra-low friction obtained on thin films based on diamond coatings. In particular the group of H. Miki *et al.* at Tohoku University, has recently highlighted a milli-range order friction, with a contact of partly-polished microcrystalline diamond layers. On the other side, LTDS has improved an experimental technique to qualify ultralow friction level, called “relaxation tribometer technique”, down to the level of  $10^{-4}$  to  $10^{-5}$ , if it happens. The complementary skills are joining in this project to go further in the knowledge of low-friction processes. In the previous ELYT-Lab project, we have explored the friction properties of partly-polished CVD diamond coatings in dry friction in air. Especially, we have quantified different components of friction: especially a solid-type friction independent of the speed and also a velocity-dependent contribution of friction, identified through the use of this technique. It should be noticed that this approach has no equivalent today. The influence of roughness was the main parameter under investigation.

### 2. Experimental

Friction characterization has been achieved thanks to the oscillating relaxation tribometer, developed at LTDS, in order to measure the kinematic friction between two sliding surfaces, as described previously [4]. This technique has been beneficially used to determine the velocity-independent and velocity-dependent friction contributions, with no need for any direct friction force measurement. The samples have been prepared at Tohoku University. The diamond coatings were

deposited by the Hot Filament CVD method on SiC ceramics substrate. Deposited microcrystalline diamond films were then carefully polished, inducing surface topography smoothening. Three levels of roughness have been investigated here:  $R_a = 1.0$  to  $1.5 \mu\text{m}$ ,  $0.4$  to  $0.7 \mu\text{m}$  and  $0.1$  to  $0.2 \mu\text{m}$ . The normal load used here is ranging from  $50$  to  $200 \text{ mN}$ , resp.  $270$  and  $430 \text{ MPa}$  of maximum Hertzian pressure. The experiments have been run in air, temperature of  $23^\circ\text{C}$  and humidity  $38 \text{ RH}\%$ .

### 3. Main results

As a result of experiments, we record the velocity time-response of the loaded contact, during its evolution from the initial situation, down to the final stop, through a damped oscillating process, for different roughness values and different normal loads. The following results have been obtained, see Fig. 1:

- from the oscillations data, we can directly compute the “friction law“, giving the dependence of the friction coefficient with sliding velocity, in non-stationary conditions;
- the effect of roughness of the coating is clearly shown: the lower the roughness, the lower the friction coefficient, as expected;
- for the better polished zone ( $R_a: 0.1$  to  $0.2 \mu\text{m}$ ), the friction laws obtained for different normal loads ( $50$ ,  $100$  and  $200 \text{ mN}$ ) are nearly superimposed, exhibiting a slight velocity-dependent contribution to friction, and a Coulomb-type friction contribution less than  $0.08$ .

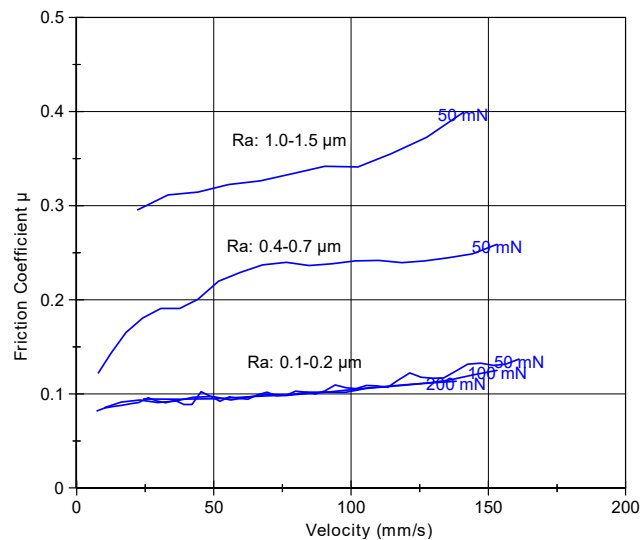


Fig. 1. Typical friction laws obtained by data processing of time-response of the velocity relaxation process.. Three different polished samples are tested:  $0.1 < R_a < 0.2 \mu\text{m}$ ,  $0.4 < R_a < 0.7 \mu\text{m}$ ,  $1.0 < R_a < 1.5 \mu\text{m}$ . We show that friction is reduced when roughness is reduced. In addition, for the low roughness sample, tested under  $50$ ,  $100$  and  $200 \text{ mN}$ , we show that the friction laws are very similar, and exhibit a slight velocity-dependent contribution to friction.

### 4. Next steps

The next steps of this ELYT Global project will include the detailed modeling of friction laws obtained with the oscillating technique, and the comparison to those obtained on a classical tribometer configuration. We will also consider i/ the effect of an applied continuous sliding velocity component, in addition to the oscillating one, and ii/ the effect of surface topcoats of diamond films. The practical goal is to reach ultralow friction with this kind of coating.

### References

- [1] Superlubricity, A. Erdemir & JM Martin Eds., Elsevier, (2007), ISBN: 978-0-444-52772-1.
- [2] J. Fontaine, M. Belin, T. Le Mogne, A. Grill, Trib. Int., **37** (2004), pp. 869-877.
- [3] H. Miki, A. Tsutsui, T. Takeno, T. Takagi, Diamond and Related Materials, **24** (2012), pp. 167–170.
- [4] E. Rigaud, J. Perret-Liaudet, M. Belin, L. Joly-Pottuz, J.M. Martin, **43** (2010), pp. 320–329.
- [5] M. Belin, H. Miki and T. Takagi, *World Tribology Congress 2017 Beijing, China, September 17 – 22, 2017*
- [6] M. Belin, H. Miki and T. Takagi, Tribology Online, submitted, 2019

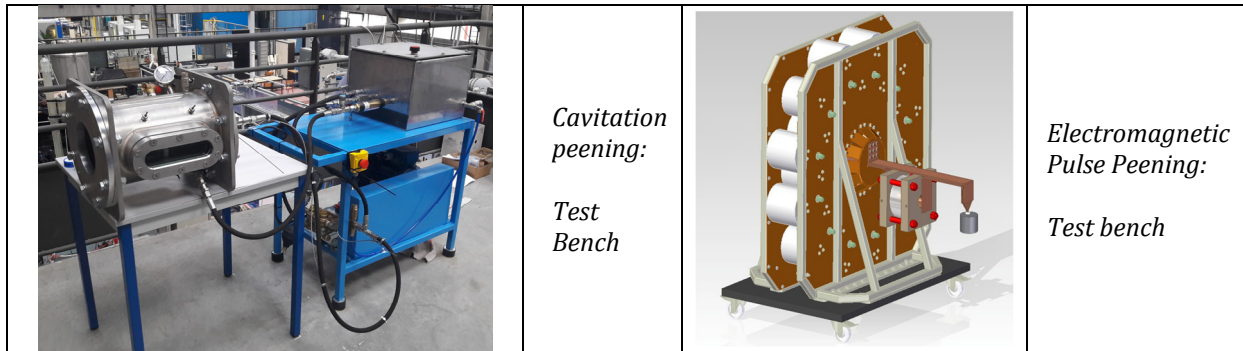


*Tuesday, March 12<sup>th</sup> – Morning*  
*Session 8 – 10:10-12:00*

## **Innovative Surface Treatments by Peening**

Daniel Nélias & Thibaut Chaise

Univ Lyon, INSA-Lyon, CNRS UMR5259, LaMCoS, F-69621, France



### Abstract:

#### **1. Introduction**

Surface treatments methods like shot peening are used to introduce compressive residual stresses in metals and alloys. These processes are carried during the manufacturing steps or for the purpose of repairing. The introduction of compressive stresses is useful to prevent the initiation and growth of cracks and hence improves the fatigue life of mechanical parts. The drawbacks and limitations of the existing processes generally used for this purpose are known and have been highlighted in many studies. These are, among others, an important surface modification (roughness), a limited compressive depth, difficulties in execution, debris and contamination problems, etc. Therefore, the interest in new surface treatment methods, which permit to obtain equivalent or even better compressive results while avoiding the previous problems, are growing. Cavitation peening and electromagnetic pulse peening are part of these innovative processes which modeling can be used for predicting purpose. The presentation will focus on these two peening processes.

#### **2. Cavitation Peening**

Cavitation peening is a process of surface treatment which acts by the generation of cavitation bubbles near the workpiece surface. The modeling of this process is challenging because of the complexity of cavitation phenomenon and the first objective is the determination of the mechanical loading on the material due the bubbles collapse. An approach of modeling for cavitation peening based on the study of the dynamics of cavitation bubbles is proposed. Spherical and aspherical collapse of bubbles near a solid surface are studied by some numerical and analytical models. These two sources of loading pressures have been compared and a macroscopic model for cavitation peening has been derived by associating the numerical simulation of the cavitation jet and the localization of the cavitation zone. The comparison between the final residual stress profile calculated with the proposed model and the experimental results is satisfactory. New experimental results will be presented.

#### **3. Electromagnetic Pulse Peening**

Electromagnetic pulse peening (EMP) is a contactless process of surface treatment that could be used to introduce compressive residual stresses in conductive materials, by the generation of a high transient electromagnetic field. Laplace forces induced in the material by magnetic induction are the

source of the material plastic deformation, which indeed produce compressive residual stresses. To predict the effects of EMP, a numerical model has been built to simulate the process. The model, based on the finite element method, is coupling electromagnetic and mechanical phenomena by using a sequential-coupled approach. Some numerical examples are provided. It is shown by calculations that much higher compressive depths than those of conventional peening processes could be achieved. A parametric study has exhibited the influence of the maximum current intensity and frequency which affect both the compressive depth and the maximum residual stress. Comparison with experiments will be discussed.

#### References :

- [1] E Sonde, T Chaise, N Boisson, D Nelias, "[Modeling of cavitation peening: Jet, bubble growth and collapse, micro-jet and residual stresses](#)", *Journal of Materials Processing Technology* **262**, 479-491, 2008.
- [2] E Sonde, T Chaise, D Nelias, V Robin, "[Numerical simulation of electromagnetic surface treatment](#)", *Journal of Applied Physics* **123**(4), 045901, 2018.
- [3] A Chazottes-Leconte, E Sonde, L Plantevin, C Joubert, T Chaise, L Morel, D Nelias, H Razik, "[The effect of an electromagnetic peening process on mumetal properties](#)" 2018 IEEE International Conference on Industrial Technology (ICIT), 859-863.

**Elaboration and characterization of new Titanium alloys for biomedical applications**

PhD thesis in cotutelle between INSA de Lyon, France and Tohoku University, Japan  
11/2018 – 10/2021

	<p><b>Manon Laurençon</b> PhD student  INSA de Lyon, MATEIS laboratory Bâtiment Saint-Exupéry, 3<sup>o</sup> étage 25 Avenue Jean Capelle 69621 Villeurbanne, France</p>
---	--

	<p><b>Prof. Damien Fabrègue</b> Supervisor INSA de Lyon, MATEIS laboratory, Bâtiment Saint-Exupéry, 3<sup>o</sup> étage 25 Avenue Jean Capelle 69621 Villeurbanne, France</p>		<p><b>Prof. Akihiko Chiba</b> Supervisor <b>Chiba Laboratory,</b> Deformation Processing, Institute for Materials Research, Tohoku University, 2-1-1 Katahira, Aoba-ku, Sendai, 980-8577 Japan</p>
---	---	---	--

Abstract :

**I. Context**

Titanium-based alloys are widely used in various areas due to their high performances. Their physical, mechanical or chemical features are directly inherited from the type (pseudo- $\alpha$ ,  $\alpha$ ,  $\alpha+\beta$ , near  $\beta$ , metastable  $\beta$  or stable  $\beta$ ) and microstructure of the alloys, driven by their chemical composition and thermomechanical history. These alloy variations provide a good compromise between lightness, mechanical strength and corrosion resistance. Thus, they are very attractive for demanding applications that possess high requirements like transportation and biomedicine. For this latter, materials biocompatibility is crucial, which reduces drastically the range of alloying elements used. During several years,  $\alpha$ -cp titanium and TA6V alloy, initially designed for aircraft structures, appeared as preferential solutions for designing implants. However, along

with practical feedbacks, some limits in the use of this type of alloys raised, showing the cytotoxicity of vanadium and aluminum elements of TA6V among other things. In addition to this lack of biocompatibility, the mismatch of Young's modulus between the alloy (110 GPa) and the receiving bone (around 20 GPa for cortical bone and 3 GPa for cancellous bone) revealed deleterious impacts on structural integrity such as the stress shielding effect because of unbalanced distribution of stresses between the implant and the bone, leading to an implant loosening at the interface [1].

To adapt the biological and mechanical behaviour to biomedical requirements, many studies focused on the development of Ti-based alloys aiming for low stiffness alloys with biocompatible alloying elements. The design of such alloys significantly spread with investigation on combinatorial metallurgy. Basing on molecular orbital calculations, « d-electron method » (or cluster method, « Discrete Variation » -X) developed by Morinaga [2, 3] gives information on phases stability, associated to the Molybdenum equivalence  $Mo_{eq}$  and the covalent electron number per atom  $e/a$  ratio. This main method relies on local electronic structures calculations for a given cluster, corresponding to a single crystal structure, of the alloying element X in a matrix M (M-X couple). From these calculations, two parameters can be extracted: the bond order ( $Bo$ ) and the metal-orbital energy level ( $Md$ ). Characterizing respectively the covalent bond strength of d-orbitals between M and X and, the mean energy of d-orbitals levels of M and X, the  $Bo-Md$  map enables to assess the phase stability and deformation mechanisms depending on the chemical composition of the alloys. Firstly used for designing steels, this method was gradually adapted for titanium alloys design, first binary then ternary for some combinations [4]. With the relatively good experimental reliability of this approach comes hypothesis that limit its use for complex alloys. Consequently, new alloys design methods are in development, via big data approaches for example.

The objectives of the current work is first to provide some understanding on the « d-electron method » by Morinaga, in order to design new metastable  $\beta$ -titanium alloys with desired deformation mechanisms for biomedical applications, without any cytotoxic element such as vanadium or aluminum. Initially developed for their lower stiffness, this type of alloys offers attractive possibilities regarding the precipitation of metastable phases and the deformation mechanisms. Metastable  $\beta$  alloys are obtained by adding some  $\beta$ -stabilizing elements to the chemical composition in order to retain  $\beta$  phase at room temperature after quenching from  $\beta$  field at high temperature (above  $\beta$  transus temperature). Most of the time, titanium alloys are reputed for their high mechanical resistance but they usually exhibit low ductility and strain hardening. However, many studies investigated the improvement of ductility in metastable  $\beta$  Ti-based alloys, especially by the combination of TWinning Induced Plasticity (TWIP) and TRansformation Induced Plasticity (TRIP) [5]. The obtained composite effect is represented in orange on  $Bo-Md$  map (Fig. 1) like a very restricted domain. In this study, we aim to maximize these effects by promoting the  $\omega$  martensite precipitation in  $\beta$  matrix, which could encourage and accommodate the formation of twins and martensite under stresses, without affecting  $\beta$  phase stability and chemical composition. This effect of ultra fine  $\omega$  phase in  $\beta$  matrix has been shown in Ti-12Mo alloy in 2017 [6] using flash low-temperature aging (LTA) treatments, previously studied in Ti-Nb superelastic metastable  $\beta$ -titanium alloy [7].

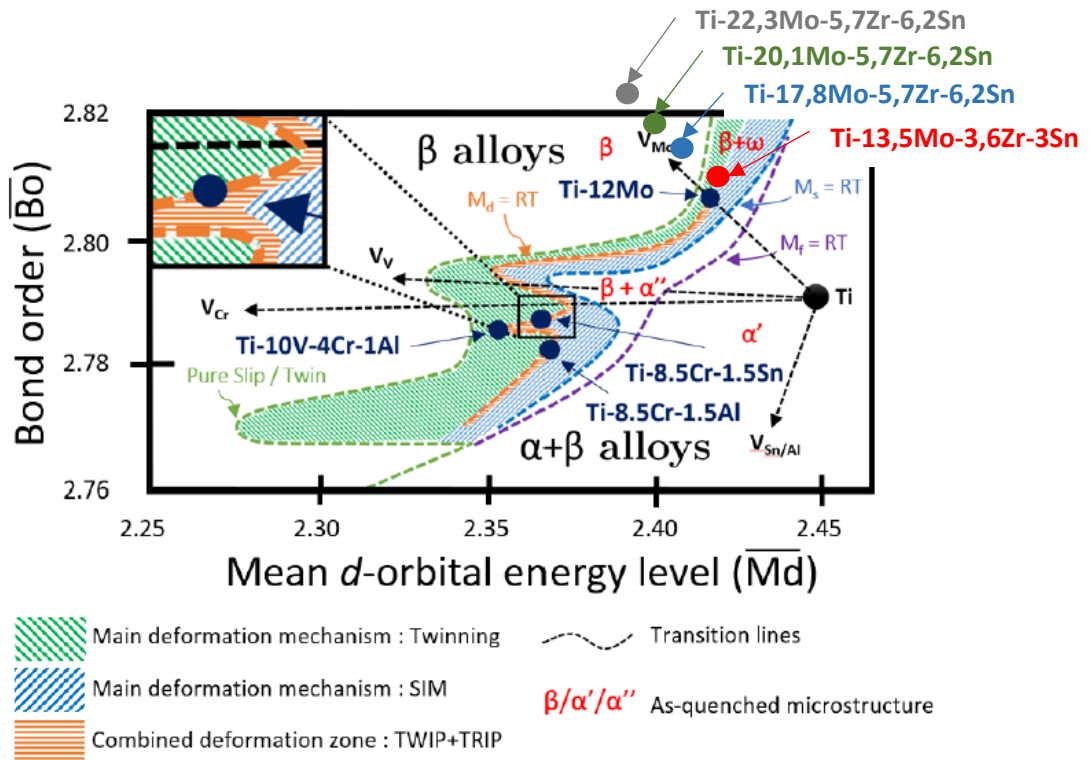


Fig. 1. Bo-Md map of « d-electron method » with deformation mechanisms and new variations of Ti-based alloys [4].

## II. Experimentation and discussion

A first quaternary metastable  $\beta$  Ti-based alloy T1 was designed, with contents of 13.5% Mo, 3.6% Zr and 3% Sn (mass fraction). Thanks to its location on the *Bo-Md* map in Fig. 1, this alloy is expected to combine both TWIP and TRIP effects to improve its ductility up to 40-50%, while exhibiting high mechanical resistance. In addition, three other variations, derived from the first one, have been elaborated with chemical composition presented in Table 1.

Tab. 1. Chemical composition of elaborated alloys.

Material reference	Ti (wt. %)	Mo (wt. %)	Zr (wt. %)	Sn (wt. %)
T1	Base	13.5	3.6	3
T2	Base	17.8	5.7	6.2
T3	Base	20.1	5.7	6.2
T4	Base	22.3	5.7	6.2

These four alloys have been elaborated by cold crucible levitation melting at INSA de Rennes in France. Ingots thus obtained were then cold rolled (for 17.8%, 20.1% and 22.3% of Mo contents) or hot rolled (for 13.5% of Mo content) before being quenched from 800 °C/1 h to room temperature. Specimens were then characterized by Optical Microscopy (MO), Scanning Electron Microscopy (SEM), Electron BackScatter Diffraction (EBSD), Energy Dispersive X-Ray Spectrometry (EDX) and X-Ray Diffraction (XRD). They showed heterogeneities in chemical composition of T3 and T4 materials which probably

indicate a lack of mixing during the melting or a spinodal decomposition. Diffraction of X-rays, completed with EBSD, showed that extremely low  $\alpha$  phase is present in T1 alloy, and only  $\beta$  phase is present in other ones. Vickers micro hardness has been assessed and seems to decrease lightly with the increase of Mo content.

In further research work, deformation mechanisms will be investigated in order to control the reliability of the « d-electron method » for the design of TWIP/TRIP metastable  $\beta$  titanium alloys. After that, heat treatments will be carried out to nucleate  $\omega$  phase and optimize microstructure, alongside with hot deformation. Characterization of metallurgical states of the materials will be iteratively performed before conducting tensile/compression tests, fatigue tests, corrosion tests and other experiments that will bring some new understanding upon the behaviour of such materials. Finally, cytotoxicity experiments will be run on the designed alloys in order to assess their biocompatibility and lifetime.

#### References :

- [1] R. Huiskes, H. Weinans, B. Vanrietbergen, The relationship between stress shielding and bone-resorption around total hip stems and the effects of flexible materials, *Clinical Orthopaedics and Related Research* (1992) 124–134.
- [2] M. Morinaga, N. Yukawa, T. Maya, K. Sone, and H. Adachi, "Theoretical Design of Titanium Alloys," in *Sixth World Conference on Titanium III*, 1988, 1601.
- [3] M. Morinaga and N. Yukawa, "Alloy Design Based on Molecular Orbital Method." *Computer Aided Innovation of New Materials*. ed. M. Doyama et al. (Amsterdam : North-Holland, 1991), 803-808.
- [4] C. Brozek, F. Sun, P. Vermaut, Y. Millet, A. Lenain, D. Embury, P.J. Jacques, F. Prima, A  $\beta$ -titanium alloy with extra high strain-hardening rate: Design and mechanical properties, *Scripta Materialia*, Vol. 114 (2016) 60-64.
- [5] J. Y. Zangh, F. Prima, M. Marteleur, P. Vermaut, P. Castany, P. J. Jacques, D. Lail  , T. Gloriant, C. Curfs, F. Sun, Investigation of early stage deformation mechanisms in a metastable  $\beta$  titanium alloy showing combined twinning-induced plasticity and transformation-induced plasticity effects, *Acta Materialia* (2013) 61(17)
- [6] F. Sun, J. Y. Zhang, P. Vermaut, D. Choudhuri, T. Alam, S. A. Mantri, P. Svec, T. Gloriant, P. J. Jacques, R. Banerjee & F. Prima, Strengthening strategy for a ductile metastable  $\beta$ -titanium alloy using low-temperature aging, *Materials Research Letters* 5:8 (2017) 547-553.
- [7] F. Sun, S. Nowak, T. Gloriant, et al., Influence of a short thermal treatment on the superelastic properties of a titanium-based alloy, *Scr Mater.* (2010) 63 (11): 1053–1056.

## **Development of fluoropolymer coating using Cold-spray**

Project ELyT lab: R6 – Resilient Polymeric cold spray coating

W. Lock Sulen<sup>1</sup>, K. Ravi<sup>1,2</sup>, C. A. Bernard<sup>1,2,3</sup>, N. Mary<sup>2</sup>, Y. Ichikawa<sup>1,2</sup>, K. Ogawa<sup>1,2</sup>



<sup>1</sup>Fracture and Reliability Research Institute, Tohoku University, Sendai, Japan

<sup>2</sup>ELyTMax, UMI 3757, CNRS—Université de Lyon—Tohoku University International Joint Unit,  
Tohoku University, Sendai, Japan

<sup>3</sup>Frontier Research Institute for Interdisciplinary Sciences, Tohoku University, Sendai, Japan

### Abstract :

Fluoropolymer particles are difficult to be deposited using cold-spray, highly attributed to its low surface energy property. In general, a low deposition efficiency is associated with this material as compared to metallic materials despite interests in its attractive properties including inertness and (super) hydrophobic properties. Thus, a study on material modifications and spray condition were conducted to evaluate and improve the deposition efficiency of fluoropolymer coating using cold-spray.

### **1. Introduction**

Fluoropolymer are highly durable even in extreme weather condition, non-adherent with extreme hydrophobicity, which is ideal for protective coatings [1]. However, depending on the fabrication method, fabricating their coating could be a challenging task [2]. A more environmentally friendly method besides using halogenated compounds is an attractive proposition. A cold-spray (CS) technique is one of the potential fabrication techniques, an ultra-high velocity solid-state particle deposition method onto a substrate. Since the discovery by Papyrin et al in 1980s, cold spray has gained considerable interests due to its novelty and simplicity, an attractive criterion in which eliminates the necessity of multi-steps procedure, resulting in a more economical and viable solution to be used at the sites [3]. It is a one-step process, and less hazardous solution. In contrast to metal-metal cold spray deposition, only a few reported studies on polymer-metal, despite considerable interests in them. Nevertheless, previous study had shown the possibility of ultra-high molecular weight polyethylene polymer deposition using cold spray onto metals substrate [4]. In the present work, we aim to study the effect of hydrophobic type fumed nano- alumina (FNA) on fluoropolymer deposition; perfluoroalkoxy (PFA) particles, on a metallic substrate by cold spray.

### **2. Hydrophobic fumed nano-ceramic effects**

The modification on the 20 - 50  $\mu\text{m}$  virgin PFA particles by homogenous dispersion of hydrophobic type FNA and FNS on the particles surface. Direct sonication method was employed on the PFA-FNC suspension to ensure a homogenous distribution of the FNC particles throughout the

suspension. A low-pressure cold spray device, Dymet 423 with a de Laval nozzle of 120.0 mm long were used (Figure 8). Gas pressure and temperature as indicated in Figure 8, were employed.

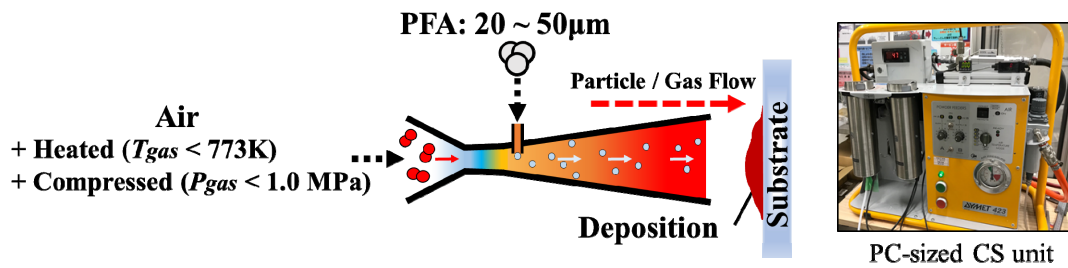


Figure 8: Diagram of a low-pressure cold-spray device.

A homogenously dispersed FNA additives onto the virgin PFA particles surface has improved the interlayers formation of the coating using cold spray. As a result, the deposition efficiency of PFA with FNA addition increased compared to without FNA addition.

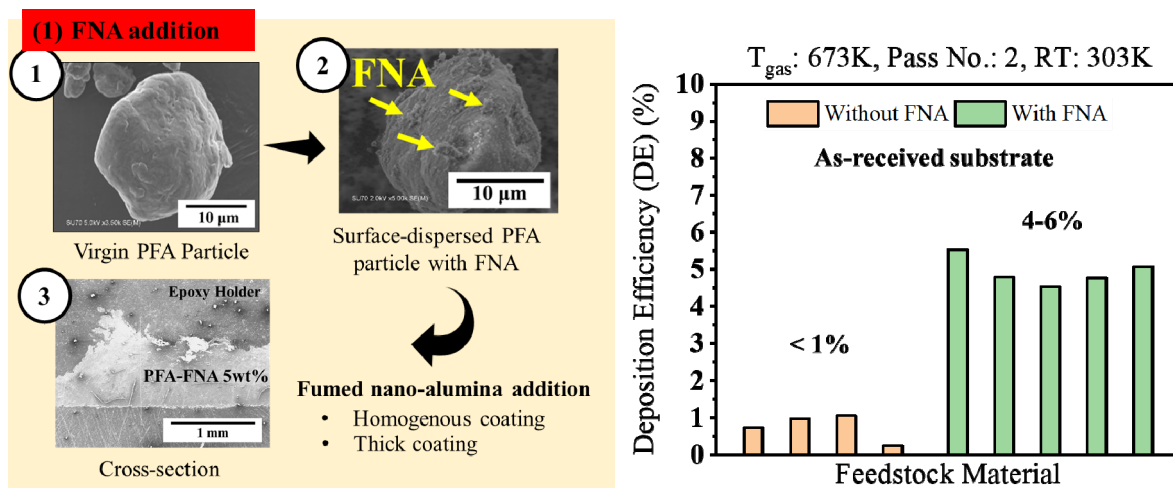


Figure 9: Deposition efficiency of PFA with and without hydrophobic type FNCs.

The PFA+FNA coating was found to retain its hydrophobicity and is useful for various application that requires such property. However, it is also important to note that further study has to be conducted to improve the adhesion strength of such coating, including understanding the effect of FNA addition to the deposition of the material.

#### References :

- [1] R. E. Banks, B. E. Smart, and J. C. Tatlow, Eds., *Organofluorine Chemistry*. Boston, MA: Springer US, 1994.
- [2] J. Gardiner, "Fluoropolymers: Origin, Production, and Industrial and Commercial Applications," *Aust. J. Chem.*, vol. 68, no. 1, pp. 13–22, 2015.
- [3] A. Papyrin, *Cold spray technology*. Elsevier, 2007.
- [4] K. Ravi, T. Deplancke, K. Ogawa, J. Y. Cavallé, and O. Lame, "Understanding deposition mechanism in cold sprayed ultra high molecular weight polyethylene coatings on metals by isolated particle deposition method," *Addit. Manuf.*, vol. 21, no. March 2017, pp. 191–200, 2018.

## Influence of the C composition on properties of Co based alloys

	<p><b>AOTA Shoya,</b> <i>Laboratoire MATEIS, UMR CNRS 5510, 20 Avenue Albert Einstein, 69621 Villeurbanne Cedex, France</i></p>		<p><b>CHIBA Akihiko,</b> <i>Institute for Materials Research, Tohoku University, Sendai, Japan</i></p>		<p><b>MAIRE Eric,</b> <i>Laboratoire MATEIS, UMR CNRS 5510, 20 Avenue Albert Einstein, 69621 Villeurbanne Cedex, France</i></p>		<p><b>FABREGUE Damien,</b> <i>Laboratoire MATEIS, UMR CNRS 5510, 20 Avenue Albert Einstein, 69621 Villeurbanne Cedex, France</i></p>
	<p><b>YAMANAKA Kenta,</b> <i>Institute for Materials Research, Tohoku University, Sendai, Japan</i></p>						

### Abstract :

#### **1. Introduction**

Co based alloys are widely used for biomedical applications every time high mechanical strength and high wear resistance are needed. Moreover, to answer to new applications' challenges (personalized shape,...), the additive manufacturing techniques are more and more used nowadays. For new applications, the wear resistance may be the real keypoint to extend the life duration of the part. Thus, the influence of the C content, which is known to increase the hardness of the alloys, should be studied. However, the behavior during the additive manufacturing technique can also change according to this composition. Thus, this project deals with the evaluation of the quality of the parts made by Electron Beam Melting for a Co based alloys according to its composition in Carbon.

#### **2. Experimentation, discussion**

Different Co-Cr6Mo alloys containing C content varying from 0.44wt% and 2.5wt% were used to manufacture tensile samples. The raw powder has been characterized in terms of initial porosity by 3D X-ray CT. Then the tensile samples have also been studied. The link between the composition and the number of defects in the samples has been determined.

It has been shown that the porosity and pore size increase with the carbon content. This is due to the fact that the solidification path is changing with the carbon content going from columnar to dendritic and thus eutectic microstructure with increasing C content. These

results are of first importance when optimization of the alloy is considered for biomedical applications.

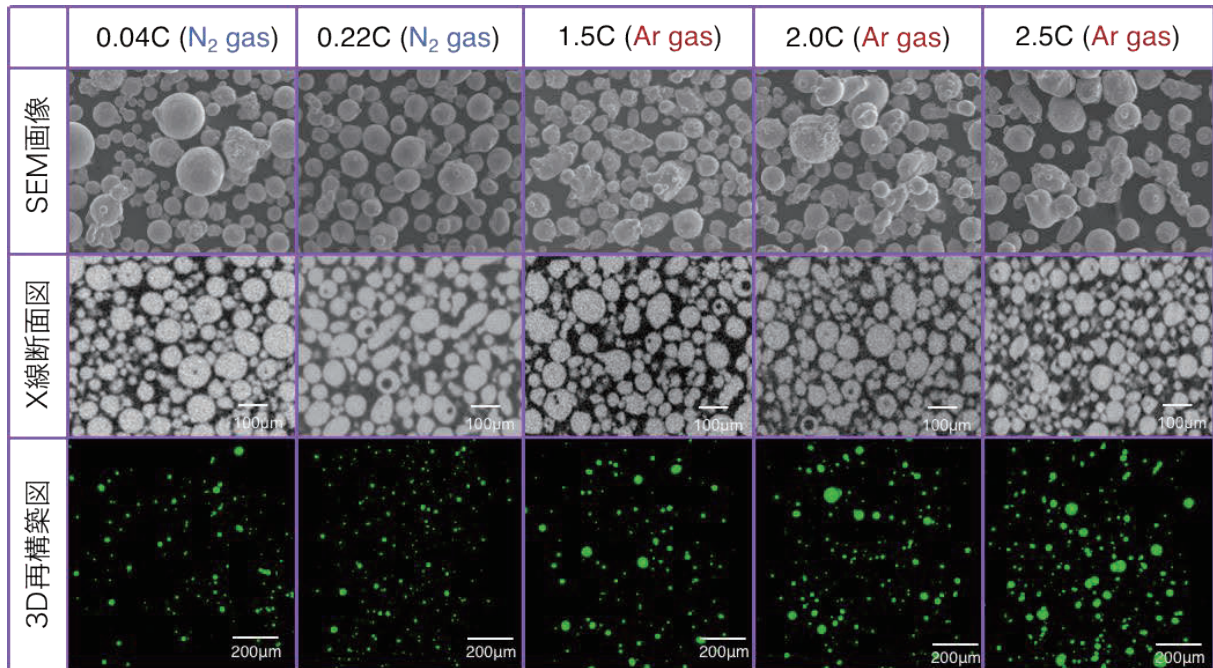


Fig.1: Evolution of the powder shape and internal porosity according to the C content by 3D X-Ray CT

